6-25-2018

Wave Attenuation by Constructed Oyster Reef Breakwaters

Jason M. Chauvin
Louisiana State University and Agricultural and Mechanical College, jchauvin10@gmail.com

WAVE ATTENUATION BY CONSTRUCTED OYSTER REEF BREAKWATERS

A Thesis

Submitted to the Graduate Faculty of the
Louisiana State University and
Agricultural and Mechanical College
in partial fulfillment of the
requirements for the degree of
Master of Science

in

The Department of Civil and Environmental Engineering

by
Jason Michael Chauvin
B.S., Louisiana State University, 2011
August 2018

For my family

ACKNOWLEDGMENTS

I would like to thank my parents, Tommy and Charlene Chauvin for their unconditional love and support. They have made many sacrifices so that my brothers and I could pursue our goals and aspirations. Through their example, my dad and mom instilled in me the value of hard work and commitment. I would like to thank Amanda for her continuous love, encouragement, and patience. I would like to thank my brothers, Jamie and Eric for their support and always pushing me to be my best. I would also like to thank all of my family and friends for their support throughout my studies, especially Maw Maw Hazel and Maw Maw Alma for their countless prayers.

Dr. Qin Jim Chen has had the greatest influence on my academic growth in coastal engineering. His undergraduate course, Introduction to Coastal Engineering, sparked my interest in pursuing an advanced degree in the subject. His guidance as my advisor for this research has helped me grow as an engineer and scientist. I am sincerely grateful for the time and devotion that he has given me. I would also like to thank my co-advisor Dr. Navid Jafari, and my committee members Dr. John Pardue and Dr. Kevin Xu for their time and guidance. Thomas Everett, Cody Johnson, Kelin Hu, and Arash Karimpour of Dr. Chen's research group provided invaluable assistance and insight.

I would like to thank my employer T. Baker Smith, Kenny Smith, and my colleagues for their support and encouragement in pursuing my studies. I would also like to acknowledge the Coastal Protection and Restoration Authority, Micaela Coner, and Josh Carter for their support of this project.

TABLE OF CONTENTS

LIST OF TABLES

LIST OF FIGURES

ABSTRACT

Biloxi Marsh, located along the shoreline of Eloi Bay in St. Bernard Parish, Louisiana has experienced significant shoreline erosion in recent years. The Living Shoreline Demonstration Project, completed in November 2016, constructed three miles of living shoreline structures to attenuate waves and thus combat marsh edge erosion along the shoreline of Eloi Bay. Several types of constructed oyster reef breakwaters were installed for this demonstration project. Due to the experimental nature of these products, available performance characteristics are limited.

This research measures wave attenuation across the constructed oyster reef breakwaters using bottom-mounted pressure gauges. Seven pressure gauges were deployed to obtain wave characteristics on the unprotected and protected sides of four types of breakwater structures. The raw pressure data were processed to determine water surface elevations, significant wave heights, and peak wave periods. In addition to the wave gauges, two water level sondes were deployed to record water surface elevations at the site. Topographic and bathymetric surveys were also conducted along cross-shore transects at the wave gauge locations to provide a profile of the shoreline and structures. The wave attenuation and transmission characteristics of the oyster reef breakwaters from the field measurements are presented. A range of transmission coefficients were calculated for each breakwater structure type.

1. INTRODUCTION

1.1 REGIONAL BACKGROUND

Coastal Louisiana is an important natural, cultural, and economic resource. The current Mississippi River delta along with its prehistoric and historic delta lobes shaped the Louisiana coastline and its unique ecosystems. The Louisiana coast is losing valuable wetlands at a rate of 16.57 square miles per year (Couvillion et al., 2011). This land loss, if occurring at a constant rate, would equate to Louisiana losing an area the size of one football field per hour (Couvillion et al., 2011). Figure 1.1 shows the land area change in coastal Louisiana from 1932 to 2010 and an enlarged view of the temporal categorization of land area change in the Pontchartrain Basin, located east of the Mississippi River.

Much of this wetland loss is due to the erosion of shorelines by natural forces. Natural waves account for 26% of coastal land loss in the Mississippi River delta plain (Penland et al., 2000). Figure 1.2 shows land loss along the shoreline of Eloi Bay is predominantly caused by natural waves.

In many coastal areas, landowners and stakeholders attempt to combat shoreline erosion by armoring the land/water interface. This is mostly accomplished by the use of limestone riprap, concrete mats, or sheet pile walls composed of wood, vinyl or steel. Recently, more attention has focused on the use of living shorelines as a means of shoreline protection. A living shoreline is a term that encompasses a range of shoreline stabilization techniques that has a footprint made up of native material. Living shorelines maintain continuity of coastal processes and reduce erosion while providing habitat value and enhancing coastal resilience (NOAA, 2015).

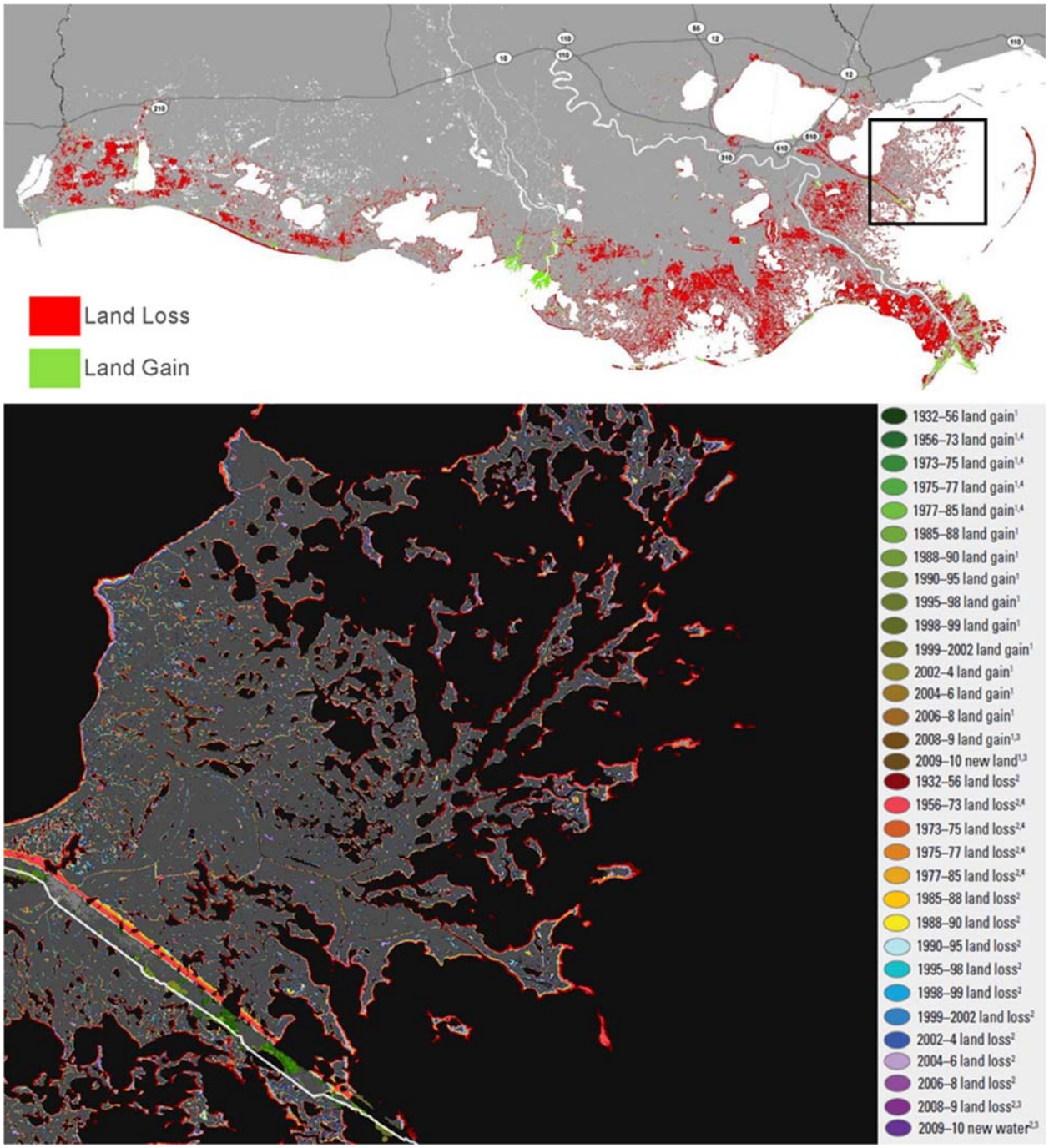

Figure 1.1: Land area change in coastal Louisiana from 1932 to 2010; (top) Louisiana coastal zone (CPRA, 2017; data from Couvillion et al., 2011), (bottom) enlarged view of the temporal categorization of land area change in the Pontchartrain Basin (modified from Couvillion et al., 2011).

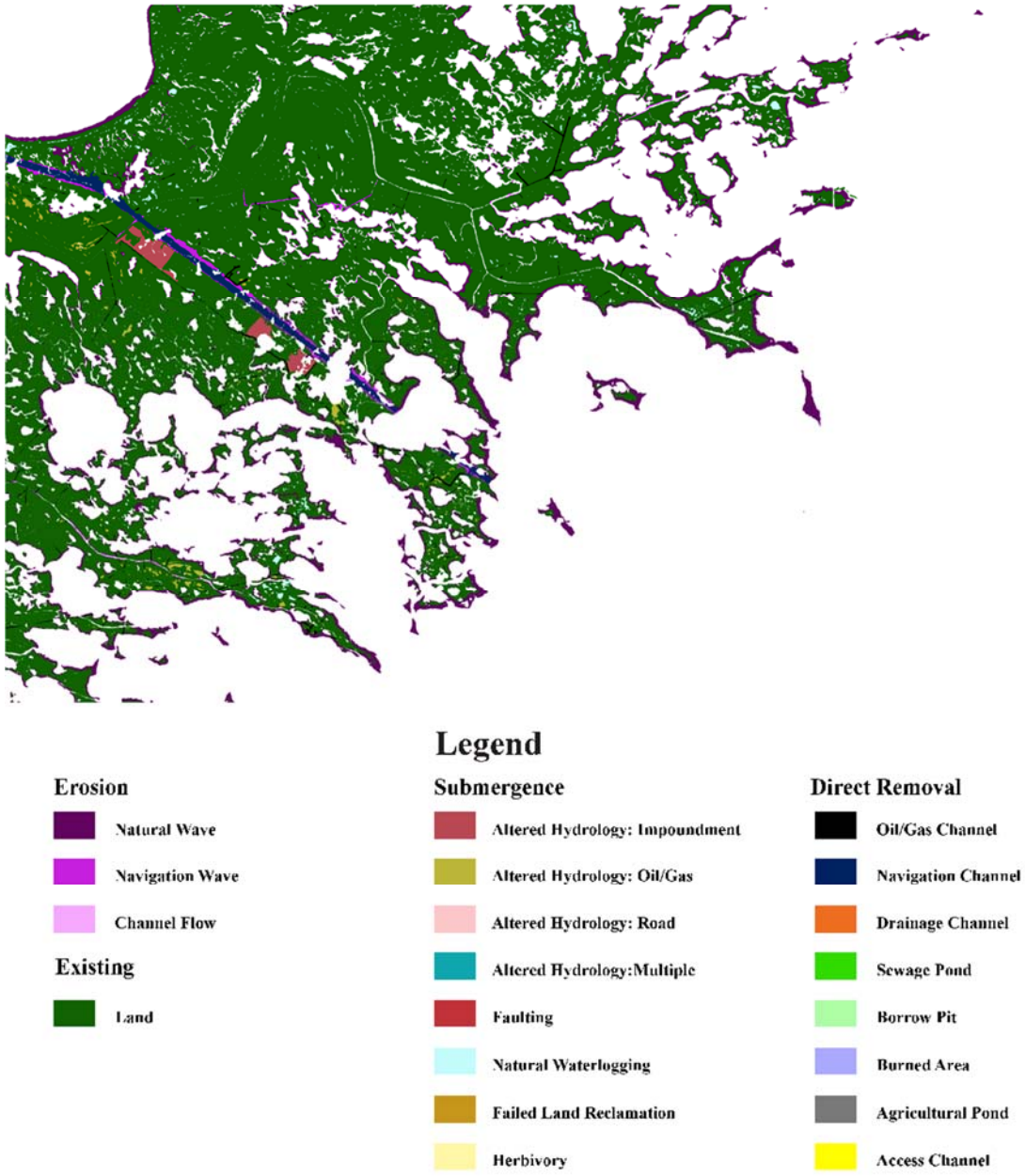

Figure 1.2: Process classification of coastal land loss between 1932 and 1990 in the Mississippi River delta plain, southeastern Louisiana (modified from Penland et al., 2000).

Louisiana's Comprehensive Master Plan for a Sustainable Coast (CPRA, 2017) includes many projects that build or maintain land and reduce risk to communities. One project type included in the master plan is oyster barrier reef projects. The master plan defines oyster barrier reef projects as bioengineered oyster reefs that improve oyster cultivation and reduce wave

energies on shorelines in open bays and lakes. One of the attributes of oyster barrier reef projects is wave attenuation, which is the percent of wave energy deflected away/prevented from contact with the shoreline by the project. Wave attenuation was calculated for oyster barrier reefs in the master plan on a per-project basis using methodology found in the United States Army Corps of Engineers (USACE) Coastal Engineering Manual (CEM) (2008). This study contributes to the quantification of wave attenuation for a master plan oyster barrier reef project by leveraging field recorded wave data.

1.2 STUDY SITE

The study site for this research is located off the shoreline of Eloi Bay in St. Bernard Parish, Louisiana. The study area is located within the Pontchartrain Basin and encompasses the eastern shoreline of Biloxi Marsh at Eloi Point and the adjacent water near the mouth of Bayou La Loutre (see Figure 1.3). Breton Sound and Chandeleur Sound separate the study site from the Gulf of Mexico. The Chandeleur Islands and other barrier islands that separate the sounds from the Gulf of Mexico are located approximately 20 miles away from the study site and provide little protection from the wind induced wave energy at the site.

The Living Shoreline Demonstration Project (PO-148), completed in November 2016, was constructed with the primary goal of combating shoreline erosion at the study site. This project, sponsored by the Coastal Protection and Restoration Authority (CPRA) and included in the master plan, created three miles of oyster barrier reefs demonstrating multiple types of oyster-promoting products. The breakwater products OysterBreaks, Reef Balls (Type 1 and Type 2), Wave Attenuation Devices (WAD), and ShoreJax were constructed along the -3.0 foot contour. Additionally, ReefBlk units were constructed along the -1.5 foot contour at the gaps of the breakwater structures. Figure 1.4 shows the types of structures constructed for PO-148. Along with

the primary goal of shoreline protection, secondary goals of the project include oyster growth and colonization, sediment accretion, and performance demonstration of the selected products. The cost of this project was approximately $15.3 million and was funded through the Coastal Impact Assistance Program (CIAP). The results of PO-148, along with the performance and cost of the structures, will be considered in the design of a larger, adjacent project, the Biloxi Marsh Living Shoreline Project (PO-0174). PO-0174 is currently in the engineering and design phase and will provide approximately 13 miles of oyster barrier reefs. This project has an estimated cost of $57.7 million and is funded by the Resources and Ecosystems Sustainability, Tourist Opportunities and Revived Economies of the Gulf Coast States Act of 2012 (RESTORE Act).

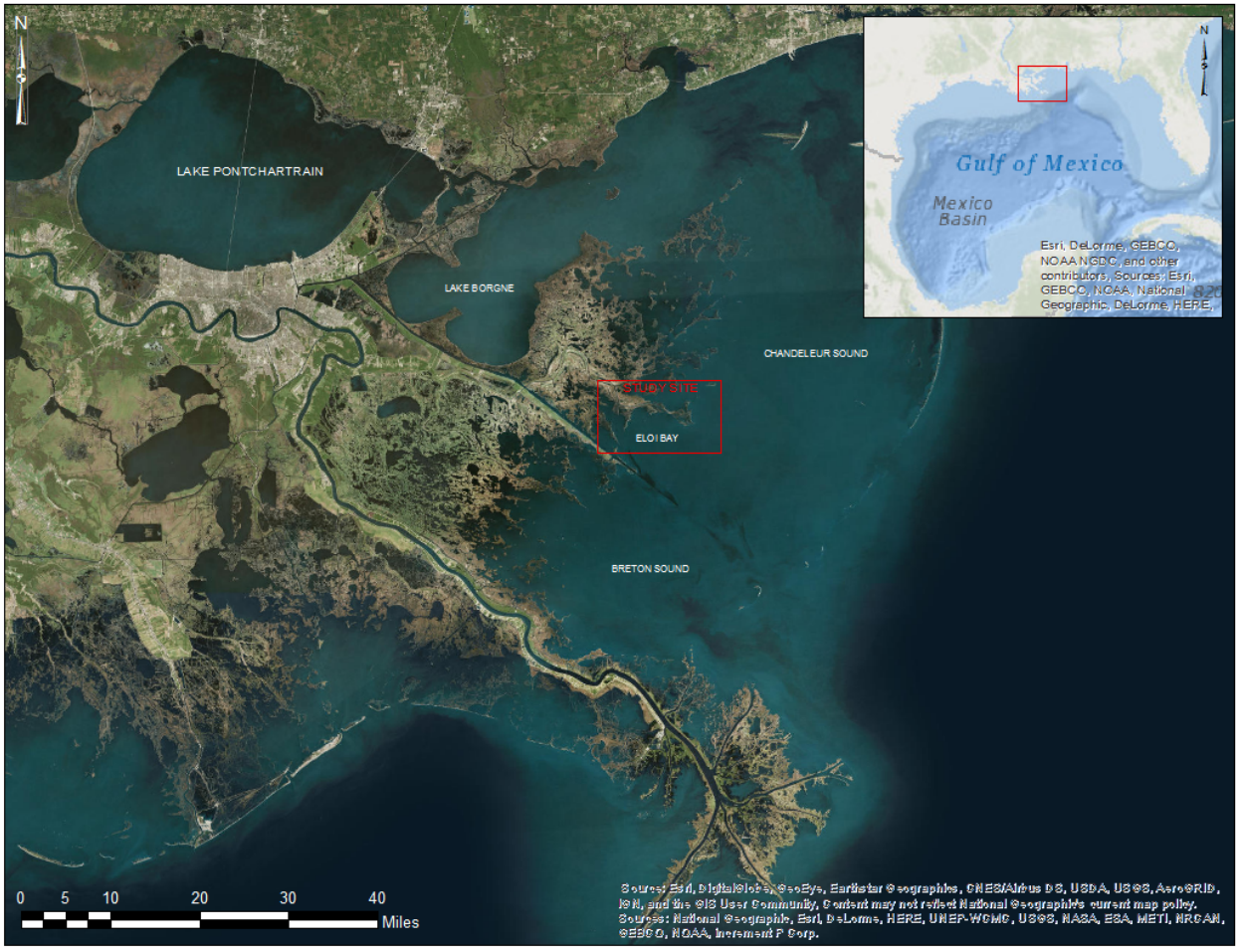

Figure 1.3: Study site vicinity map.

Figure 1.4: PO-148 shoreline protection structures (photo credits: OysterBreak – Wayfarer Environmental Technologies; WAD - Mott MacDonald; Reef Ball - Tetra Tech, Inc.; ReefBlk - Beth Maynor Young, 2010; ShoreJax - ACF Environmental. Sketches: Coast and Harbor Engineering, 2015).

1.3 OBJECTIVES

Performance characteristics of constructed oyster reef breakwaters are limited due to the relatively recent implementation of these structures as a means of shoreline protection. Engineers and stakeholders are still experimenting and studying the most productive and cost effective methods to construct each of the different structure types to maximize shoreline protection while also providing a substrate for oyster accruement. There is limited data on the shoreline protection

benefits of oyster reef breakwaters. The objective of this research is to quantify shoreline protection of these structures by determining the transmission coefficients of the oyster reef breakwaters constructed for the Living Shoreline Demonstration Project (PO-148). This is accomplished through data analysis of in-situ wave measurements using bottom-mounted pressure gauges.

2. LITERATURE REVIEW

2.1 WAVE CLIMATE IN ESTUARIES

A Coastal Engineering and Alternatives Analysis was conducted by Coast and Harbor Engineering (CHE, 2014) for PO-148 to develop an understanding of water level and wave conditions at the project site. Water surface elevation (WSEL), wind, and wave data were selected from stations in the project vicinity for coastal processes analysis. Available meteorological data stations in the project vicinity were described in the Data Collection Summary and New Data Collection Plan Technical Memorandum (CHE, 2013) and shown in Figure 2.1. Measured wind and wave data were obtained from the National Oceanic and Atmospheric Administration's (NOAA) National Data Buoy Center (NDBC) stations (NOAA, 2012) shown as green points in Figure 2.1. Wind and wave data produced from hindcast models were obtained from the USACE Wave Information Studies stations (WIS, 2012) shown as yellow points in Figure 2.1.

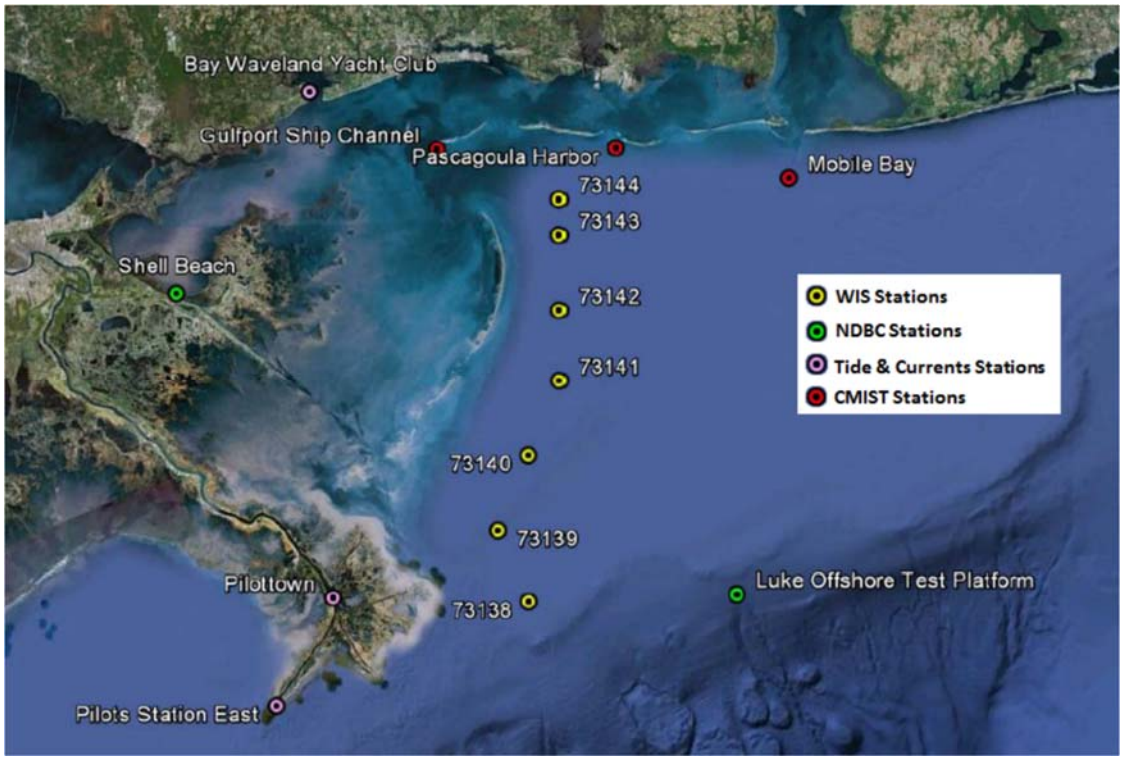

Figure 2.1: Available meteorological data stations near the project site (CHE, 2013).

Tidal elevations for the project site were established by CHE using NOAA's VDatum software (NOAA, 2013) and are listed in Table 2.1.

Table 2.1: Tidal datums at project site and Bay Waveland (CHE, 2014).

Water Level	Project Site (feet) (NAVD88)	Bay Waveland (feet) (NAVD88)
Mean Higher-High Water (MHHW)	1.32	1.42
Mean High Water (MHW)	1.28	1.32
Mean Sea Level (MSL)	0.60	0.56
Mean Low Water (MLW)	-0.13	-0.20
Mean Lower-Low Water (MLLW)	-0.19	-0.31

Tidal elevations were also obtained by CHE for the Bay Waveland Yacht Club station (Tides and Currents, 2013) for comparative purposes. An extreme value analysis was performed by CHE using the Bay Waveland Yacht Club station data to provide anticipated water level estimates during extreme events. These results are summarized in Table 2.2.

Table 2.2: Extreme value analysis for water surface elevation (CHE, 2014).

Return Period (years)	Water Surface Elevation (feet) (NAVD88)
1	4.3
2	5.6
5	7.8
10	9.8
25	12.8

Wave roses of WIS Station 73141 developed by CHE are shown in Figure 2.2. Wave heights were sorted by summer months, April-September (Figure 2.2, a), winter months, October-March (Figure 2.2, b), all months (Figure 2.2, c), and winter months having wave height ≥ 8 ft. (Figure 2.2, d).

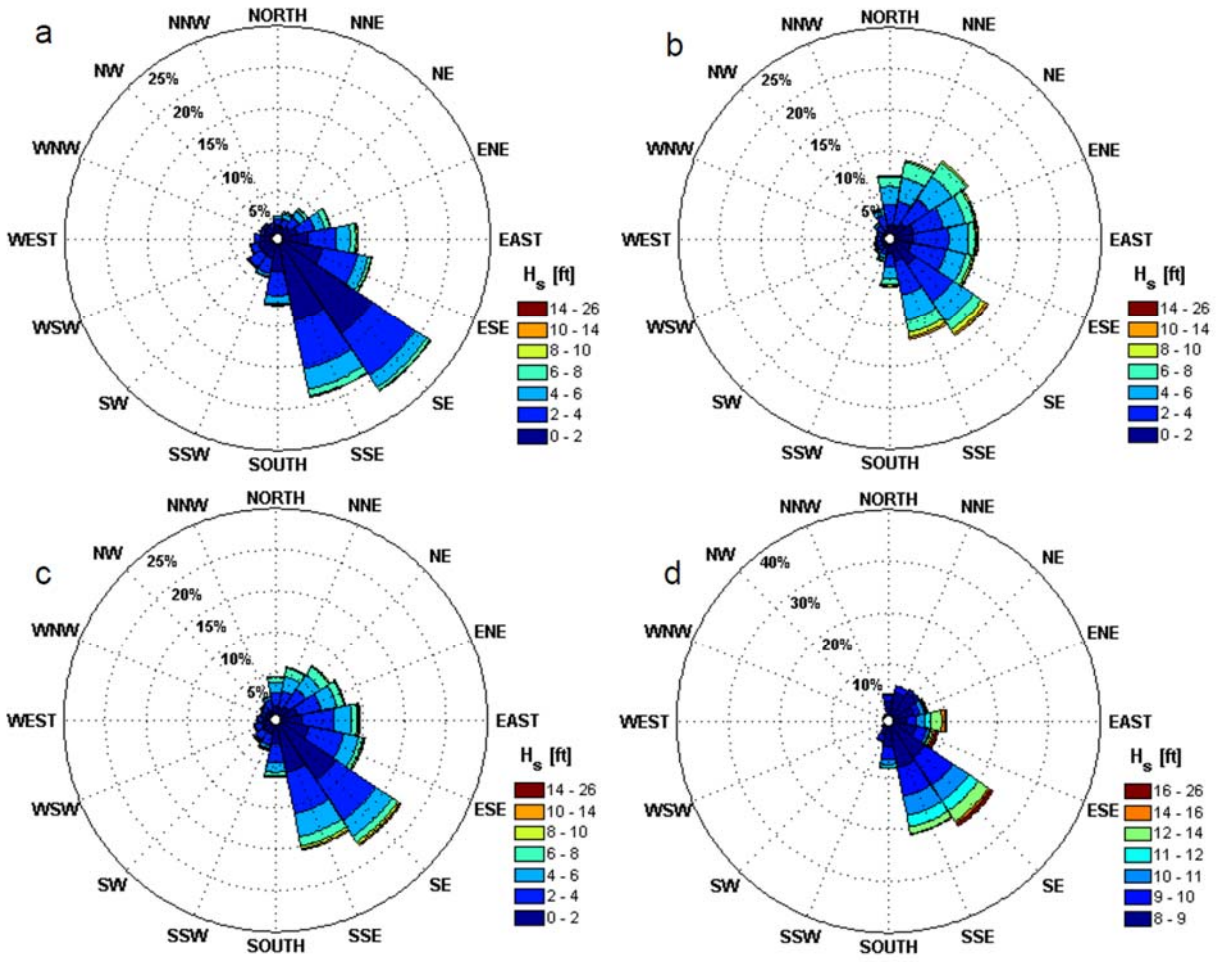

Figure 2.2: Wave roses for WIS Station 73141 (a) summer months, (b) winter months, (c) winter months, and (d) winter waves ≥ 8 ft. [NOTE: (d) is on a different radial scale] (CHE, 2014).

WIS Station 73141 wave data were analyzed by CHE to produce monthly and general wave statistics shown in Table 2.3. An extreme value analysis was conducted by CHE to determine extreme wave heights and corresponding wave period. The wave period was correlated to the extreme wave height through a joint wave height – wave period distribution (CHE, 2014). The results of the extreme value analysis of wave heights are shown in Table 2.4.

Table 2.3: Monthly statistics of significant wave height and peak wave period at WIS Station 73141 (CHE, 2014).

Month	Mean H_s (feet)	Range of H_s Min – Max (feet)	Standard Deviation H_s (feet)	Mean T_p (sec)	Maximum T_p (sec)	Standard Deviation T_p (sec)	Mean Wave Direction (deg TN)
Jan	3.8	0 – 15.5	2.2	5.1	11.1	1.4	86
Feb	4.0	0 – 17.1	2.3	5.2	11.1	1.5	100
March	3.8	0 – 13.8	2.2	5.3	11.1	1.6	121
April	3.5	0 – 10.8	1.9	5.1	10.0	1.4	127
May	2.7	0 – 12.3	1.6	4.7	10.0	1.1	134
June	2.3	0.2 – 10.4	1.5	4.5	11.1	1.2	151
July	1.7	0.1 – 16.1	1.2	4.0	10.0	1.0	164
Aug	1.8	0.1 – 18.7	1.5	4.1	15.0	1.2	137
Sept	2.8	0.1 – 26.4	2.2	4.7	14.3	1.5	103
Oct	3.5	0 – 21.9	2.3	5.0	16.7	1.7	81
Nov	3.9	0 – 17.4	2.1	5.1	15.0	1.4	87
Dec	3.9	0 – 14.3	2.1	5.1	12.5	1.3	89
Overall	3.1	0 – 26.4	2.1	4.8	3.3 – 16.7	1.4	116

Table 2.4: Extreme value analysis of wave heights at WIS Station 73141 (CHE, 2014).

Return Period (years)	Significant Wave Height, H_s (feet)	Peak Wave Period, T_p (sec)
1	13.3	9.2
2	15.4	10.0
5	18.6	11.2
10	21.1	12.1
25	24.7	13.4
50	27.5	14.4

WIS Station 73141 does not accurately represent wave conditions at the study site due to its location in the Gulf of Mexico, offshore of the barrier islands. CHE performed wind wave generation and transformation modeling for the project vicinity to determine wave characteristics at the shoreline. This was conducted using the two-dimensional SWAN (Simulating Waves Nearshore) model, which utilizes bathymetry, incident wave spectra, and local wind conditions to generate and transform waves into the nearshore environment (CHE, 2014). Wave transformation from WIS Station 73141 to the project site was modeled for average conditions and storm

conditions. Figure 2.3 shows the modeling results for average conditions from the northeast direction. The SWAN model was also used to transform a time series of waves from the WIS station to the nearshore region from 1980 – 2012, where wave height, period, and direction were extracted. A transfer function was developed between the WIS input and the nearshore results to generate the full time series along the project shoreline. Figure 2.4 shows the long-term average significant wave height and peak wave period at the -4.5 ft (NAVD88) contour (CHE, 2014). This model was not validated with in-situ wave measurements at the study site.

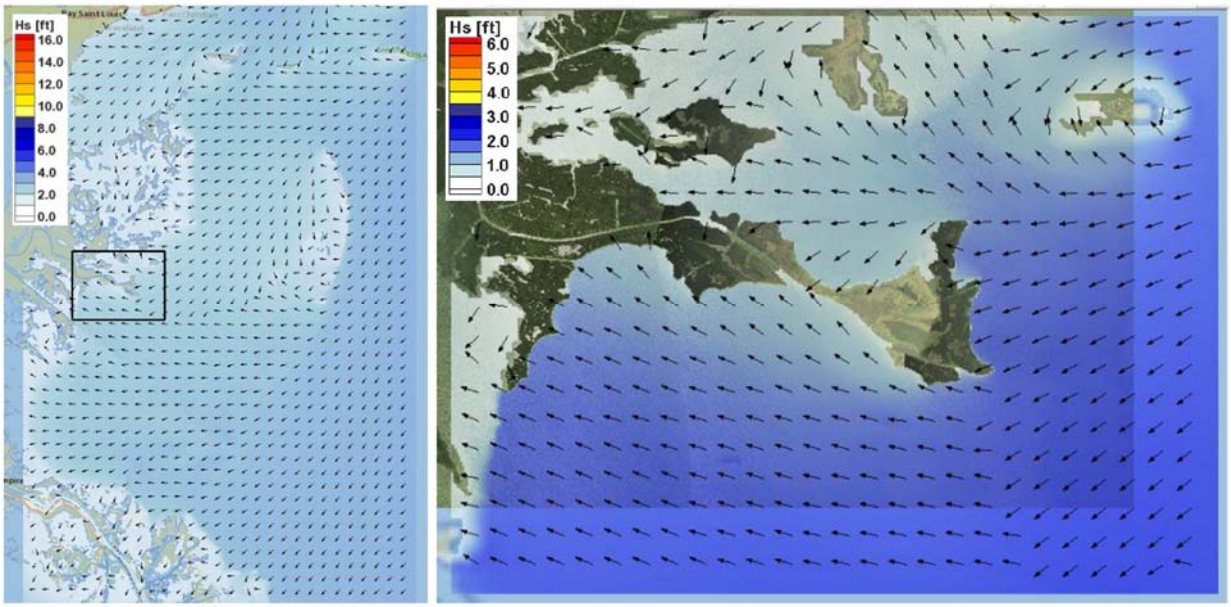

Figure 2.3: Wave heights results from the SWAN model for average conditions from northeast; (left) offshore grid, (right) nearshore grid (CHE, 2014).

Wave parameters can be calculated using parametric wave hindcasting models. Parametric wave hindcasting determines wave height (H) and wave period (T) from fetch (F), wind duration (t), and depth of water (d). The JONSWAP method of wave hindcasting models wave properties in deep water (Hasselmann et al., 1973). Young and Verhagen (1996) developed commonly used equations for depth and fetch limited wave parameters:

$$H_{m0}^{*} = 0.24\left\{\tanh[0.49(d^{*})^{0.75}]\tanh\left[\frac{0.0031(F^{*})^{0.57}}{\tanh[\,0.49(d^{*})^{0.75}]}\right]\right\}^{0.87} \quad (1)$$

$$T_{p}^{*} = 7.54\left\{\tanh[0.33(d^{*})]\tanh\left[\frac{0.00052(F^{*})^{0.73}}{\tanh[\,0.33(d^{*})]}\right]\right\}^{0.37} \quad (2)$$

where H_{m0}^{*} is the dimensionless zero-moment wave height, T_{p}^{*} is the dimensionless peak wave period, d^{*} is the dimensionless depth, and F^{*} is the dimensionless fetch.

$$H_{m0}^{*} = \frac{gH_{m0}}{U_{10}^{2}} \quad (3)$$

$$T_{p}^{*} = \frac{gT_{p}}{U_{10}} \quad (4)$$

$$d^{*} = \frac{g\bar{d}}{U_{10}^{2}} \quad (5)$$

$$F^{*} = \frac{gF}{U_{10}^{2}} \quad (6)$$

$$\bar{d} = \frac{1}{x}\int_{0}^{x} d_{x}(x)dx \quad (7)$$

$$\overline{U}_{10} = \frac{1}{x}\int_{0}^{x} U_{10}(x)dx \quad (8)$$

where g is the acceleration of gravity, $\overline{U}_{10}$ is the wind velocity at 10 meters above the water surface averaged over the fetch, and $\bar{d}$ is the average water depth along the fetch. The formulas developed by Young and Verhagen (1996) are applicable for shallow coastal estuaries and bays because of the depth and fetch limited parameters.

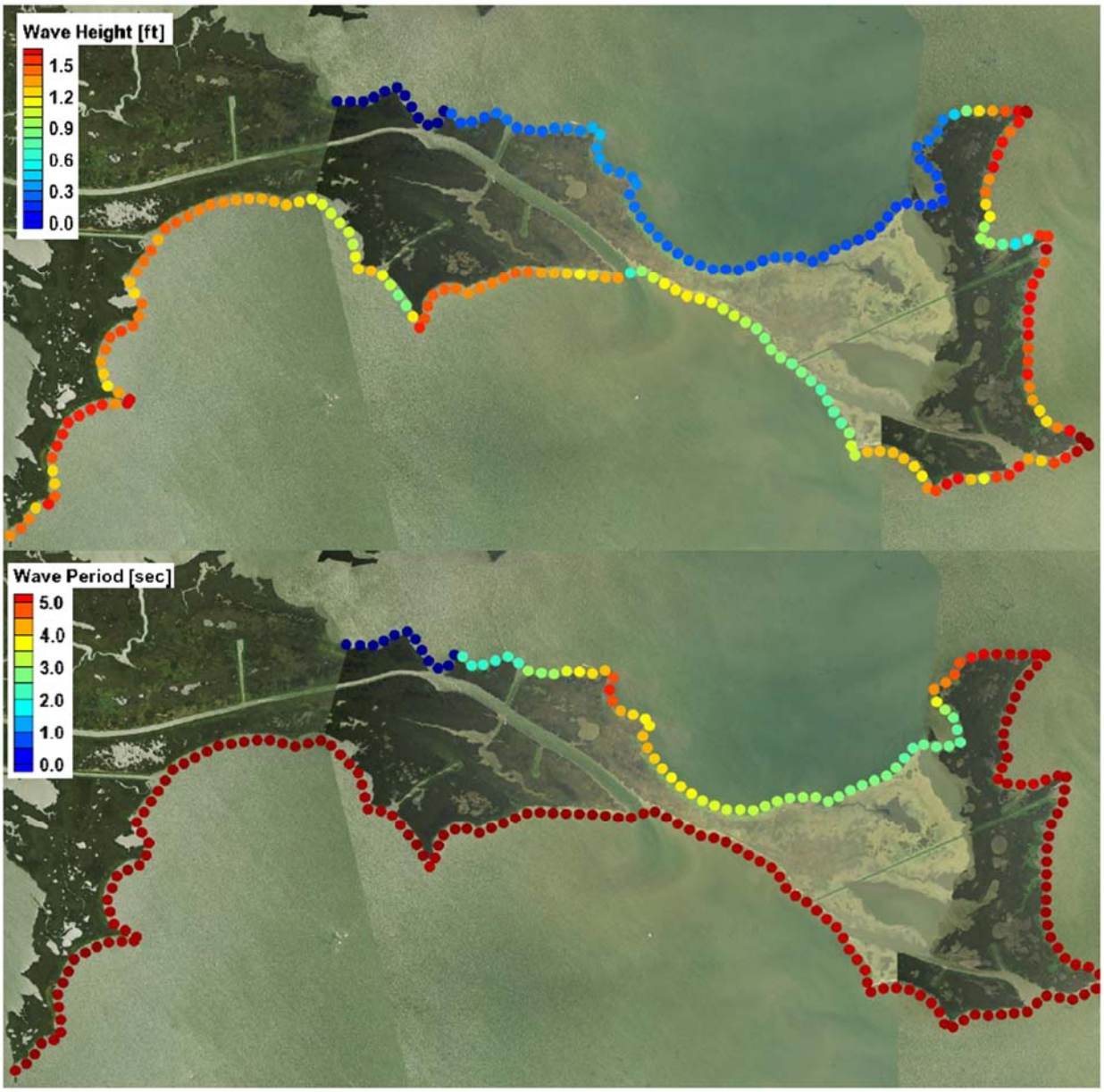

Figure 2.4: Average (top) wave heights and (bottom) peak wave periods as computed by the SWAN model from 1980-2012 (CHE, 2014).

Studies have shown that wind wave energy in wetland dominated estuaries can accelerate wetland loss rates (Karimpour et al., 2016; Marani et al., 2011). Karimpour et al. (2017) developed a set of parametric wave growth equations that demonstrate wave growth rate in shallow estuaries as a function of wind fetch to water depth ratio:

$$\hat{k}_p\hat{h} = 1.363\left(\tanh\left(3.356\hat{h}\right)\right)^{0.315} \leq 1.363 \quad (9)$$

$$\hat{k}_p\hat{h} = \frac{1}{1.14641}\tan^{-1}\left(\frac{\hat{E}}{3\times10^{-5}}\right) \leq 1.363 \quad (10)$$

for $\hat{E} \leq 3.64 \times 10^{-3}$; where $\hat{k}_p$ is dimensionless peak wave number, $\hat{h}$ is dimensionless water depth, and $\hat{E}$ is dimensionless wave energy.

Leonardi et al. (2016) determined a linear relationship between wind wave energy and salt marsh response with no critical threshold in wave energy above which salt marsh erosion drastically accelerates. They found that violent tropical storms contribute less than 1% to long-term salt marsh erosion rates and moderate storms with a return period of 2.5 months cause the most marsh deterioration. This shows that salt marshes are very susceptible to above average wind produced waves.

2.2 OYSTER REEFS AS BREAKWATERS

Eastern oysters (*Crassostrea virginica)* are important to Louisiana's coastal ecosystem because of the many ecosystem services they provide (Coen et al., 2007). The shell reefs created by oysters provide unique, structurally complex habitat that supports distinct and diverse aquatic communities, functions as nursery habitat for many fish and shellfish species, and enhances local productivity (Soniat et al., 2004; Plunket and La Peyre, 2005; Schyphers et al., 2011). Oyster reefs can improve recreational fisheries by providing valuable foraging sites for transient, predatory fishes such as flounder, drum, and speckled trout (Plunket and La Peyre, 2005; Schyphers et al., 2011). Oysters also enhance water quality by filtering large volumes of water daily to feed. By removing large amounts of carbon, phosphorus, and nitrogen incorporated into phytoplankton biomass, oysters can mitigate nutrient loading and help prevent eutrophication and hypoxia (Wall

et al., 2011). It is estimated that 85% of the filtration capacity of oysters in the United States has been lost in the past century (Zu Ermagassen et al., 2012).

Oyster reefs are frequently found near the marsh edge, and the vertical structure serves to attenuate wave energies and reduce water velocities resulting in reduced erosion as well as increased sediment deposition behind the reef, both of which act to stabilize the shoreline (Campbell, 2004; Piazza et al., 2005). With adequate oyster recruitment and survival over time, living oyster reefs can promote continuous three-dimensional reef growth. The potential for oyster reefs to be self-sustaining shoreline protection structures can make them a preferable alternative to traditional shoreline structures such as rubble mound breakwaters, which are unnatural and require maintenance to combat settlement and sea level rise.

Bioengineered oyster reefs, which are man-made structures designed to promote the formation of marsh-fringing oyster reefs, have been implemented in many locations in Louisiana (Furlong, 2012; La Peyre et al., 2013). Although most of these projects have been constructed too recently to determine their long term effectiveness, those that have been monitored have shown they can significantly reduce shoreline recession while also supporting adequate oyster recruitment and survival such that the reefs may be sustainable (Piazza et al., 2005; Melancon et al., 2013).

Oyster reefs may be a preferable method of shoreline protection in south Louisiana for several reasons: it is native to the area, it is lighter than traditional materials (e.g. limestone), it is conducive to oyster spat production and growth, it has potential for sustainability, and it can support aquatic wildlife.

2.3 WAVE TRANSMISSION AND ATTENUATION BY BREAKWATERS

Several studies have been conducted to measure the transmission and attenuation of waves by breakwaters. Wave attenuation is described by the wave transmission coefficient, K_t (Jeffreys, 1994):

$$K_t = \frac{H_t}{H_i} \tag{11}$$

where H_t is the transmitted wave height and H_i is the incident wave height.

Wave transmission can be characterized as a function of non-dimensional ratios of structure geometry and hydrodynamic parameters (Goda et al., 1967):

$$K_t = f\left(\frac{R_c}{H_i}, \frac{B}{h_i}, \frac{h_c}{h_i}, \frac{h_i}{L_i}, \frac{H_i}{h_i}\right) \tag{12}$$

where R_c is the structure crest freeboard, B is the crest width, h_i is the water depth, h_c is the structure crest height above the bottom, and L_i is the incident wavelength.

Seelig (1980) conducted two-dimensional laboratory tests on smooth impermeable breakwaters, rubble mound breakwaters, and breakwaters armored with dolos units. Seelig (1980) developed empirical equations for smooth and impermeable sloped breakwaters using the runup prediction equation developed by Franzius (1965):

$$R = \overline{H_i} C_1 \left(0.123 \frac{L_i}{\overline{H_i}}\right)^{\left(C_2\sqrt{\overline{H_i}/h_i} + C_3\right)} \tag{13}$$

$$\overline{H_i} = 0.63 H_i \tag{14}$$

where R is the runup, $\overline{H_i}$ is the mean wave height, H_i is the incident significant wave height at the breakwater seaward toe, L_i is the wavelength, and h_i is the water depth. C_1, C_2, and C_3 are empirical coefficients which can be linearly interpolated. The recommended values of the empirical coefficients are given in Table 2.5.

Table 2.5: Empirical wave runup prediction coefficients for smooth impermeable slopes (Seelig, 1980).

Front-face slope of breakwater	C_1	C_2	C_3
Vertical	0.958	0.228	0.0578
1:0.5	1.280	0.390	-0.091
1:1	1.469	0.346	-0.105
1:1.5	1.991	0.498	-0.185
1:2.25	1.811	0.469	-0.080
1:3	1.366	0.512	0.040

$$K_t = C\left(1 - \frac{R_c}{R}\right) \tag{15}$$

$$C = 0.51 - 0.11\left(\frac{B}{h_c}\right) \tag{16}$$

where K_t is the transmission coefficient with a minimum value of 0 and a maximum value of 1. C is the empirical coefficient, R_c is the crest freeboard, B is the crest width, and h_c is the height of the breakwater. For C, the term $\left(\frac{B}{h_c}\right)$ has a maximum value of 0.86 due to the data set analyzed by Seelig (1980).

van der Meer et al. (2005) focused on wave transmission at low-crested structures. The primary parameters describing wave transmission are identified in Table 2.6 and shown in Figure 2.5. van der Meer et al. (2005) developed an empirical transmission coefficient equation for rough and permeable breakwaters:

$$K_t = -0.4\frac{R_c}{H_i} + 0.64\left(\frac{B}{H_i}\right)^{-0.31}\left(1 - e^{-0.5\xi_{op}}\right) \tag{17}$$

with a minimum K_t = 0.075 and a maximum K_t = 0.8 [0.75, van der Meer and Daemen (1994)].

van der Meer et al. (2005) developed an empirical transmission coefficient equation for smooth and impermeable sloped breakwaters:

$$K_t = \left[-0.3\frac{R_c}{H_i} + 0.75\left(1 - e^{-0.5\xi_{op}}\right)\right]\cos^{\frac{2}{3}}\beta \tag{18}$$

with a minimum K_t = 0.075 and a maximum K_t = 0.8, and limitations: $1 < \xi_{op} < 3$; $0° < \beta < 70°$; $1 < \frac{B}{H_i} < 4$.

Table 2.6: Governing parameters of wave transmission (van der Meer et al., 2005).

Wave Transmission Parameter Definitions	
H_i	incident significant wave height, preferably H_{m0i}, at the seaward toe of the structure
H_t	transmitted significant wave height, preferably H_{m0t}
T_p	peak period
s_{op}	wave steepness, $s_{op} = \frac{2\pi H_i}{gT_p^2}$
R_c	crest freeboard
h_c	structure height
B	crest width
D_{n50}	nominal diameter of armour rock (rubble mound structure)
K_t	transmission coefficient $\frac{H_t}{H_i}$
ξ_{op}	breaker parameter $\xi_{op} = \frac{\tan\alpha}{(s_{op})^{0.5}}$
$\tan\alpha$	seaward slope of structure
β	angle of incidence

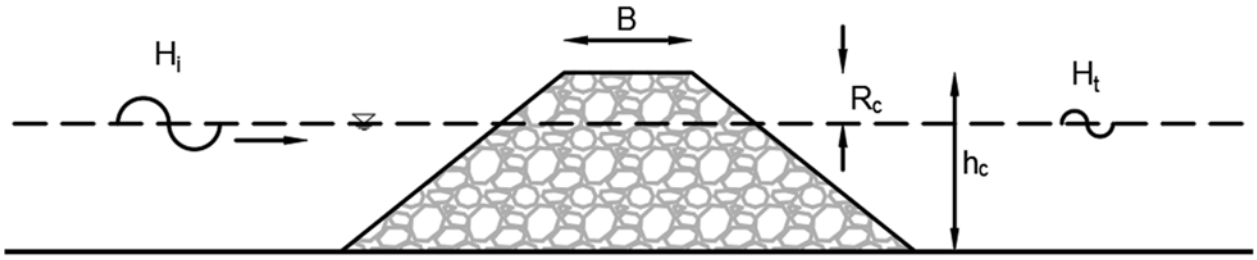

Figure 2.5: Governing parameters for wave transmission calculations.

The Seelig (1980) experiments were conducted on regular waves and used mean wave height while van der Meer et al. (2005) considered random waves and used significant wave height. The equations proposed by van der Meer et al. (2005) have been used to predict wave transmission coefficients for engineering calculation (e.g. Chen et al. 2014).

Teh (2013) developed empirical equations for wave transmission of free surface semicircular breakwaters (SCB). Sharma et al. (2016) concluded that wave attenuation units (WAUs) were effective at mitigating erosion in the northern Gulf of Mexico. Geometry based wave transmission calculations are used for the engineering and design of breakwaters as referenced in the USACE Coastal Engineering Manual (USACE, 2008).

Buccino and Calabrese (2007) developed a semi-empirical model to predict wave transmission of low-crested, detached breakwaters for a wide range of engineering conditions. CHE (2014) used the Buccino and Calabrese method for average wave conditions modeled at the PO-148 project site (H_s = 1.6 ft, T_p = 5 sec) to determine the baseline geometry that will reduce wave transmission by 50%. Results of this analysis are shown in Figure 2.6.

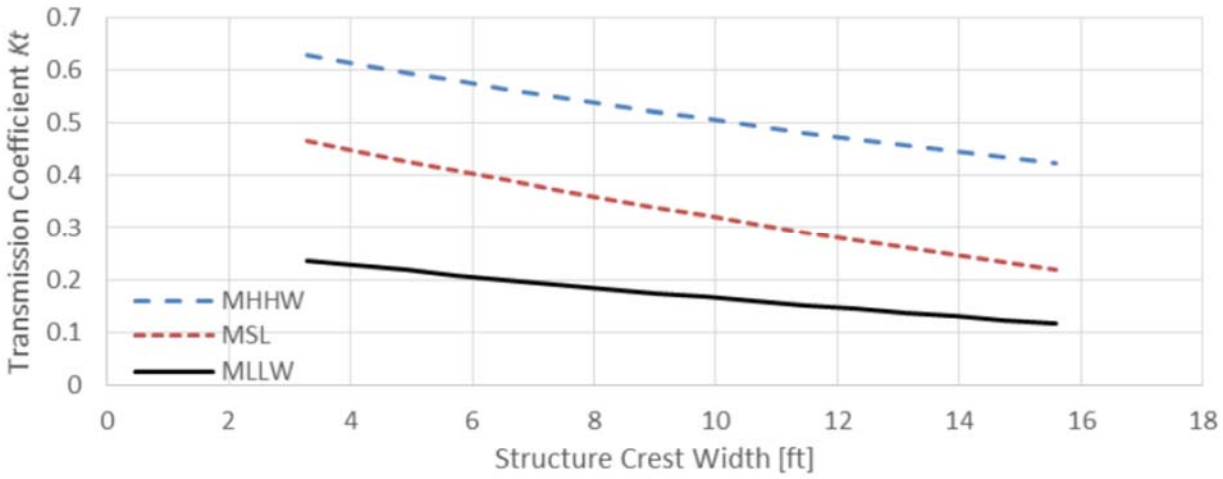

Figure 2.6: Wave transmission as a function of crest width and water level for average wave conditions (CHE, 2014).

Several studies and publications discuss wave transmission of rubble mound breakwaters; however, there is little literature on wave transmission of oyster reef breakwaters such as the products constructed for PO-148. Webb and Allen (2015) conducted scaled laboratory experiments to measure wave transmission behind bagged oyster shell breakwaters, concrete wave transmission

frustums (WTF), and ReefBLK units. The results revealed strong correlations between wave transmission and simple, dimensionless parameters; however, existing methods for estimating wave transmission through rubble mound structures did not provide accurate estimates for these structures (Webb and Allen, 2015). Empirical equations to estimate wave transmission coefficients based on the laboratory experiments were not found in the literature.

CHE (2014) modeled wave transmission through the PO-148 structure alternatives using FLOW-3D, a computational fluid dynamics (CFD) software program. Figure 2.7 shows a series of CFD model frames displaying wave transmission for the OysterBreak and Reef Ball breakwaters (Carter et al., 2015).

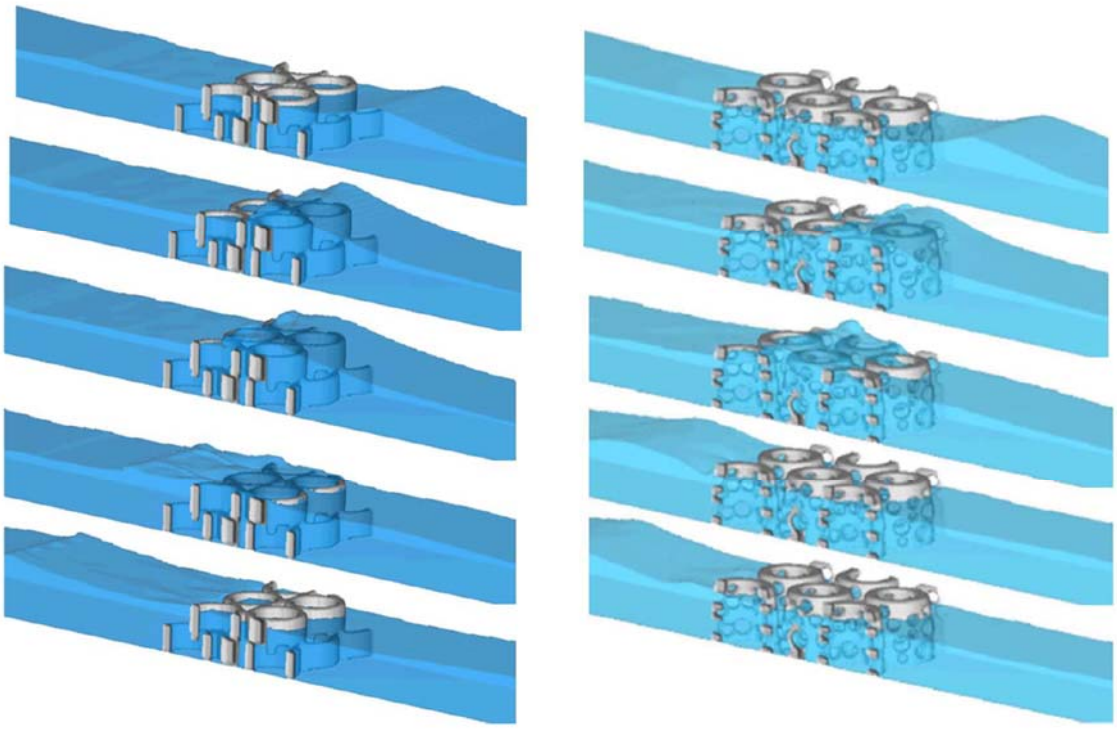

Figure 2.7: FLOW-3D computation of waves interacting with OysterBreaks (left) and Reef Balls (right) over one wave phase (Carter et al., 2015).

Wave transmission results computed using the CFD model were plotted and compared to transmission coefficients computed by the Buccino and Calabrese (2007) method for a structure

with similar geometry but no porosity (i.e. transmission through the structure was not included in the empirical method; all transmission is the result of overtopping) (CHE, 2014). The results show that all structures used for PO-148 are more porous than a rubble mound structure. They were also compared to CIRIA's (2007) rule of thumb for wave transmission of rubble mound structures. The results indicate that all PO-148 structures have higher transmission rates compared to the rule of thumb (CHE, 2014). However, there are no field measurements nor reliable empirical equations for the prediction of wave transmission through oyster breakwater structures. The objective of this study is to fill this knowledge gap.

3. DATA COLLECTION

3.1 EXPERIMENTAL DESIGN

Wave attenuation of the oyster reef breakwaters constructed for the Living Shoreline Demonstration Project (PO-148) was investigated for this study. The breakwater structure types investigated include Oysterbreaks, WADs, and Reef Balls (Types 1 and 2). Seven wave gauges were deployed from 21 November 2017 to 14 February 2018 to measure the wave characteristics on the unprotected and protected sides of the structures. Two water surface elevation (WSEL) gauges were deployed from 21 September 2017 to 14 February 2018 to measure water levels at the study site. Topographic and bathymetric surveys were conducted on 12 – 13 December 2018 and 15 January 2018 along cross-shore transects corresponding with the wave gauge locations. Table 3.1 provides a summary of the instruments used for data collection. Table 3.2 lists the instruments sampling settings. The instruments and deployments are described in further detail in sections 3.2.2 and 3.2.3. An overview of the study site with the wave gauge locations, WSEL gauge locations, survey transects, and PO-148 as-built structures is shown in Figure 3.1.

Table 3.1: Data collection instruments summary.

Gauge	Instrument	# of Units	Output Parameters
WSEL Gauge (001 & 002)	YSI 600LS Level Sonde	2	Water Level
Wave Gauge (501 – 507)	Wave Gauge OSSI-010-003C	7	Wave Height, H_{m0} Peak Wave Period, T_p Water Depth, h

Table 3.2: Data collection instruments sampling settings.

Gauge	Instrument	Sampling Interval (min)	Sampling Duration (min)	Sampling Frequency (Hz)	Sampling Parameter
WSEL Gauge (001 - 002)	YSI 600LS Level Sonde	15	-	-	Water Level (ft)
Wave Gauge (501 – 507)	Wave Gauge OSSI-010-003C	30	20	10	Pressure (bar)

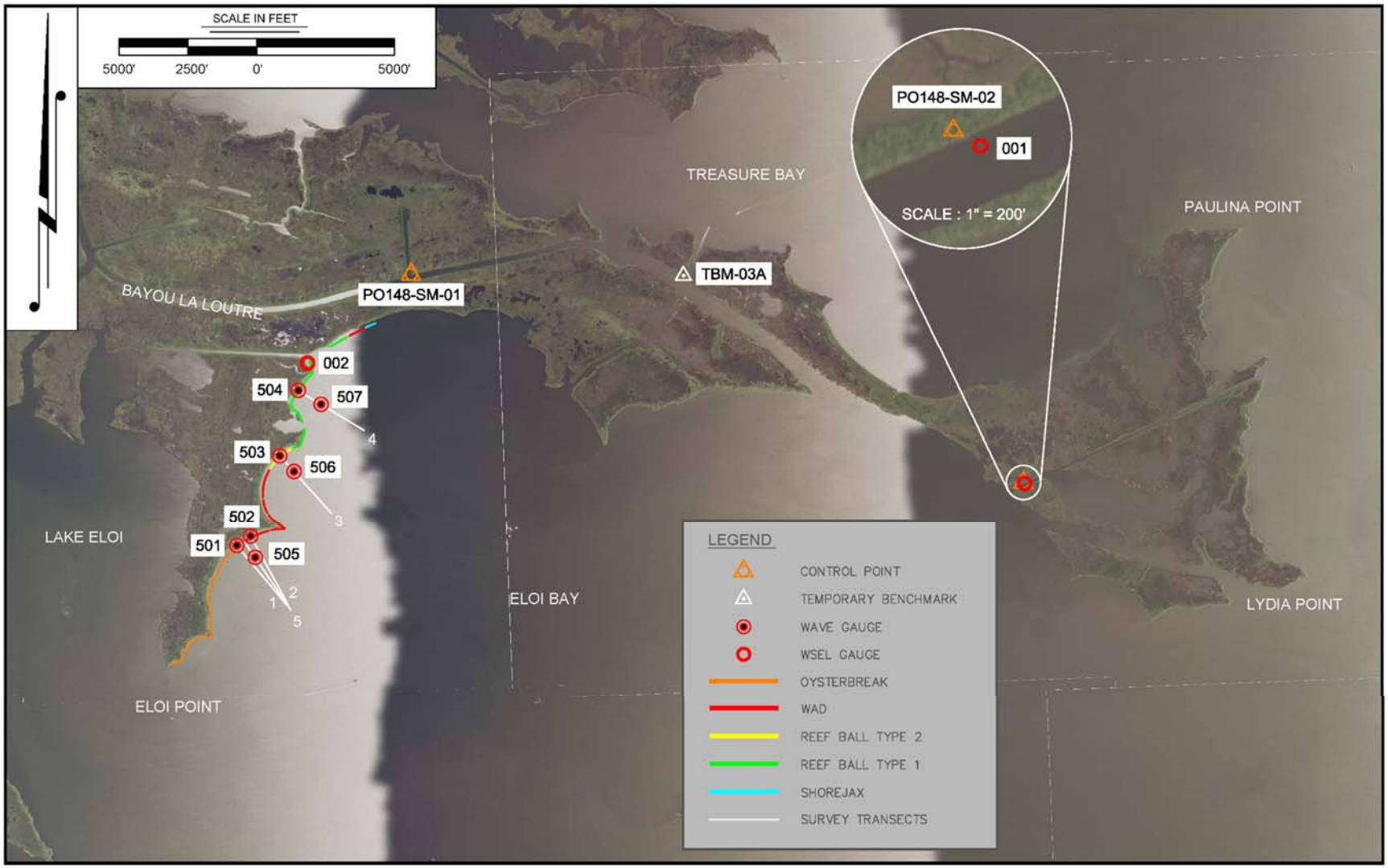

Figure 3.1: Study site overview depicting survey benchmarks, survey transects, gauges, and PO-148 as-built breakwater structures.

3.2 INSTRUMENTATION AND METHODOLOGY

3.2.1 Surveys

Survey data were collected using a Trimble R10 GNSS (Global Navigation Satellite System). This system includes a Trimble TSC3 controller and two Trimble R10 receivers. One R10 receiver is used for a base station and the other as a rover unit. This system is referred to as a RTK GPS (Real Time Kinematic Global Positioning System) unit. Equipment datasheets are located in Appendix A. All survey data were recorded using established control from CPRA secondary benchmarks PO148-SM-01 and PO148-SM-02. The established horizontal datum for the benchmarks is U.S. State Plane 1983, Louisiana South Zone (1702) North American Datum of 1983 (NAD83), U.S. survey feet. The vertical datum is North American Vertical Datum of 1988 (NAVD88) (Geoid 12A). Survey benchmark datasheets for PO148-SM-01 and PO148-SM-02 are located in Appendix B.

The RTK base station was set up on the secondary benchmark PO148-SM-01 or PO148-SM-02 and used to transmit real time corrections to the rover unit, where horizontal and vertical positions were established (see Figure 3.2 showing the base station setup). The rover unit was used to collect topographic point data. For quality assurance and quality control (QA/QC) purposes, the positions of the secondary benchmark and field data collected were verified by checking into the other CPRA secondary benchmark or the temporary benchmark (TBM), “TBM-03A”.

Bathymetric survey data were collected using an Odom Hydrotrac single frequency echo-sounder (datasheet located in Appendix A) interfaced with HYPACK hydrographic survey software in conjunction with the RTK GPS unit previously mentioned. HYPACK receives real-time position data from the RTK GPS rover unit and digital water depth data from the echo-sounder. HYPACK uses this data to establish real time tide corrections and computes centimeter

level positioning of each sounding. The software accounts for heave, pitch, and roll of the survey vessel and displays course corrections to help the surveyor navigate the predefined track lines.

Figure 3.2: Setup of RTK GPS base station on secondary benchmark PO148-SM-01 on 14 February 2018.

The digital echo-sounder was calibrated for sound velocity, draft, and index corrections. This was accomplished utilizing the bar check method of lowering an acoustic target, with precisely measured marks, below the transducer to various depths. The sound velocity, draft, and

index were then adjusted so that the echo-sounder reads the precise depth of the acoustic target. The tide corrections of the onboard GPS system were checked by comparing top of water elevations to the real-time tide corrections in HYPACK. Bathymetric survey data was transferred from the onboard laptop computer to the office for processing.

Topographic and bathymetric surveys were performed along five transects in line with the location of the wave gauges (see Figure 3.1 for transect locations). The survey transects and the wave gauge locations were chosen to align with as-built survey transects previously completed for the Living Shoreline Demonstration Project (PO-148). Each survey transect is 3000 feet in length. Topographic survey data was collected by a T. Baker Smith, LLC (TBS) survey crew from 13 to 14 December 2017. The crew accessed the site using a 24-foot survey vessel with dual outboards. Bathymetric survey data was collected on 15 January 2018 using a 24-foot survey vessel with dual outboards. All survey field notes are located in Appendix C.

3.2.2 Water Surface Elevation (WSEL) Gauges

Two water surface elevation (WSEL) gauges were installed to collect water level data at the study site. Water levels were recorded using an YSI 600LS Water Level Sonde. The sonde has a differential strain gauge transducer to measure pressure. One side of the transducer is exposed to the water while the other side is vented to the atmosphere. The vent allows the transducer to measure only the pressure exerted by the water column. Atmospheric pressure is ignored and changes in atmospheric pressure do not affect the reading (YSI, 2012). The YSI 650 Multiparameter Display System (650 MDS) was used to calibrate, program, and deploy the sondes for unattended sampling. The sondes were calibrated according to the YSI 6 Series User manual (YSI, 2012). They were programed for unattended recordings of temperature, specific conductivity, salinity, and depths at 15 minute intervals. Figure 3.3 shows the YSI 600LS Water

Level Sonde and the YSI 650 MDS. The specification sheets for the YSI 600LS and the YSI 650 MDS are located in Appendix A.

Figure 3.3: YSI 600LS Water Level Sonde (left) and YSI 650 Multiparameter Display System (650 MDS) (right) (YSI, 2017).

Several factors were considered when choosing the two WSEL gauge locations, i.e., avoiding areas of potential obstructions to boat traffic, protection from waves, adequate water level, and accessibility. A few potential locations were selected based on a desktop review of the study site using aerial photography, and the two final locations were selected in the field. Some potential locations were eliminated in the field due to shallow water depths. WSEL Gauge 001 was installed in the pipeline canal near secondary benchmark PO148-SM-02. WSEL Gauge 002 was installed on the protected side of the Reef Balls (Type 1) where an oil and gas well canal meets the northwest portion of Eloi Bay. The locations of the WSEL gauges are indicated in Figure 3.1. Table 3.3 lists the locations and elevations of the WSEL gauges.

Table 3.3: WSEL gauge locations and elevations.

WSEL Gauge	Northing (ft., La. State Plane, NAD83)	Easting (ft., La. State Plane, NAD83)	Top of Lock Box (ft., NAVD88)	Sensor Elevation (ft., NAVD88)	Mudline (ft., NAVD88)
001	468737.00	3919756.11	4.72	-1.41	-3.7
002	473080.36	3893714.93	4.88	-1.37	-3.2

The water level sonde sits inside a fabricated aluminum housing. The housing consists of a vertical aluminum pipe that the sonde slides down and rests on the bottom. The pipe is open on one side at the bottom of the pipe to allow water to enter. The top of the pipe opens to a fabricated aluminum lock box where the excess field cable is stored. The aluminum housing was mounted to a 4 inch by 4 inch by 14 foot treated timber post. The timber post was manually hammered into the soil using a post driver. The sonde housing was then mounted to the post using stainless steel lag screws. The 4 inch by 4 inch post was additionally supported using two 2 inch by 2 inch timbers. A timber staff gauge was installed on the post and surveyed following CPRA standards (CPRA, 2016).

The WSEL gauges were deployed on 21 September 2017. On 21 November 2017, the gauges were checked, maintained, surveyed, and an attempt was made to download the data. At WSEL Gauge 002, the sonde and 650 MDS failed to connect and there appeared to be water damage at the sonde and field cable connection. The sonde at that location was replaced with another sonde and field cable. At WSEL Gauge 001, a connection was made between the sonde and the 650 MDS. However, the 650 MDS froze during the upload process and was unable to complete the upload. This sonde was returned to the housing to continue field recording. No data was uploaded during the 21 November 2017 site visit. On 15 January 2018, the gauges were again checked, maintained, and surveyed. The data from each sonde was uploaded directly to a laptop computer using the EcoWatch Lite software. On 14 February 2018, the sondes were retrieved and

the sonde housings were removed from the 4 inch by 4 inch timbers. The timbers and the staff gauges were left in place for future reference. Upon return from the field, the data were uploaded from each sonde using EcoWatch Lite. Figure 3.4 shows WSEL 002 after installation. All field notes pertaining to the deployment, maintenance, data download, and retrieval of the WSEL gauges are located in Appendix C.

Figure 3.4: WSEL Gauge 002 deployment on 21 September 2017.

3.2.3 Wave Gauges

Seven submersible wave gauges were deployed to measure wave properties at the study site. In-situ wave properties were recorded using Ocean Sensor Systems, Inc. Wave Gauge OSSI-

010-003C. The instrument is a tubular shape with a gauge pressure transducer located at the center of a circular cap on one side. The pressure transducer measures the total pressure, which is gauge pressure plus atmospheric pressure. The gauges were configured using the Ocean Sensor Systems Wave Gauge Interface software according to the OSSI-010-003 Wave Gauge User Manual (OSSI, 2015). The instrument stores data in units of bars to a removable compact flash card. Measurement data can be downloaded from the compact flash card using the interface software. The wave gauges were programed to collect data in the burst sampling mode; sampling one burst for 20 minutes at 30 minute intervals and at a 10 Hz sample rate. The wave gauges were secured in fabricated metal baseplates to allow for deployment on the water bottom with no movement or drift. Installation on the bay bottom allows the gauges to withstand high wave energy environments while recording water surface oscillations. Ropes were tied to the baseplates and a buoy attached on the tag end to allow for identification and recovery of the units. The gauge and baseplate housing are shown in Figure 3.5. The OSSI-010-003C datasheet is located in Appendix A.

Figure 3.5: Fabricated baseplates (top left); assembled baseplate and OSSI-010-003C Wave Gauge (bottom left); wave gauge secured in baseplate housing (right) (Parker, 2014).

Several factors were considered when selecting the locations of the wave gauges. Ideally, a control gauge is proposed to measure wave characteristics at the study site that are not influenced by the breakwaters. Due to the geomorphology of the PO-148 project shoreline and Eloi Bay, an acceptable location for a control site was not found. The bathymetry offshore of the structures in Eloi Bay differs greatly between the southwestern and northeastern extents of the study site. In addition, there is no satisfactory location along the project shoreline where a potential control gauge would not be impacted by wave reflection and diffraction caused by the breakwater structures. Due to the absence of a control site, the wave characteristics were measured on the unprotected and protected sides of the structures and consequently compared. The locations and orientations of the four different breakwater structures were also considered. Structures with similar orientations within the natural bights of the shoreline were chosen so waves propagate toward each structure type similarly. The locations of the wave gauges in relationship to the as-built PO-148 breakwater structures are shown in Figure 3.6.

The wave gauges were deployed and surveyed on 21 November 2017. The deployment duration was scheduled for one month; however, the meteorological conditions at the study site were also monitored to ensure that useful data would be collected. The criteria monitored included wind speeds above 15 knots and east to south wind directions (90 to 180 degrees). Meteorological data were acquired from NOAA station 8761305 Shell Beach, Louisiana (NOAA, 2018). The original one-month deployment was extended to over two and a half months to allow for at least four extended occurrences of the meteorological criteria. Figure 3.7 shows the instances where both criteria were met.

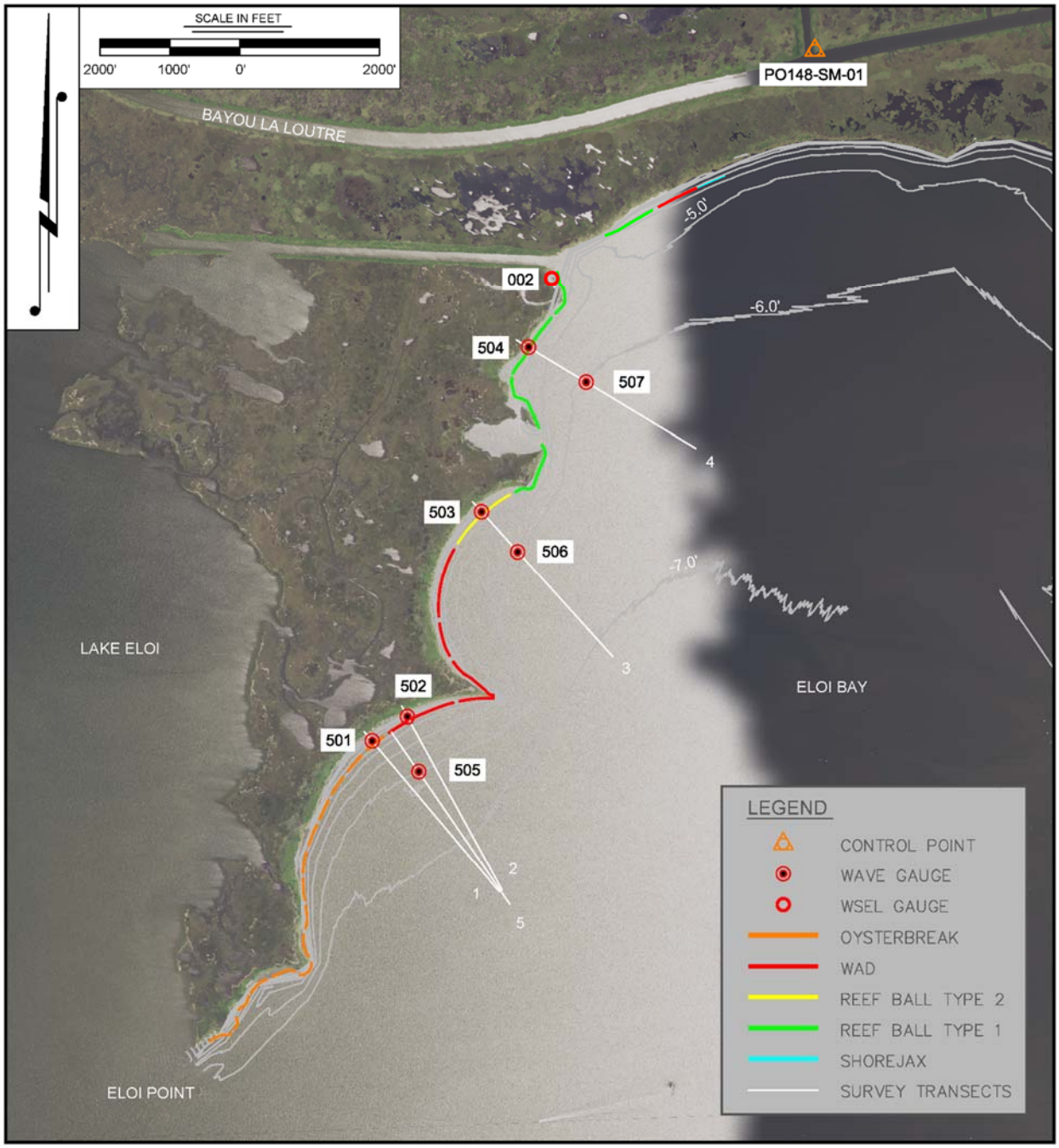

Figure 3.6: Wave gauge locations and PO-148 as-built structures.

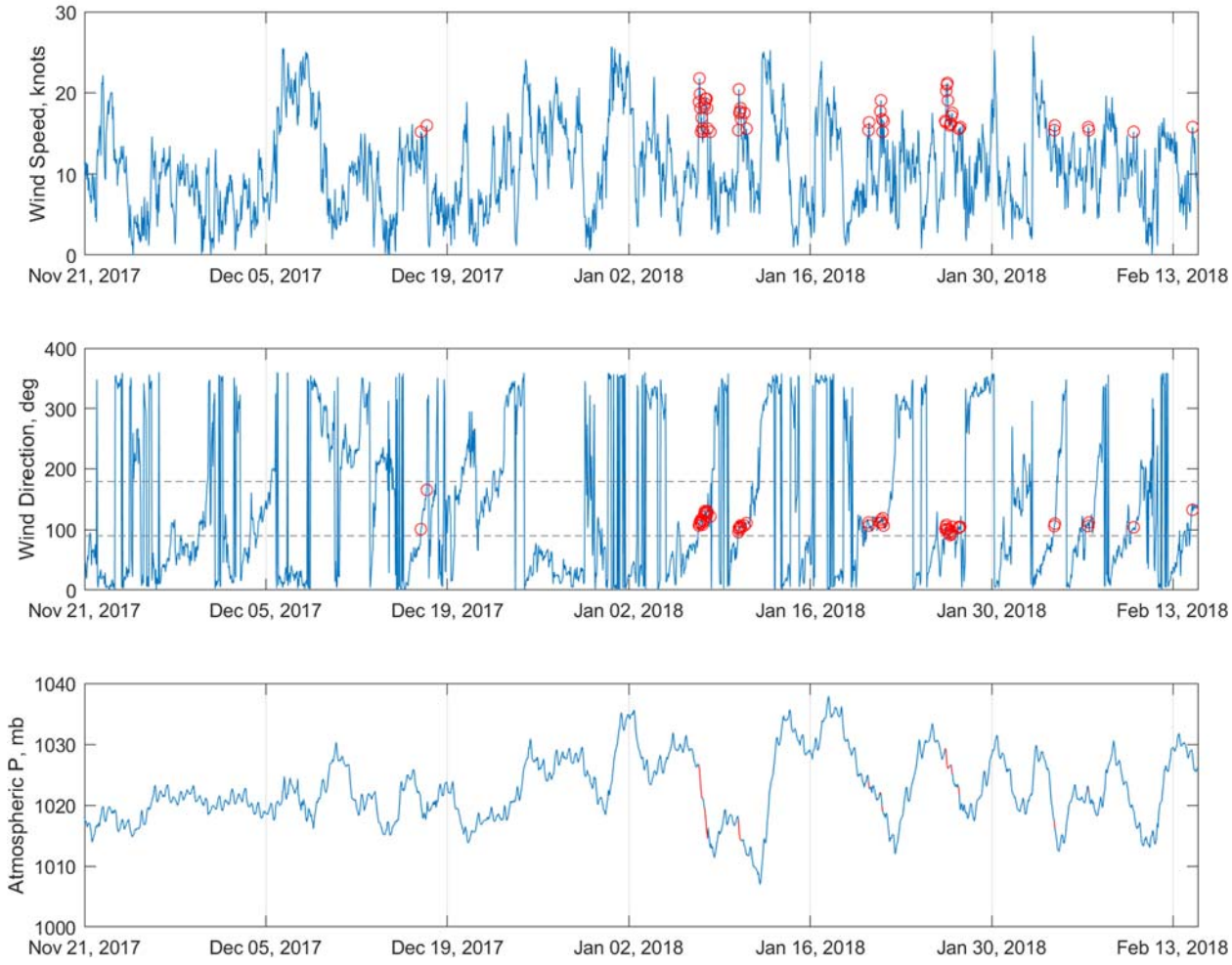

Figure 3.7: NOAA Shell Beach meteorological data. Red circles indicate instances where meteorological criteria were met.

All seven gauges were surveyed and recovered on 14 February 2018. The survey data indicated that none of the wave gauges shifted or moved horizontally. There was minimal vertical settlement on the gauges. Upon return from the field, the raw data were uploaded from the compact flash cards. During this procedure, it was discovered that wave gauge 506 malfunctioned and did not record any data. The other six wave gauges recorded data as expected. Table 3.4 lists each wave gauge's location, identification, and elevation. Figure 3.8 shows the deployment of Wave Gauges 505 and 502. Field notes from deployment and retrieval are located in Appendix C.

Table 3.4: Wave gauge locations and elevations.

Wave Gauge	Location	Northing (ft., La. State Plane, NAD83)	Easting (ft., La. State Plane, NAD83)	Sensor Elevation (ft., NAVD88)	Mudline Elevation (ft., NAVD88)
501	OB - Near	466454.20	3891146.30	-1.47	-1.68
502	WAD - Near	466794.42	3891651.98	-1.79	-2.00
503	RB 2 - Near	469737.20	3892709.69	-2.24	-2.45
504	RB 1 - Near	472087.53	3893383.84	-2.47	-2.68
505	OB/WAD - Off	466015.34	3891812.77	-5.99	-6.20
506	RB 2 - Off	469163.17	3893228.13	-6.36	-6.57
507	RB 1 - Off	471586.82	3894206.85	-6.33	-6.54

Figure 3.8: Deployment of Wave Gauge 505 (left) and Wave Gauge 502 (right) on 21 November 2017 (photo credit: (left) Navid Jafari, (right) Thomas Everett).

4. DATA ANALYSIS

4.1 METHODOLOGY

4.1.1 Survey Data

Topographic survey data were downloaded from the controller into the Trimble Business Center software for processing. This software allows for QA/QC of GPS data including checks for instrument setup errors, antenna height errors, and other errors. Topographic data were exported from Trimble Business Center as digital point files and then imported into AutoCAD Civil 3D software for grouping, management and further QA/QC. Bathymetric survey data were processed using HYPACK's Single Beam Editor. Single Beam Editor displays all sounding measurements graphically and provides a number of methods to edit the raw data. Sounding outliers were manually removed and the edited soundings were smoothed. The processed HYPACK files were exported as digital point files and imported into AutoCAD Civil 3D for grouping, management, and QA/QC. The topographic and bathymetric survey point data imported into AutoCAD Civil 3D were used to create profile drawings of the survey transects.

4.1.2 Water Surface Elevation (WSEL) Data

Time series water level data were uploaded from each sonde using YSI's EcoWatch Lite Software. Once uploaded, the file was then exported as a Microsoft Excel file using EcoWatch Lite. The time series data are referenced to Coordinated Universal Time (UTC). A QA/QC review of the data was performed, and the raw water level data were converted to water elevations in NAVD88. The raw data were converted to elevations by applying an adjustment based on the sensor elevation. The sensor elevation was calculated for each instrument by subtracting raw water levels recorded by the sonde from water surface elevations at specific time stamps. Water elevations were obtained from RTK GPS top of water shots along with reference nail shots and

hand measurements to the water surface. Several calculated sensor elevations were averaged to produce one sensor elevation for each instrument (included in Table 3.3). During site visits that included instrument maintenance and/or data upload, a water level was calculated from the top of water elevation surveyed at the gauge. This water level was recorded as a "clean" reading. A water level reading was also extracted from the sonde data set at the same time stamp of the field survey and recorded as a "dirty" reading. If the percent difference between the dirty and clean readings was greater than 5%, then a shift factor due to biofouling would be applied to the data. A shift factor was not needed for WSEL 001 or WSEL 002 data.

Erroneous water level data were removed from the data set during periods of maintenance and data uploads when the sonde was out of the water. This occurred during 21 November 2017 and 15 January 2018. A review of the data indicated that the water levels fell below the sensors of both sondes during periods of low tides in December 2017 and January 2018. All of these instances were removed from the data set.

4.1.3 Wave Gauge Data

The wave gauge data were processed using MATLAB (matrix laboratory), a computational, coding, and programming software package. The software was used to process raw pressure data uploaded from the wave gauges into formats of water depth, significant wave height, and peak wave period. This was accomplished in two main steps: (1) conversion of raw pressure to water depths and (2) conversion of time series of water depths to significant wave height and peak wave period using OCEANLYZ, a MATLAB toolbox (Karimpour, 2015).

Raw hydraulic pressure observations were transformed into water depths above the sensor using the equation:

$$h = \frac{P}{\rho g} \tag{19}$$

where h is the water depth above the sensor (m), P is pressure (Pa), ρ is the density of water (kg/m^3), and g is the acceleration due to gravity (m/s^2) . Water density $\rho = 1015\ kg/m^3$ was selected for the study site based on salinity measurements recorded at WSEL 002 throughout the deployment. Atmospheric pressure readings, averaged from the first four bursts of data collected on 21 November 2017 prior to the submersion of the gauges, were used to correct the raw instrument readings. Time series atmospheric pressure measured at NOAA Station 8761305 Shell Beach, LA was used to correct the wave gauge pressure readings by accounting for changes in atmospheric pressure during the deployment (NOAA, 2018).

Two methods can be used for short-term wave analysis: (1) time domain analysis using the zero-crossing method and (2) frequency domain analysis using spectral analysis method. These methods are described in further detail in the literature (Dean and Dalrymple, 1991; Holthuijsen, 2007; Kamphuis, 2010; Karimpour and Chen, 2017). Spectral analysis was used for this study. This method uses a Fast Fourier Transform (FFT) to convert the water surface measurements from the time domain to the frequency domain. A wave energy spectrum is then calculated for each burst. Wave properties were calculated from the water surface elevation power spectral density ($S_{\eta\eta}$), which is estimated from the dynamic pressure power spectral density (S_{PP}) (Karimpour and Chen, 2017):

$$S_{\eta\eta} = \frac{1}{K_p^2} \times \frac{S_{PP}}{\rho^2 g^2} \tag{20}$$

$$K_p(f) = \frac{\cosh kd_s}{\cosh kh} \tag{21}$$

where K_p is the dynamic pressure to the surface elevation conversion factor (pressure response factor), f is the wave frequency, k is the wave number, d_s is the distance of the pressure sensor from the bed, and h is the local water depth. The pressure response factor (K_p) is used to correct

the attenuation of the dynamic pressure signal in the water column as depth increases. Accounting for pressure attenuation using this method can cause unrealistic amplification of shorter waves with large frequencies. To prevent this, a high-cutoff frequency ($f_{maxpcorr}$) is selected to limit the minimum value of K_p (Karimpour and Chen, 2017). For this study, a $f_{maxpcorr}$ value of 0.60 was selected for the offshore gauges and 0.65 was selected for the nearshore gauges based on water depths. A wave energy density spectrum is shown in Figure 4.1.

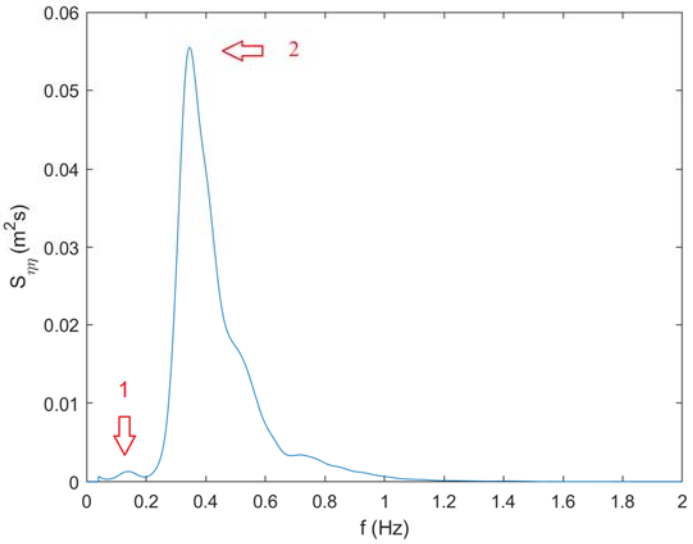

Figure 4.1: Wave energy density spetrum for a single burst (Wave Gauge 505, 8 January 2018, 07:00 UTC). The peak (1) swell component and (2) sea component of the wind induced wave are identified.

The zero-moment wave height (H_{m0}) is calculated:

$$H_{m0} = 4\sqrt{m_0} \tag{22}$$

where m_0 is the zero-moment of the spectrum. The peak wave period (T_p) is calculated:

$$T_p = \frac{1}{f_p} \tag{23}$$

where f_p is the peak wave frequency. The peak wave period was limited to 10 seconds to eliminate overestimation during calm, low wave energy days.

Significant wave height (H_s) is defined as the mean of the top one-third of wave heights for a time period record, or in this case a twenty minute burst. H_s is calculated from the time domain analysis using the zero-crossing method. In deep water, H_s is close to H_{m0}. Since the wave gauges located behind the oyster breakwaters for this study are in shallow water, H_s was calculated using the zero-crossing method and compared to H_{m0}.

Data analysis revealed that water depth values for wave gauges 501 and 507 were observed to have some drift. This drift refers to an offset error in the raw sampling data from its original calibration. This may be caused by physical changes to the sensor's components or biofouling. To adjust for this drift, gauge 501 water depths were adjusted using an offset value of -0.310 feet. This value was calculated by taking the mean of the time series differences between water levels at gauges 502 and 501. The standard deviation of the differences in water levels between 502 and 501 is 0.149 feet. Gauge 507 water depths were adjusted using an offset value of +0.219 feet. This value was calculated by taking the mean of the time series differences between water levels at gauges 505 and 507. The standard deviation of the differences in water levels between 505 and 507 is 0.029 feet. The mean differences of water levels was taken from the beginning of the deployment through 31 December 2017. The differences caused by adjusting the mean water levels for gauges 501 and 507 were analyzed. The adjustment has very minor implications on the calculation of the wave heights.

4.1.4 Wave Transmission

The relationships between incident significant wave heights (H_i) and transmitted significant wave heights (H_t) at each structure were compared by plotting the variables using a linear regression analysis (H_{m0} offshore vs. H_{m0} nearshore). The wave heights were grouped into five water level (WL) elevation ranges (ft., NAVD88): WL less than -0.5 ft., WL greater than or

equal to -0.5 ft. and less than 0.5 ft., WL greater than or equal to 0.5 ft. and less than 1.0 ft., and WL greater than or equal to 1.5 ft.

Wave transmission at each structure was evaluated by plotting the wave transmission coefficient (K_t) vs. the relative freeboard ($\frac{R_c}{H_i}$). When the entire data set was plotted, K_t was inconsistent and scattered when H_i was less than 0.4 feet. All incident wave heights (H_i) less than 0.4 feet were subsequently removed and the plots were reproduced.

4.2 RESULTS

4.2.1 Survey Data

Land and hydrographic surveys were conducted along Transects 1 – 5 that correspond to the wave gauge locations. The surveys recorded the as-is elevations and dimensions of the structures along with the topographic and bathymetric features of each cross-shore transect at the time of the study. Table 4.1 shows the surveyed crest elevation and dimensions for each structure type. Figure 4.2 shows the survey transect cross sections and the locations of the wave gauges. Photographs of the breakwater structures (Figure 4.3) were taken during the 15 January 2018 field survey. Low water levels that day allowed for more of the structures to be exposed. The OysterBreak structure consists of rows of units that are stacked two units high. There are three rows of units at the base and two rows of units at the crest. The WAD and Reef Ball Type 2 structures consist of two rows of units parallel to the shoreline. The Reef Ball Type 1 structure has three rows of units.

Table 4.1: Breakwater structures surveyed elevations and widths.

Structure	Survey Transect	PO-148 Baseline Station	Crest Elevation (ft., NAVD88)	Crest Width (ft.)	Base Width (ft.)
OysterBreak	1	56+00	1.05	8.49	13.84
WAD	2	62+00	1.93	13.41	17.20
Reef Ball Type 2	3	106+00	1.78	7.11	9.82
Reef Ball Type 1	4	137+00	1.20	12.27	15.59

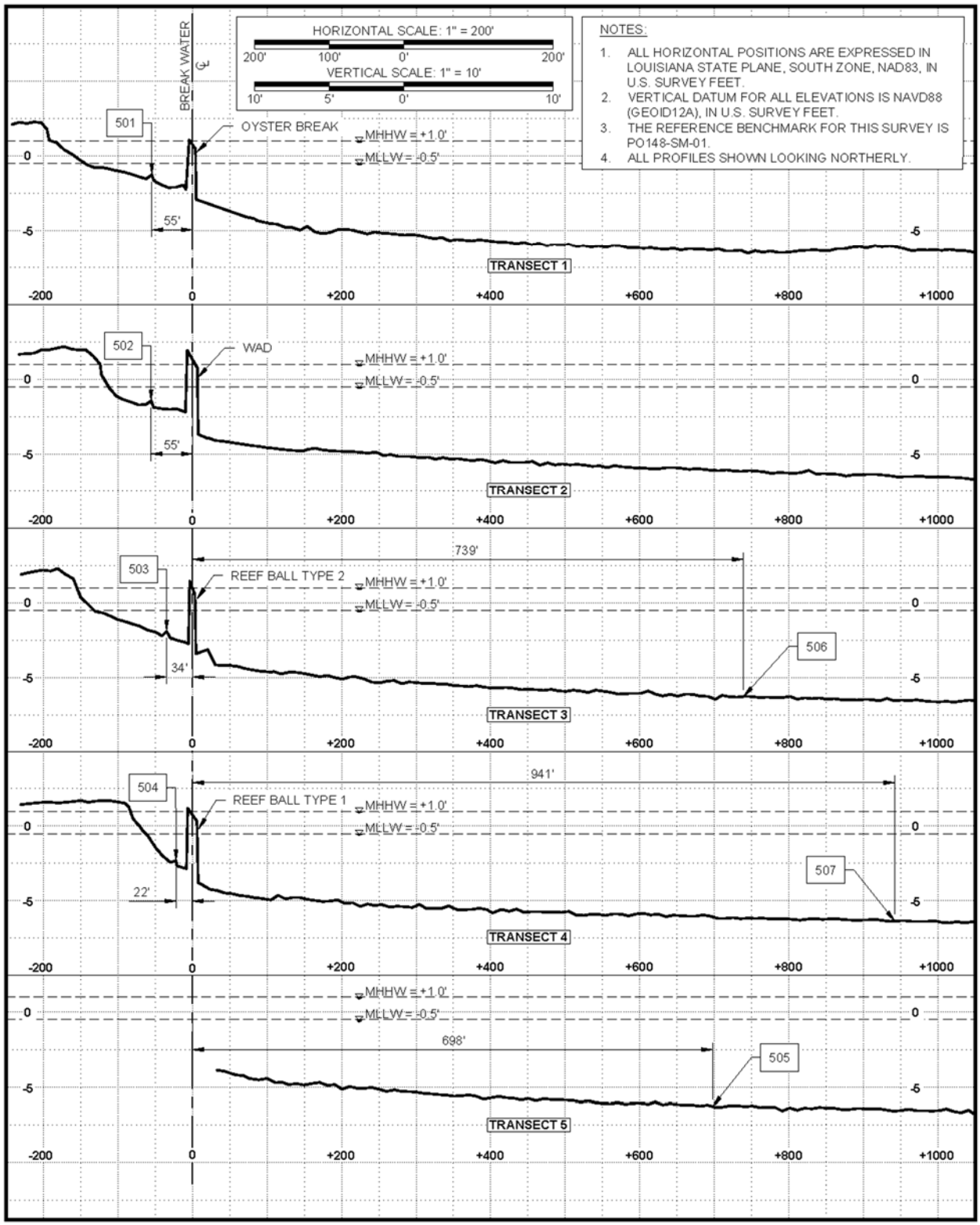

Figure 4.2: Survey transect cross sections.

Figure 4.3: OysterBreak (top left), WAD (top right), Reef Ball Type 2 (bottom left), Reef Ball Type 1 (bottom right). Photos taken 15 January 2018.

4.2.2 Water Surface Elevation (WSEL) Data

The adjusted water surface elevation data were compared to nearby Coastwide Reference Monitoring System (CRMS) sites 0147, 1024, 1069, and 4557 (CPRA, 2018). CRMS site locations are shown in Figure 4.4. Table 4.2 lists the CRMS sites location and elevation information.

Figure 4.4: CRMS site locations.

Table 4.2: CRMS site locations and elevation summary.

CRMS Site	Northing (ft., La. State Plane, NAD83)	Easting (ft., La. State Plane, NAD83)	Sensor Elevation (ft., NAVD88)	Top of 4x4 Post (ft., NAVD88)	Nail Elevation (ft., NAVD88)
0147	428002.52	3829822.58	-1.75	5.94	3.66
1024	505272.96	3900312.77	-2.01	7.01	2.67
1069	568363.95	3948984.76	-1.21	6.74	2.33
4557	485819.61	3838960.52	-0.51	7.25	3.78

The water elevation data from both WSEL 001 and WSEL 002 matched favorably with CRMS sites 0147, 4557, and 1069 (see Figure 4.5 for water level comparison). CRMS 1024 matched favorably with WSEL 001 and WSEL 002 on some days and other days resulted in 1.0 feet water

level difference. This difference may be due to the specific topographic and hydrodynamic conditions or sensor issues at CRMRS 1024. On the morning of 8 October 2017, Hurricane Nate, a Category 1 hurricane, tracked approximately eighteen miles east of the project area causing significant storm surge. Peak water surface elevations associated with Hurricane Nate are listed in Table 4.3 for WSEL 001 and the investigated CRMS sites. Water levels fell below the WSEL 001 sensor elevation on 30 December 2017, 1, 3, 4, 12-19, 30, and 31 January 2018 during periods of low tide. Water levels fell below WSEL 002 sensor elevation on 9, 12, and 30 December 2017, 1, 3, 4, 12-17, 19, 30, and 31 January 2018 during periods of low tide.

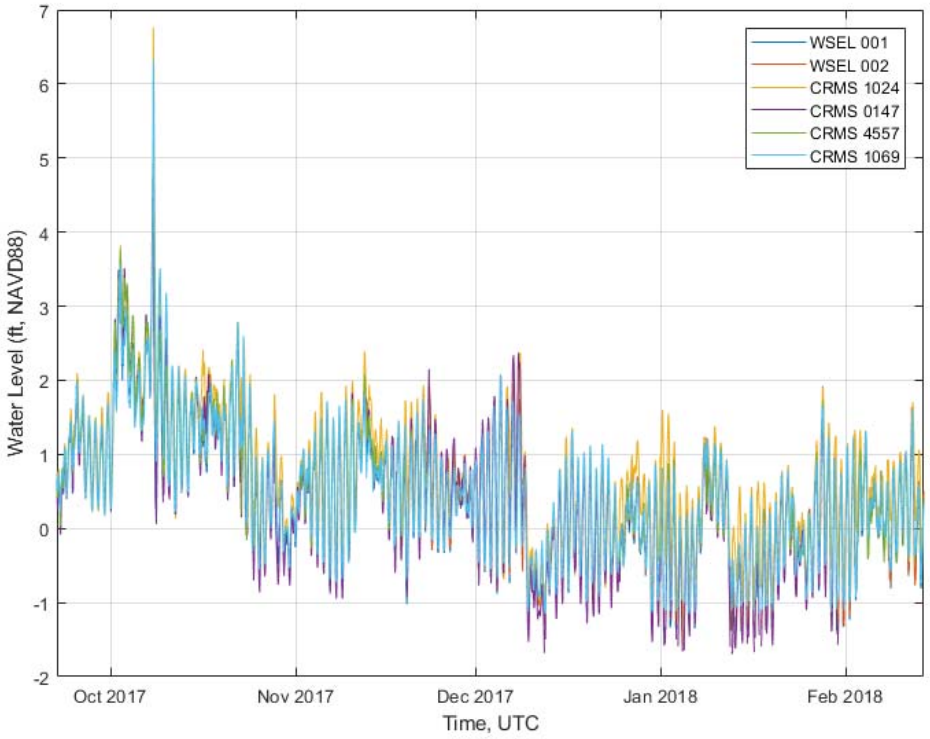

Figure 4.5: WSEL comparison between WSEL 001, WSEL 002, CRMS 1024, CRMS 0147, CRMS 4557, and CRMS 1069.

Table 4.3: Hurricane Nate peak storm surge.

Gauge	WSEL (ft., NAVD88)	Date Time (UTC)
WSEL 001	4.75	10/08/2017 2:00
CRMS 0147	5.08	10/08/2017 3:00
CRMS 1024	6.76	10/08/2017 3:00
CRMS 1069	6.32	10/08/2017 3:00
CRMS 4557	5.13	10/08/2017 4:00

4.2.3 Wave Gauge Data

The wave gauge data were analyzed in the frequency domain using the spectral analysis method. Results of the data analysis, including the time series of water depths, wave heights (H_{m0}) and peak wave periods (T_p), are shown in Figures 4.6 – 4.11.

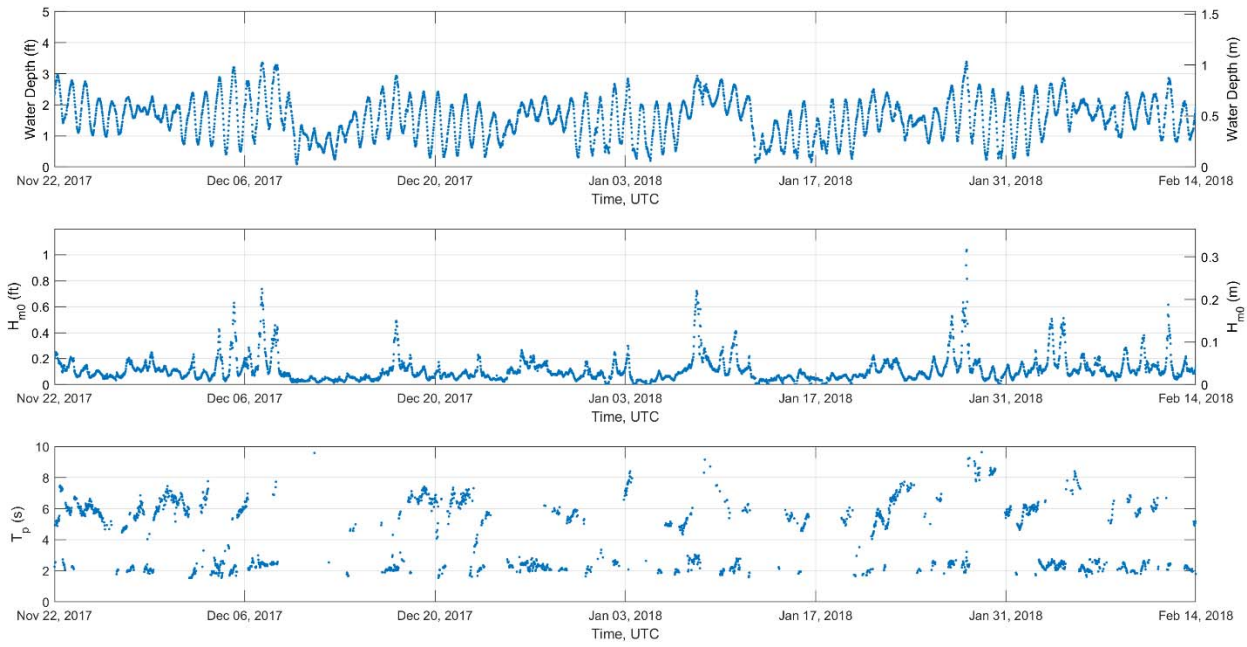

Figure 4.6: Wave Gauge 501 water depth, wave height (H_{m0}), and peak wave period (T_p).

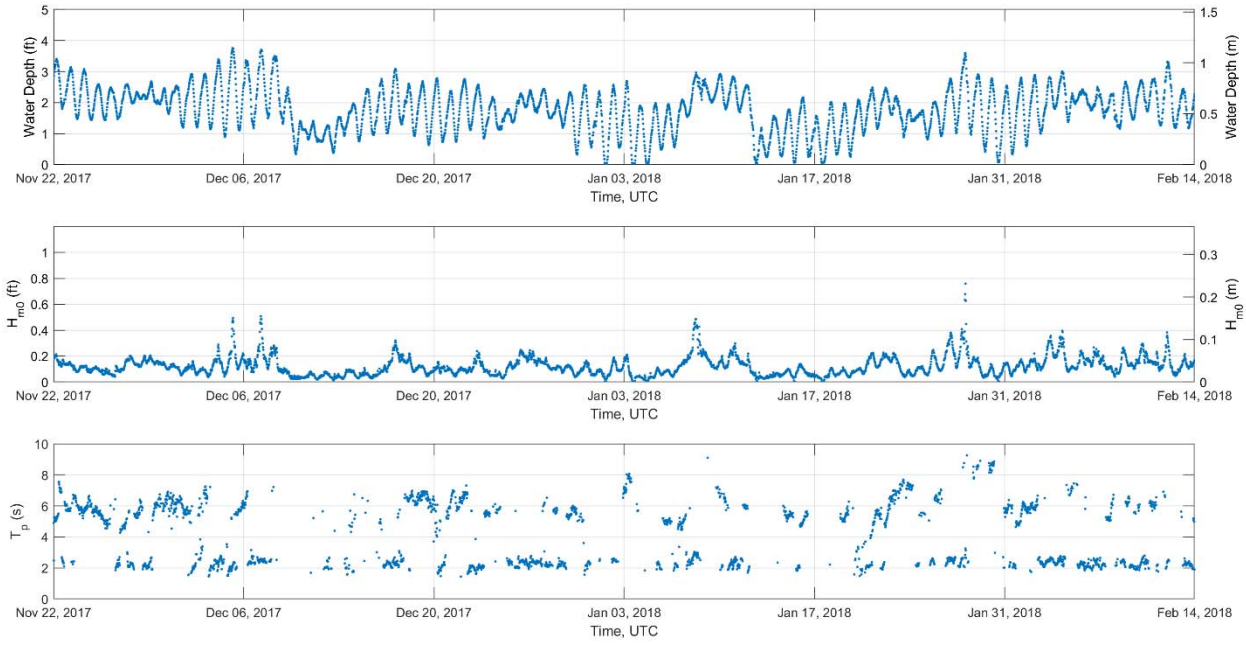

Figure 4.7: Wave Gauge 502 water depth, wave height (H_{m0}), and peak wave period (T_p).

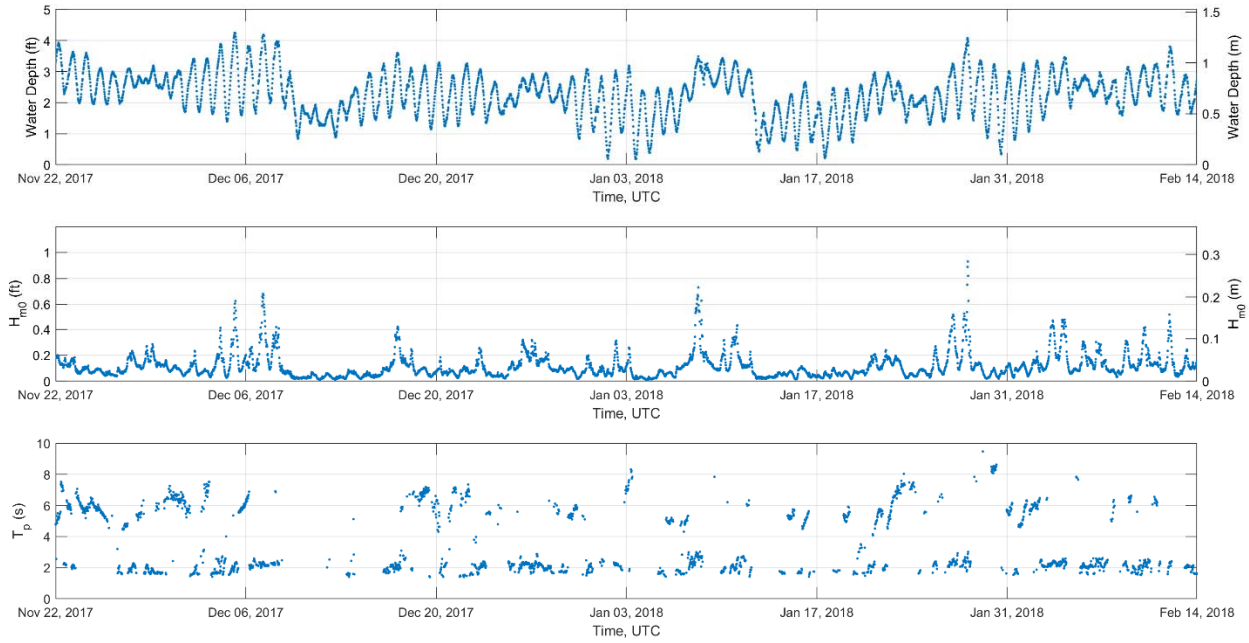

Figure 4.8: Wave Gauge 503 water depth, wave height (H_{m0}), and peak wave period (T_p).

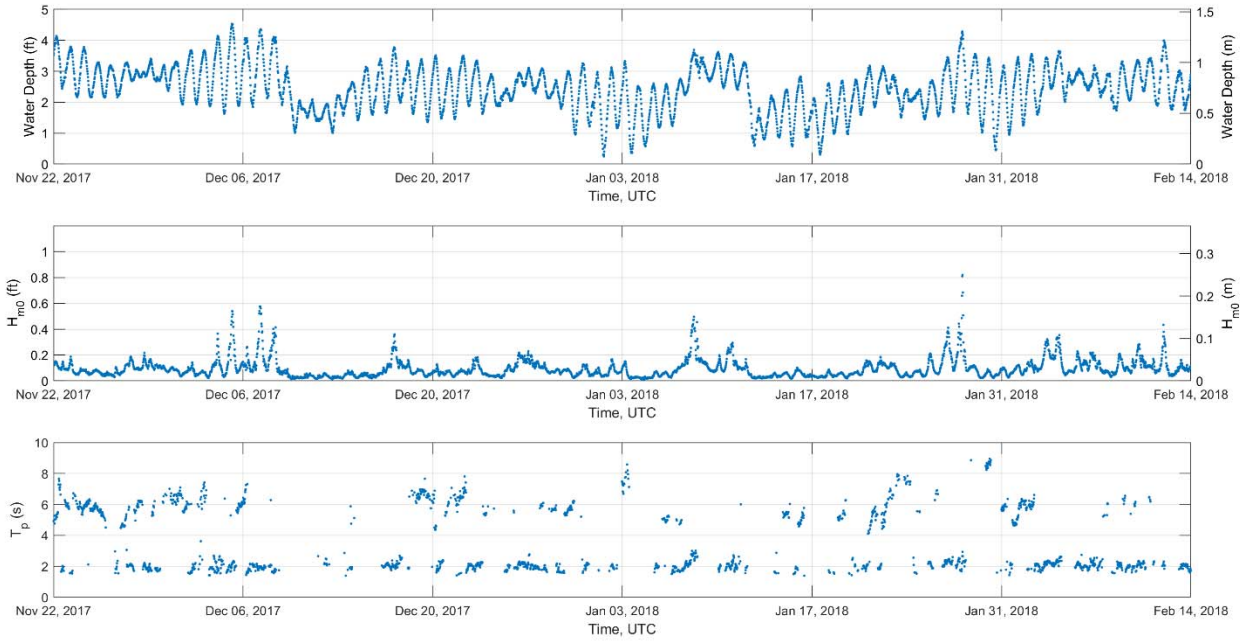

Figure 4.9: Wave Gauge 504 water depth, wave height (H_{m0}), and peak wave period (T_p).

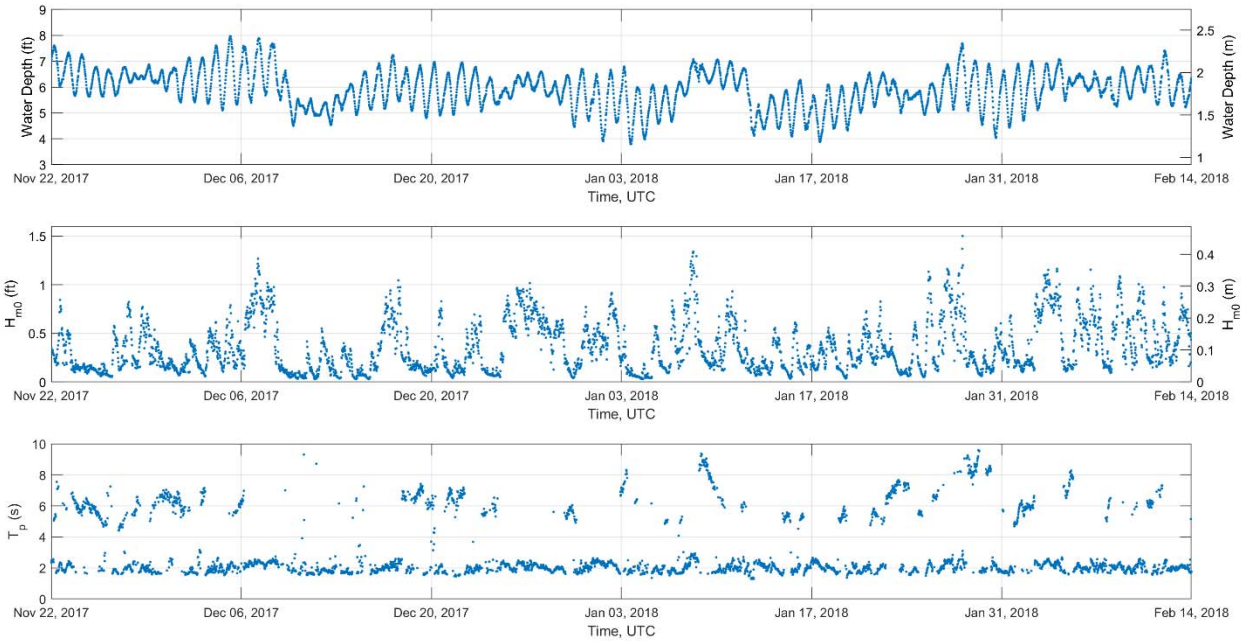

Figure 4.10: Wave Gauge 505 water depth, wave height (H_{m0}), and peak wave period (T_p).

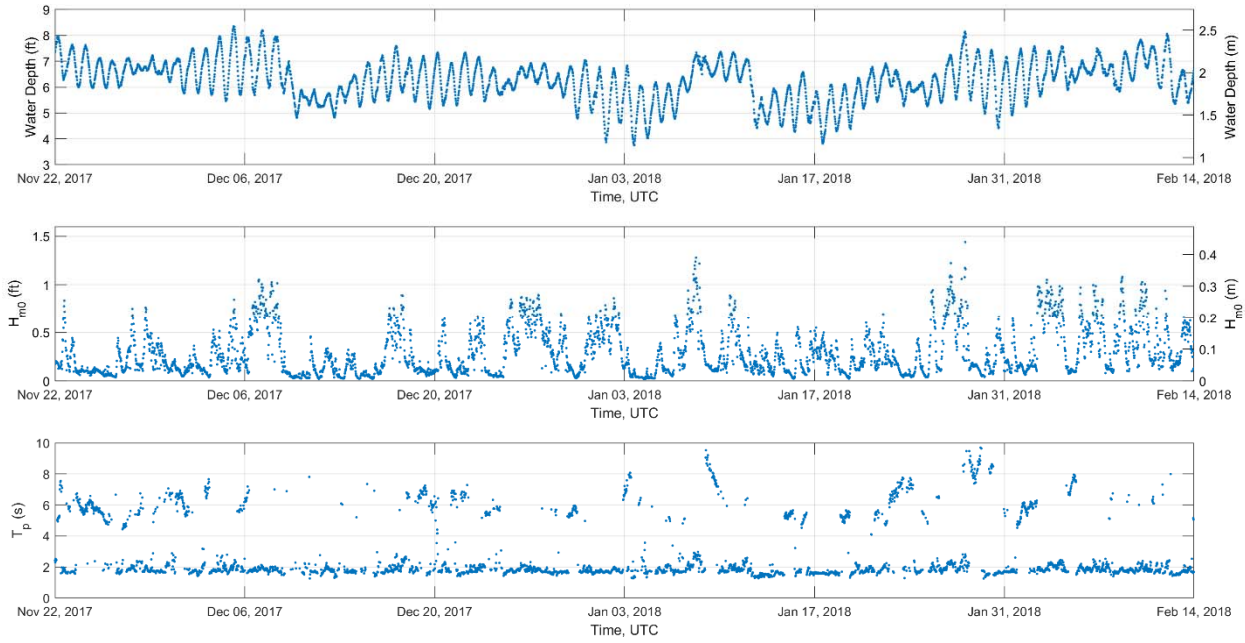

Figure 4.11: Wave Gauge 507 water depth, wave height (H_{m0}), and peak wave period (T_p).

The largest wave heights correspond to periods of high winds; especially prolonged south to southeast winds, i.e., 8 January 2018 and 28 January 2018. The maximum H_{m0} recorded for the offshore gauges is 1.50 feet at Wave Gauge 505 on 28 January 2018. The maximum H_{m0} recorded for the nearshore gauges is 1.04 feet at Wave Gauge 501 on 28 January 2018. The average H_{m0} for the offshore gauges is 0.33 feet and the average H_{m0} for the nearshore gauges is 0.11 feet. The wave gauge data statistics are listed in Table 4.4. Note that the peak wave period statistics listed in Table 4.4 are of locally generated wind waves. The swell wave energy is small in comparison to local wind waves during cold front passages. This is evident in the wave energy density spectrums (example Figure 4.1) where the sea component of the wind wave dominates the energy spectrum.

Table 4.4: Wave gauge data statistics.

Wave Gauge	Min Water Depth (ft.)	Max Water Depth (ft.)	Mean Water Depth (ft.)	Min H_{m0} (ft.)	Max H_{m0} (ft.)	Mean H_{m0} (ft.)	Min T_p (sec)	Max T_p (sec)	Mean T_p (sec)
501	0.09	3.38	1.57	0.00	1.04	0.11	1.54	3.87	2.25
502	0.03	3.75	1.78	0.00	0.76	0.12	1.44	3.92	2.29
503	0.19	4.25	2.27	0.01	0.93	0.12	1.39	3.98	2.05
504	0.25	4.53	2.45	0.01	0.82	0.09	1.39	3.62	2.00
505	3.80	7.97	5.92	0.03	1.50	0.35	1.29	3.91	2.02
507	3.75	8.35	6.26	0.02	1.44	0.30	1.25	3.59	1.83

Wave heights were also analyzed in the time domain using the upward zero-crossing method and compared to the spectral analysis results. Figures 4.12 – 4.17 show the comparison of wave heights using the spectral analysis (H_{m0}) and zero-crossing method (H_s). The results show that H_{m0} is typically larger than H_s which is consistent with the literature (e.g. Thompson and Vincent, 1985). The best fit line that passes through the origin of the linear regression (y = ax) is shown for the data. The average "a" is 0.9186 for the nearshore gauges and 0.9344 for the offshore gauges.

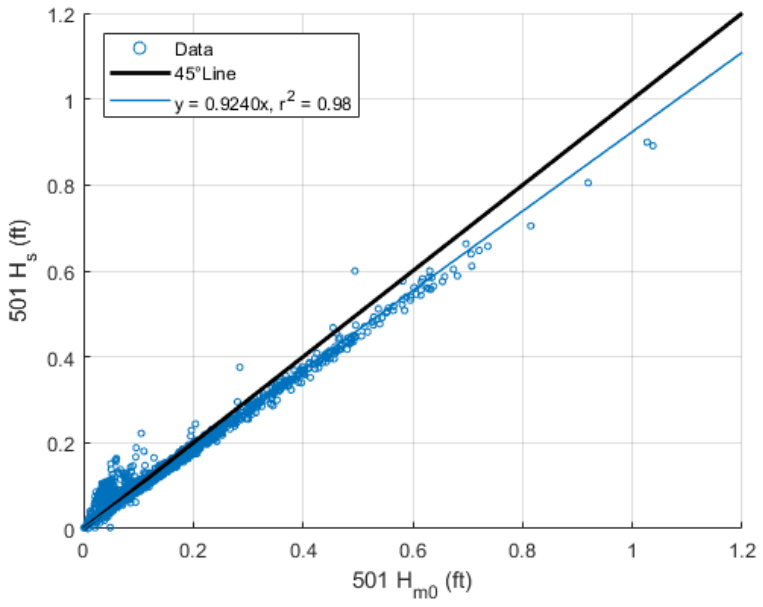

Figure 4.12: Wave heights comparison between spectral analysis (H_{m0}) and zero-crossing method (H_s) for wave gauge 501.

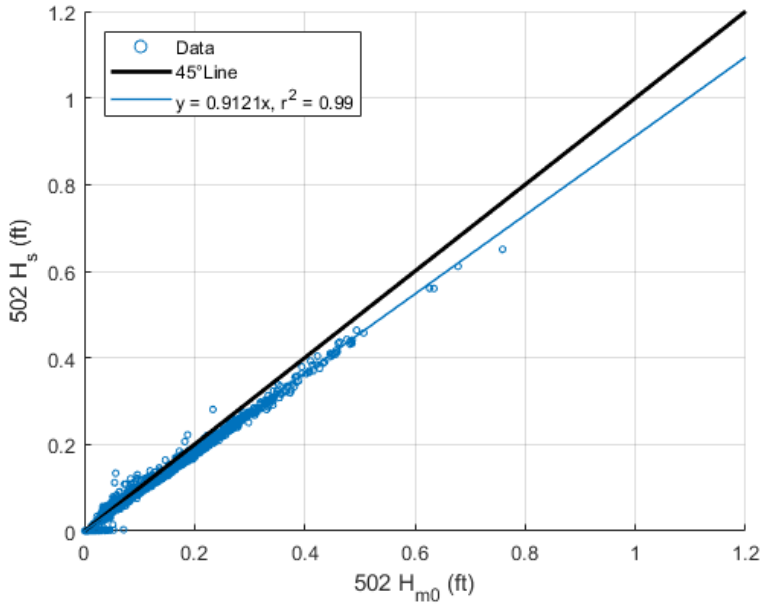

Figure 4.13: Wave heights comparison between spectral analysis (H_{m0}) and zero-crossing method (H_s) for wave gauge 502.

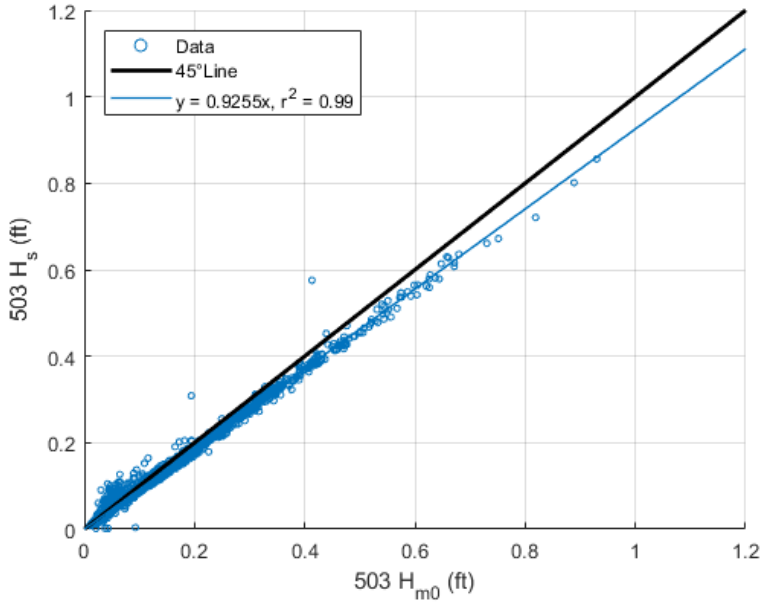

Figure 4.14: Wave heights comparison between spectral analysis (H_{m0}) and zero-crossing method (H_s) for wave gauge 503.

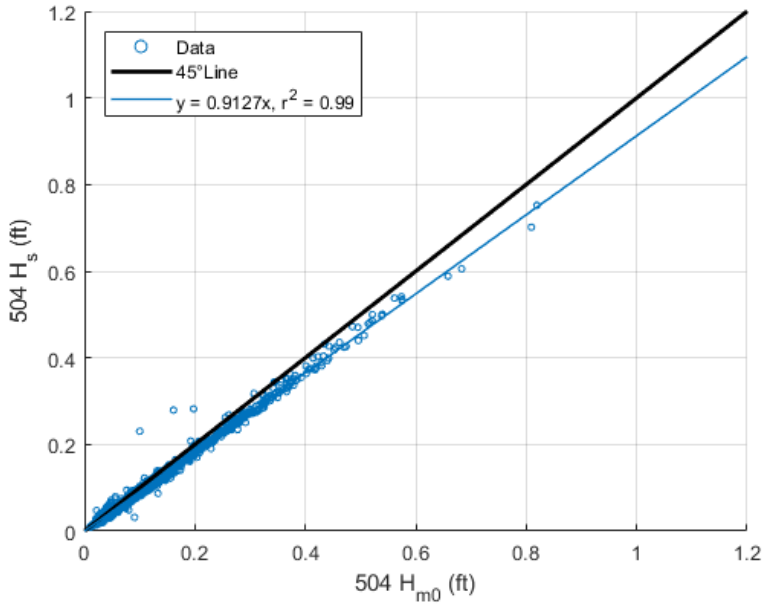

Figure 4.15: Wave heights comparison between spectral analysis (H_{m0}) and zero-crossing method (H_s) for wave gauge 504.

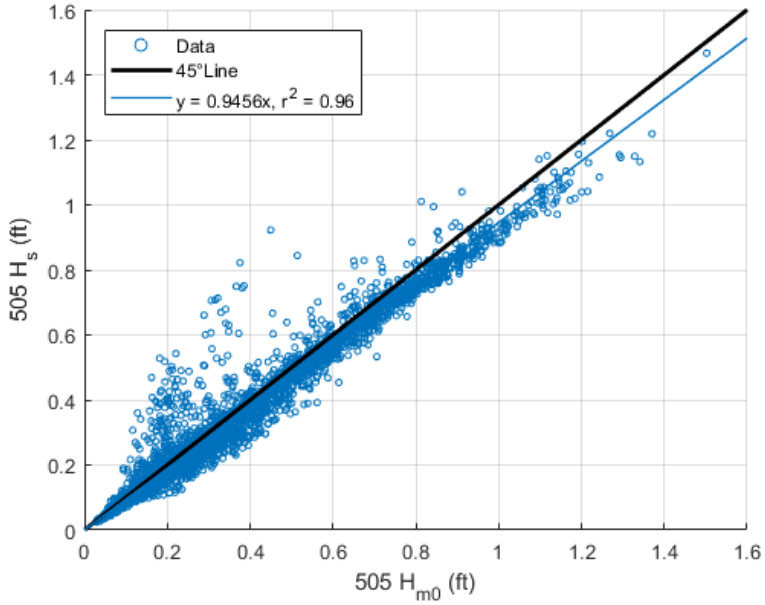

Figure 4.16**:** Wave heights comparison between spectral analysis (H_{m0}) and zero-crossing method (H_s) for wave gauge 505.

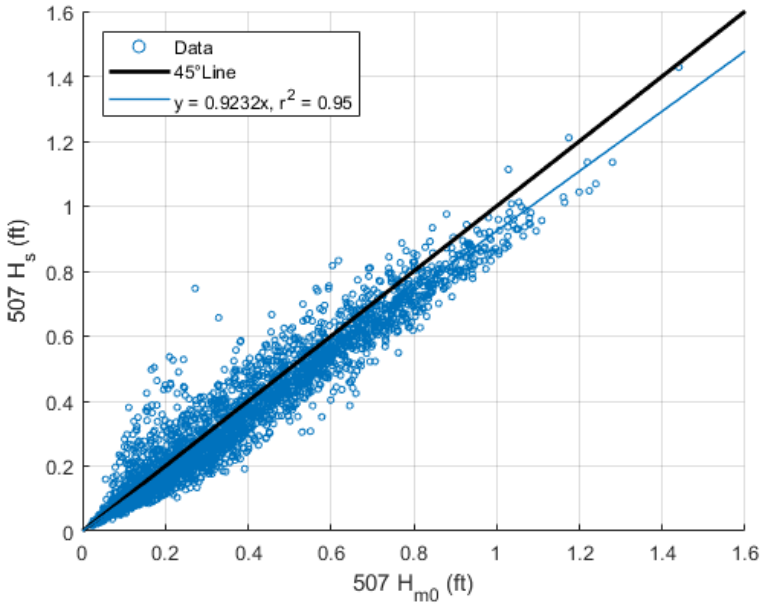

Figure 4.17: Wave heights comparison between spectral analysis (H_{m0}) and zero-crossing method (H_s) for wave gauge 507.

4.2.4 Wave Transmission

The relationships between incident significant wave heights (H_i) and transmitted significant wave heights (H_t) at each structure are shown in Figures 4.18 – 4.21. The wave heights are grouped into five water level (WL) elevation ranges (ft., NAVD88), i.e., WL less than -0.5 ft., WL greater than or equal to -0.5 ft. and less than 0.5 ft., WL greater than or equal to 0.5 ft. and less than 1.0 ft., and WL greater than or equal to 1.5 ft. The best fit line that passes through the origin of the linear regression analysis (y = ax) is shown for each group. The results show that wave heights on the protected side of the structures are a function of water levels and the incident wave heights. H_{m0} data at Wave Gauge 506 were estimated by calculating the mean between Wave Gauges 505 and 507.

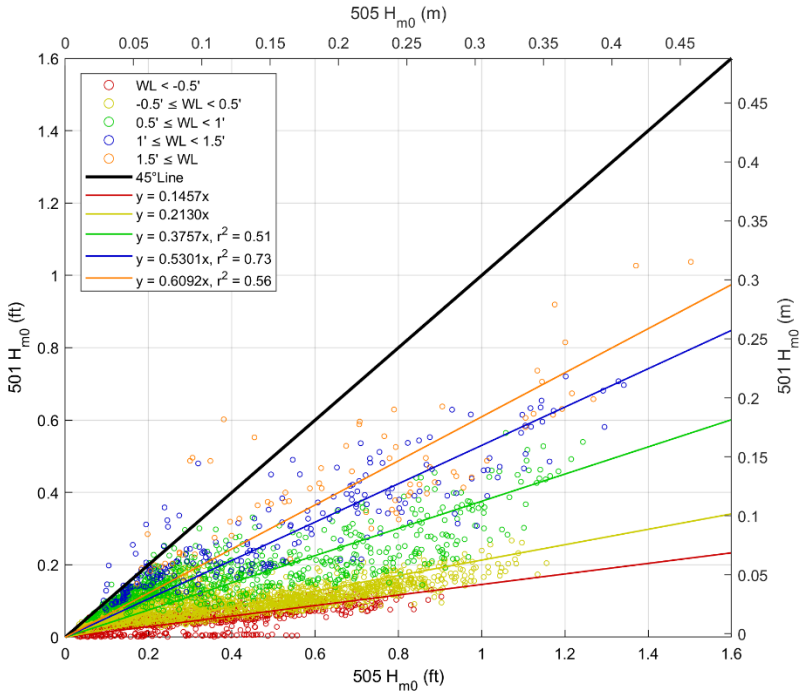

Figure 4.18: OysterBreak incident significant wave heights (505) and transmitted significant wave heights (501) comparison grouped by water level elevations (ft., NAVD88).

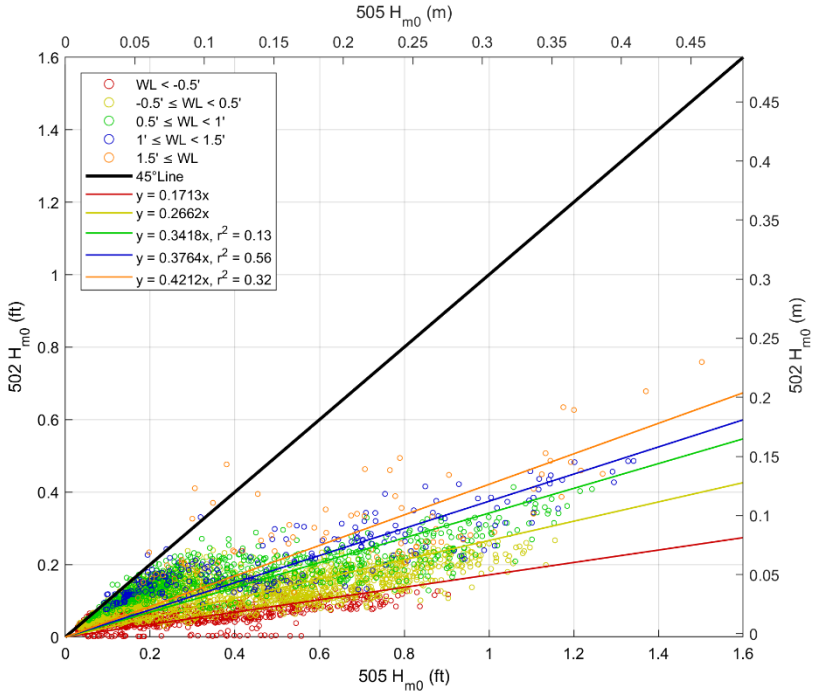

Figure 4.19: WAD incident significant wave heights (505) and transmitted significant wave heights (502) comparison grouped by water level elevations (ft., NAVD88).

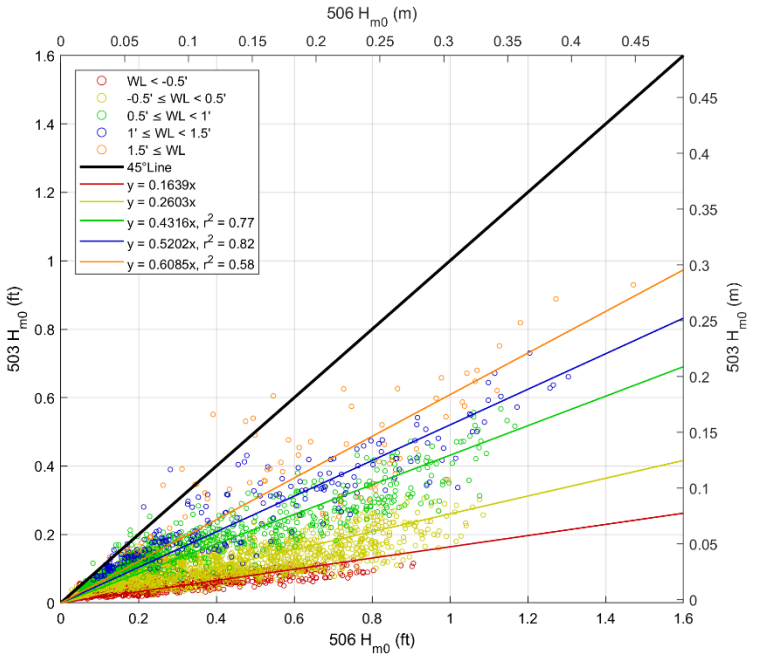

Figure 4.20: Reef Ball Type 2 incident significant wave heights (506) and transmitted significant wave heights (503) comparison grouped by water level elevations (ft., NAVD88).

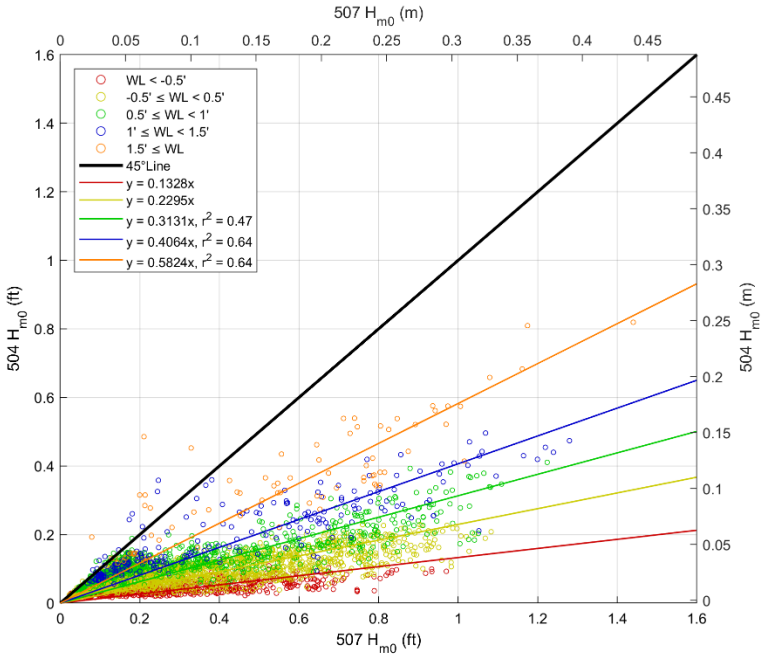

Figure 4.21: Reef Ball Type 1 incident significant wave heights (507) and transmitted significant wave heights (504) comparison grouped by water level elevations (ft., NAVD88).

Wave transmission was evaluated by plotting K_t vs. $\frac{R_c}{H_i}$ for each structure type. Small waves were removed from the data set by omitting all incident wave heights (H_i) less than 0.4 feet. These graphs are shown in Figure 4.22. Although the graphs indicate more of a trend in the data after the small incident wave heights were removed, the results are still scattered. This scattering of the data may be caused by effects of wave direction, structure width, and wave period.

As an application of the transmission relationships obtained from the field data, the transmission coefficient (K_t) is found for each structure type by observing the data at fixed water levels and a fixed incident wave height (H_i) of 1.0 feet. For example, to find the K_t range for the OysterBreak structure at water level -0.5 feet, R_c and $\frac{R_c}{H_i}$ is calculated:

$$R_c = h_c - WL \tag{24}$$

$$R_c = 1.05 - (-0.5) = 1.55\ feet \tag{25}$$

$$\frac{R_c}{H_i} = \frac{1.55}{1.0} = 1.55\ feet \tag{26}$$

The K_t range is determined visually from Figure 4.22 using the calculated $\frac{R_c}{H_i}$ value. The K_t range for the OysterBreak structure at water level -0.5 feet and with a H_i of 1.0 feet is 0.14 to 0.30. The K_t ranges for all structure types are listed in Table 4.5. It is observed that the Reef Ball Type 1 structure has the lowest K_t range of the four structures under the given conditions. Note that this may not be the case as the water level increases because the crest elevation of this structure type is relatively low. The wave transmission coefficient depends on the structure type and configuration as well as the water level.

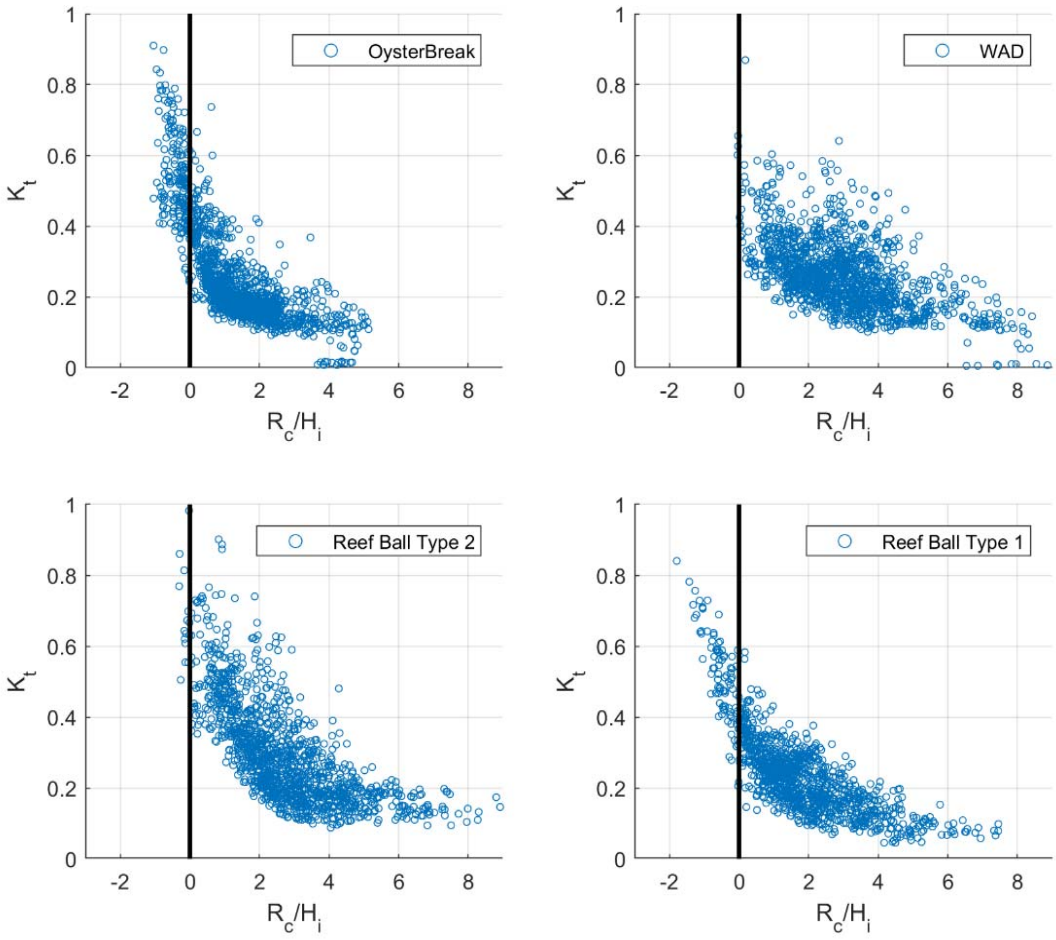

Figure 4.22: Influence of the relative freeboard (R_c/H_i) on the wave transmission coefficient (K_t) for OysterBreak (top left), WAD (top right), Reef Ball Type 2 (bottom left), and Reef Ball Type 1 (bottom right).

Table 4.5: Comparison of K_t values by structrue type and water level at H_i = 1.0 feet.

Structure	Water Level (ft., NAVD88)	R_c/H_i	K_t Range
OysterBreak	-0.5	1.55	0.14 – 0.30
	1.0	0.05	0.37 – 0.60
WAD	-0.5	2.43	0.16 – 0.56
	1.0	0.93	0.22 – 0.60
Reef Ball Type 2	-0.5	2.28	0.15 – 0.60
	1.0	0.78	0.22 – 0.62
Reef Ball Type 1	-0.5	1.70	0.11 – 0.34
	1.0	0.20	0.15 – 0.45

5. DISCUSSION

5.1 DISCUSSION ON THE EFFECT OF SENSOR DEPTH

The offshore and nearshore wave gauges were planned for deployment at the -6.0 foot and -2.0 foot contour, respectively. These locations were determined from a survey performed prior to the construction of the Living Shoreline Demonstration Project (PO-148). The wave gauge elevations deviated slightly from the proposed elevations. This is especially evident for the nearshore gauges located on the protected side of the structures where construction activities and geomorphic shoreline changes due to the structures may have occurred. A wave shoaling analysis was conducted to determine the influence of the differences in water depths to the wave heights. Wave Gauge 505 was selected as the reference offshore gauge and Wave Gauge 503 was selected as the reference nearshore gauge. Assuming wave direction was normal to the contours, the wave shoaling analysis was conducted for 8 January 2018 at 07:00 UTC due to the large wave height recorded during this burst. Table 5.1 lists the results of the wave shoaling analysis. Wave heights for gauges 505, 507, 503, 501, 502, and 504 are recorded wave heights. 507_shoal, 501_shoal, 502_shoal, and 504_shoal designate new wave heights calculated from the shoaling analysis using the water depth at the reference gauge.

Table 5.1: Wave shoaling analysis results.

Wave Gauge	Water Depth (ft.)	Peak Wave Period, T_p (sec.)	Wave Height, H_{m0} (ft.)	Deviation from Reference Wave Height (ft.)
505	7.07	2.89	1.34	
507	7.34	2.52	1.07	
507_shoal			1.07	0.0033
503	3.49	2.76	0.73	
501	2.93	2.95	0.70	
501_shoal			0.68	0.0157
502	2.97	2.96	0.49	
502_shoal			0.48	0.0102
504	3.69	2.87	0.50	
504_shoal			0.50	-0.0030

The shoaling analysis shows that the differences in wave gauge depths have a negligible effect on the wave heights. In other words, the slight differences in the wave depths of grouped wave gauges do not affect the wave transmission analysis and comparison.

5.2 DISCUSSION ON WAVE TRANSMISSION

The wave transmission coefficient (K_t) data results are scattered, as illustrated in Figure 4.22. The K_t data were more scattered prior to the removal of all incident wave heights (H_i) less than 0.4 feet. This scattering of the data may be caused by several factors, specifically effects of wave direction, structure width, and wave period. Wave direction was not measured for this study, but Equation (18) suggests that normal incident waves lead to larger K_t and the greater the oblique incident angle results in a smaller K_t value. Future studies may consider measuring flow direction by using an acoustic Doppler current profiler (ADCP). Structure width also affects wave transmission. The width of each structure varies in the horizontal and vertical directions. Improved K_t data with better r^2 values may be obtained by focusing on stricter criteria, such as a singular cold front that produces high south winds.

The Living Shoreline Demonstration Project Coastal Engineering and Alternatives Analysis (CHE, 2014) analyzed wave transmission using nine simulated CFD model cases. The model cases include three different incident wave heights (0.6 feet, 1.6 feet, and 2.5 feet) at three different water levels (3.2 feet, 4 feet, and 4.72 feet, which is the MLLW, MSL, and MHHW, respectively). The wave parameters and water levels for each model case is listed in Table 5.2. The transmission coefficient results for each model run is listed in Table 5.3. The range of transmission coefficients from CHE is compared to that of the observed data collected for this study. The transmission coefficients from the three model runs with an incident wave height of 2.5 feet (cases

7 – 9) were omitted for this comparison because the highest incident wave height recorded during this study is 1.50 feet.

Table 5.2: Wave parameters and water levels for each CFD model case (modified from CHE, 2014).

Case	H_s (ft.)	T_p (sec)	Water Depth (ft.)	Tide Level
1	0.6	2	3.2	MLLW
2	0.6	2	4	MSL
3	0.6	2	4.72	MHHW
4	1.6	5	3.2	MLLW
5	1.6	5	4	MSL
6	1.6	5	4.72	MHHW
7	2.5	6	3.2	MLLW
8	2.5	6	4	MSL
9	2.5	6	4.72	MHHW

Table 5.3: Transmission coefficients computed by CFD model (modified from CHE, 2014).

Case	Rubble Mound	OysterBreak	Reef Ball	WAD
1	0.00	0.00	0.50	0.26
2	0.27	0.00	0.59	0.45
3	0.43	0.60	0.61	0.53
4	0.36	0.21	0.55	0.32
5	0.39	0.52	0.57	0.46
6	0.42	0.70	0.87	0.80
7	0.31	0.24	0.58	0.35
8	0.37	0.53	0.80	0.51
9	0.47	0.51	0.76	0.58

The K_t values calculated for the OysterBreak structure at H_i = 1.0 feet and water levels at -0.5 feet and 1.0 feet range from 0.14 – 0.60 (Table 4.5). This range falls within the K_t range from CHE's CFD model. The K_t values calculated for the WAD structure range from 0.16 – 0.60. Some of these values fall below the CFD model K_t range for WADs of 0.26 – 0.80. The K_t values calculated for the Reef Ball Type 1 and Reef Ball Type 2 structures range from 0.11 – 0.62. Some of these values fall below the CFD model K_t range for Reef Balls of 0.50 – 0.87. However, this evaluation only compares the transmission coefficients calculated with water levels at -0.5 feet

and 1.0 feet and an incident wave height of 1.0 feet to the CFD model with the water level and wave parameters listed in Table 5.2. Along with the differences in water levels and incident wave heights, other differences in the comparison include wave period and the locations where the incident and transmitted wave heights are measured/simulated. The CFD model simulations can be re-run using the field measurements to validate the model. A calibrated CFD model will be capable of converging the K_t range to within a smaller window for a variety of hydrodynamic conditions, which will facilitate the design of these structures for wave attenuation.

5.3 DISCUSSION ON THE LOUISIANA COASTAL MASTER PLAN

Louisiana's Comprehensive Master Plan for a Sustainable Coast estimates that 2,254 square miles of land loss will occur over the next 50 years under the medium environmental scenario if no action is taken (CPRA, 2017). A significant proportion of this land loss is caused by wind wave attack on marsh boundaries. This process produces a positive feedback cycle by increasing the fetch and depth of coastal lakes, estuaries, and bays.

Artificial or bioengineered oyster reef projects, in which reefs are created using shell or engineered products to provide substrate for oyster recruitment, are nature-based infrastructure and hence are an important restoration technique (McMann et al., 2017). The primary goal of these projects is coastal restoration, rather than management or enhancement of the oyster fishery. However, in areas suitable for oyster recruitment and growth, these reefs can provide a number of ecosystem services in addition to shoreline protection.

The master plan (Alymov et al., 2017) measures the effectiveness of shoreline protection projects by calculating the marsh edge erosion rate (MEE_{new}) as reduced by the project:

$$MEE_{new} = \left(\left(MEE_{original}\right) \left(\frac{A_{project}}{A_{total}}\right) (F_r) \right) + \left(1 - \left(\frac{A_{project}}{A_{total}}\right) \left(MEE_{original}\right) \right) \quad (27)$$

where $A_{project}$ = project edge area = shoreline protection project length * assumed marsh edge width of one 30 meter land/water pixel in morphology subroutine, A_{total} = total marsh edge area, F_r = project reduction factor = wave (erosion) attenuation rate/100%. $MEE_{original}$ can be found by estimating the marsh retreat rate at the shoreline. The linear relationships between retreat rate and wave power, that is the wave energy flux density, were analyzed in the master plan to calculate marsh retreat rate based on wave power (Allison et al., 2017). The results from this study can be used to determine the project reduction factor (F_r). F_r can then be used to calculate the reduction of marsh edge erosion for the Living Shoreline Demonstration Project (PO-148) and other restoration projects in coastal Louisiana.

6. CONCLUSIONS

A successful field study was conducted as a part of this research. Accurate survey data, water surface elevation data, and wave data were collected at the study site between September 2017 and February 2018. This data provide a better understanding of typical conditions at the site. Water level data were also collected during an extreme event when the eye of Hurricane Nate passed approximately 18 miles east of the project site on 8 October 2017.

There were some challenges experienced and lessons learned while conducting the field study. A water level sonde incurred water damage at WSEL Gauge 002 causing data to be lost. Wave Gauge 506 malfunctioned and data were not recoded. It was anticipated that wave data collection would occur for one month; however, the deployment time was extended to almost three months to ensure larger waves were recorded. Additional data processing was needed to correct for small data drift found at Wave Gauges 501 and 507 because of the deployment duration extension. It is recommended that the deployment of wave gauges for similar studies occur during the months of January through April when seasonal fronts produce high east to south winds, and thus larger waves at the study site.

Wave transmission through the types of oyster reef breakwaters investigated in this study is complex owing to variations in porosity, structure width, and crest elevations. Wave transmission strongly depends on water level and structure type. A constant wave transmission coefficient for a given type of structure was not found. This study provides a unique dataset that can be used to calibrate and validate numerical models for wave transmission though different types of constructed oyster reef breakwaters. Such models can then be used to predict the performances of each structure type under a large range of incident wave conditions, which is critical for the design of effective oyster reef breakwaters.

REFERENCES

Allison, M., Chen, Q.J., Couvillion, B., Freeman, A., Leadon, M., McCorquodale, A., Meselhe, E., Ramatchandirane, C., Reed, D., and White, E. (2017). 2017 Coastal Master Plan: Model Improvement Plan, Attachment C3-2: Marsh Edge Erosion. Version Final. (pp. 1-51). Baton Rouge, Louisiana: Coastal Protection and Restoration Authority.

Alymov, V., Cobell, Z., Couvillion, C., de Mutsert, K., Dong, Z., Duke-Sylvester, S., Fischbach, J., Hanegan, K., Lewis, K., Lindquist, D., McCorquodale, J. A., Poff, M., Roberts, H., Schindler, J., Visser, J. M., Wang, Z., Wang, Y., and White, E. (2017). 2017 Coastal Master Plan: Appendix C: Modeling Chapter 4 – Model Outcomes and Interpretations. Version Final. (pp. 1-448). Baton Rouge, Louisiana: Coastal Protection and Restoration Authority.

Buccino, M. and Calabrese, M. (2007). Conceptual approach for prediction of wave transmission at low-crested breakwaters. Journal of Waterway, Port, Coastal, and Ocean Engineering, 133(3), 213-224.

Campbell, M.D. (2004). Analysis and evaluation of a bioengineered submerged breakwater. M.S. Thesis. Louisiana State University. pp. 109.

Carter, J., Fenical, S., Harter, C., and Todd, J. (2015). CFD modeling for the analysis of living shoreline structure performance. *Coastal Structures and Solutions to Coastal Disasters 2015: Resilient Coastal Communities* 442-450.

Chen, Q., Chakrabarti, A., Yu, H. (2014). Optimizing the design of shoreline protection to reduce marsh edge erosion for Louisiana coastal protection and restoration (CPRA-2013-TO11-SB01-DR).

CIRIA, CUR, CETMEF (2007). The Rock Manual. The use of rock in hydraulic engineering. 2nd Edition. C683, CIRIA, London.

Coast and Harbor Engineering (2013). Living Shoreline Demonstration Project, Data Collection Summary and New Data Collection Plan Technical Memorandum. January 24, 2013.

Coast and Harbor Engineering (2014). Living Shoreline Demonstration Project, Coastal Engineering and Alternatives Analysis. October 9, 2014.

Coast and Harbor Engineering (2015). Living Shoreline Demonstration Project, PO-148. Project Drawings. September 24, 2015.

Coastal Protection and Restoration Authority of Louisiana (2016). A Contractor's Guide to the Standards of Practice. For CPRA Contractors Performing GPS Surveys and Determining GPS Derived Orthometric Heights within the Louisiana Coastal Zone. March 2016.

Coastal Protection and Restoration Authority of Louisiana (2017). Louisiana's Comprehensive Master Plan for a Sustainable Coast. Coastal Protection and Restoration Authority of Louisiana. Baton Rouge, LA.

Coastal Protection and Restoration Authority of Louisiana (2018). Coastwide Reference Monitoring System-Wetlands Monitoring Data. Retrieved from Coastal Information Management System (CIMS) database. http://cims.coastal.louisiana.gov. Accessed 10 March 2018.

Coen, L.D., Brumbaugh, R.D., Bushek, D., Grizzle, R., Luckenbach, M.W., Posey, M.H., Powers, S.P., and Tolley, S.G. (2007). Ecosystem services related to oyster restoration. *Marine Ecology-Progress Series* 341: 303-307.

Couvillion, B.R., Barras, J.A., Steyer, G.D., Sleavin, W., Fischer, M., Beck, H., Trahan, N., Griffin, B., and Heckman, D. (2011). Land area change in coastal Louisiana from 1932 to 2010: U.S. Geological Survey Scientific Investigations Map 3164, scale 1:265,000, 12 p. pamphlet.

Dean, R.G. and Dalrymple, R.A. (1991). *Water Wave Mechanics For Engineers and Scientists*. Advanced Series on Ocean Engineering – Volume 2. World Scientific.

Franzius, L. (1965). Wirkung und Wirtschaftlichkeit von Rauhdeckwerden im Hinblick auf den Wellenauflauf. Mitteilungen des Franzius-Instituts fur Grund-und Wasserbau der TH Hannover, Heft 25, pp. 149-268 (in German).

Furlong, J.N. (2012). Artificial oyster reefs in the northern Gulf of Mexico: management, materials, and faunal effects. M.S. Thesis. Louisiana State University. pp. 109.

Goda, Y., Takeda, H., and Moriya, Y. (1967). Laboratory Investigation on Wave Transmission over Breakwaters. Port and Harbour Technical Research Institute, Report No. 13, Ministry of Transport, Yokosuka, Japan.

Hasselmann, K., Barnett, T.P., Bouws, E., Carlson, H., Cartwright, D.E., Enke, K., Ewing, J.A., Gienapp, H., Hasselmann, D.E., Kruseman, P., Meerburg, A., Muller, P., Olbers, D.J., Richter, K., Sell, W., and Walden, H. (1973). Measurements of wind-wave growth and swell decay during the Joint North Sea Wave Project (JONSWAP). Deutsche Hydrographische Zeitschrift A80(12), 95p.

Holthuijsen, L.H. (2007). *Waves in Oceanic and Coastal Waters*. Cambridge University Press.

Jeffreys, H. (1944). Note on the Offshore Bar Problem and Reflection from a Bar. Great Britain. Ministry of Supply, Wave Report 3.

Kamphuis, J. W. (2010). *Introduction to Coastal Engineering and Management*. Advanced Series on Ocean Engineering – Volume 30. World Scientific.

Karimpour, A. (2015). OCEANLYZ, Ocean Wave Analyzing Toolbox, user manual, http://www.arashkarimpour.com/download.html.

Karimpour, A. and Chen, Q. (2016). A simplified parametric model for fetch-limited peak wave frequency in shallow estuaries. Journal of Coastal Research, 32(4), 954–965. Coconut Creek (Florida), ISSN 0749-0208.

Karimpour, A., Chen, Q., and Twilley, R. (2016). A Field Study of How Wind Waves and Currents May Contribute to the Deterioration of Saltmarsh Fringe. *Estuaries and Coasts* 39(4), 935–950.

Karimpour, A. and Chen, Q. (2017). Wind wave analysis in depth limited water using OCEANLYZ, A MATLAB toolbox. *Computers & Geosciences*, 106, 181-189.

Karimpour, A., Chen, Q., and Twilley, R. (2017). Wind Wave Behavior in Fetch and Depth Limited Estuaries. Scientific Reports 7:40654; DOI: 10.1038/srep40654.

La Peyre, M. K., Schwarting, L., and Miller, S. (2013). Preliminary assessment of bioengineered fringing shoreline reefs in Grand Isle and Breton Sound, Louisiana: U.S. Geological Survey Open-File Report 2013–1040, pp. 34.

Leonardi, N., Ganju, N. K., and Fagherazzi, S. (2016). A linear relationship between wave power and erosion determines salt-marsh resilience to violent storms and hurricanes. *Proceedings of the National Academy of Sciences*, 113(1), 64-68.

Marani, M., dAlpaos, A., Lanzoni, S. and Santalucia, M. (2011). Understanding and predicting wave erosion of marsh edges. *Geophysical Research Letters*, 38(21).

McMann, B., Schulze, M., Sprague, H, and Smyth, K. (2017). 2017 Coastal Master Plan: Appendix A: Project Definition. Version Final. (pp.1- 119). Baton Rouge, Louisiana: Coastal Protection and Restoration Authority.

Melancon, E.J. Jr., Curole, G.P., Ledet, A.M., and Fontenot, Q.C. (2013). 2013 Operations, Maintenance, and Monitoring Report for Terrebonne Bay Shore Protection Demonstration (TE-45), Coastal Protection and Restoration Authority of Louisiana, Thibodaux, Louisiana. pp. 75 and Appendices.

NOAA. (2012). http://www.ndbc.noaa.gov/.

NOAA. (2013). http://vdatum.noaa.gov/.

NOAA. (2015). Guidance for Considering the Use of Living Shorelines. Available at http://www.habitat.noaa.gov/pdf/noaa_guidance_for_considering_the_use_of_living_shorelines_2015.pdf.

NOAA. (2018). https://tidesandcurrents.noaa.gov/stationhome.html?id=8761305.

OSSI-010-003 Wave Gauge User Manual. (2015). Ocean Sensor systems, Inc. Coral Springs, FL. USA.

Parker, K.R. (2014). Field and numerical investigation of wave power and shoreline retreat in Terrebonne Bay, Southern Louisiana. M.S. Thesis. Louisiana State University.

Penland, S., Wayne, L., Britsch, D., Williams, S.J., Beall, A., and Butterworth, V., (2000). Process classification of coastal land loss between 1932 and 1990 in the Mississippi River delta plain, southeastern, Louisiana, U.S Geological Survey Open-File Report 00-418.

Piazza, B. P., Banks, P.D., and La Peyre, M.K. (2005). The potential for created oyster shell reefs as a sustainable shoreline protection strategy in Louisiana. *Restoration Ecology* 13: 499–506.

Plunket, J.T. and La Peyre, M.K. (2005). Oyster beds as fish and macroinvertebrate habitat in Barataria Bay, Louisiana. *Bulletin of Marine Science* 77: 155–164.

Scyphers, S.B., Powers, S.P., Heck, K.L. Jr., and Byron, D. (2011). Oyster reefs as natural breakwaters mitigate shoreline loss and facilitate fisheries. *PLoS ONE* 6(8): e22396. Doi:101371/journal.pone.0022396.

Seelig, W.N. (1980). Two-deimensional tests of wave transmission and reflection characteristics of laboratory breakwaters. TR 801-, USACE, CERC, Fort Belvoir, VA.

Sharma, S., Goff, J., Cebrian, J., and Ferraro, C. (2016). A hybrid shoreline stabilization technique: Impact of modified intertidal reefs on marsh expansion and nekton habitat in the northern Gulf of Mexico. *Ecological Engineering* (90), 352-360.

Soniat, T. M., Finelli, C.M., and Ruiz, J.T. (2004). Vertical structure and predator refuge mediate oyster reef development and community dynamics. *Journal of Experimental Marine Biology and Ecology* 310: 163-182.

Teh, H. (2013). *Hydrodynamic performance of free surface semicircular breakwaters*. Ph.D. Thesis, The University of Edinburgh.

Thompson, E. F., and Vincent, C.L. (1985). Significant wave height for shallow water design. *Journal of Waterway, Port, Coastal, and Ocean Engineering*. 111(5) 828-842.

Tides and Currents, NOAA. (2013). http://tidesandcurrents.noaa.gov/data_menu.shtml?stn=8747437%20Bay%20Waveland%20Yacht%20Club,%20MS&type=Datums.

U.S. Army Corps of Engineers. (2008). *Coastal Engineering Manual*. Engineering Manual 1110-2-1100, U.S. Army Corps of Engineers, Washington D.C.

van der Meer, J.W., Wind, H.G., Zanuttigh, R., and Wang, B. (2005). Wave transmission and reflection at low-crested structures: design formulae, oblique wave attack and spectral change. *Coastal Engineering*, 52, 915–029.

Wall, C.C., Peterson, B.J., and Gobler, C.G. (2011). The growth of estuarine resources (*Zostera marina, Mercinaria mercenaria, Crassotrea virginica, Argopecten irradians, Cyprinodon variegatus)* in response to nutrient loading and enhanced suspension feeding by adult shellfish. *Estuaries and Coasts* 34: 1262-1277.

Wave Information Studies. (2012). http://wis.usace.army.mil/hindcasts.shtml?dmn=gomWIS.

Webb, B.M. and Allen, R. (2015). Wave transmission through artificial reef breakwaters. *Coastal Structures and Solutions to Coastal Disasters 2015: Resilient Coastal Communities* 432-441.

Young, I.R. and Verhagen, L.A. (1996). The growth of fetch limited waves in water of finite depth. part i : Total energy and peak frequency. *Coastal Engineering*, (29), 47–78.

YSI. (2017). https://www.ysi.com/.

YSI Environmental User's Manual. (2012). 6-Series Multiparameter Water Quality Sondes, Revision J. Yellow Springs, OH: YSI, Incorporated.

Zu Ermgassen, P.S., Spalding, M.D., Grizzle, R.E., and Brumbaugh, R.D. (2012). Quantifying the loss of a marine ecosystem service: filtration by the eastern oyster in US estuaries. *Estuaries and Coasts* 36:36–43 DOI 10.1007/s12237-012-9559-y.

APPENDIX A

EQUIPMENT DATASHEETS

Trimble R10

GNSS SYSTEM

A NEW LEVEL OF PRODUCTIVITY

Collect more accurate data faster and easier – no matter what the job or the environment, with the Trimble® R10 GNSS System. Built with powerful technologies integrated into a sleek design, this unique system provides Surveyors with a powerful way to increase productivity in every job, every day.

Trimble HD-GNSS Processing Engine

The advanced Trimble HD-GNSS processing engine provides markedly reduced convergence times as well as high position and precision reliability while reducing measurement occupation time. Transcending traditional fixed/float techniques, it provides a more accurate assessment of error estimates than traditional GNSS technology.

Trimble SurePoint

With Trimble SurePoint™ technology, advanced sensors onboard the Trimble R10 continuously stream pole tilt and heading information that is used to display an electronic level bubble on the Trimble controller screen, allowing surveyors to maintain focus where it matters most. Full tilt compensation allows the survey pole to be tilted up to 15° when measuring, allowing the Trimble R10 to capture points that would be inaccessible to other GNSS surveying systems.

Trimble 360 Receiver

Powerful Trimble 360 receiver technology in the Trimble R10 supports signals from all existing and planned GNSS constellations and augmentation systems. With two integrated Trimble Maxwell™ 6 chips, the Trimble R10 offers 440 GNSS channels.

Trimble CenterPoint RTX

Trimble CenterPoint® RTX delivers RTK level precision anywhere in the world without the use of a local base station or VRS network. Survey using satellite delivered, CenterPoint RTX corrections in areas where terrestrial based corrections are not available. When surveying over a great distance in a remote area, such as a pipeline or utility right of way, CenterPoint RTX eliminates the need to continuously move base stations or maintain connection to a cellular network.

Trimble xFill

Leveraging a worldwide network of Trimble GNSS reference stations and satellite datalinks, Trimble xFill® seamlessly fills in for gaps in your RTK or VRS connection stream. Maintain centimeter level accuracy beyond five minutes with a CenterPoint RTX subscription.

Smart, Versatile

A smart lithium-ion battery inside the Trimble R10 system delivers extended battery life and more reliable power. A built-in LED battery status indicator allows the user to quickly check remaining battery life.

The Trimble R10 system provides a number of communications options to support any workflow. Receive VRS corrections and connect to the Internet from the field with the integrated cellular modem. Using Wi-Fi, easily connect to the Trimble R10 system using a laptop or smartphone to configure the receiver without a Trimble controller.

The Complete Solution

Bring the power and speed of the Trimble R10 system together with trusted Trimble software solutions, including Trimble Access™ and Trimble Business Center.

Trimble Access field software provides specialized and customized workflows to make surveying tasks quicker and easier while enabling teams to communicate vital information between field and office in real time. Back in the office, users can seamlessly process data with Trimble Business Center software.

Key Features

- Cutting-edge Trimble HD-GNSS processing engine
- Precise position capture and full tilt compensation with Trimble SurePoint technology
- Trimble CenterPoint RTX provides RTK level precision anywhere without the need for a base station or VRS network
- Trimble xFill technology provides centimeter-level positioning during connection outages
- Advanced satellite tracking with Trimble 360 receiver technology
- Sleek ergonomic design for easier handling

PERFORMANCE SPECIFICATIONS		
MEASUREMENTS		
	Measuring points sooner and faster with Trimble HD-GNSS technology	
	Increased measurement productivity and traceability with Trimble SurePoint electronic tilt compensation	
	Worldwide centimeter level positioning using Trimble CenterPoint RTX satellite delivered corrections	
	Reduced downtime due to loss of radio signal with Trimble xFill technology	
	Advanced Trimble Maxwell 6 Custom Survey GNSS chips with 440 channels	
	Future-proof your investment with Trimble 360 GNSS tracking	
	Satellite signals tracked simultaneously:	GPS: L1C/A, L1C, L2C, L2E, L5 GLONASS: L1C/A, L1P, L2C/A, L2P, L3[1] SBAS: L1C/A, L5 (For SBAS satellites that support L5) Galileo: E1, E5A, E5B, E5 AltBOC BeiDou (COMPASS): B1, B2, B3[2]
	CenterPoint RTX, OmniSTAR® HP, XP, G2, VBS positioning	
	QZSS, WAAS, EGNOS, GAGAN, MSAS	
	Positioning Rates	1 Hz, 2 Hz, 5 Hz, 10 Hz, and 20 Hz
POSITIONING PERFORMANCE[3]		
CODE DIFFERENTIAL GNSS POSITIONING		
	Horizontal	0.25 m + 1 ppm RMS
	Vertical	0.50 m + 1 ppm RMS
	SBAS differential positioning accuracy[4]	typically <5 m 3DRMS
STATIC GNSS SURVEYING		
High-Precision Static		
	Horizontal	3 mm + 0.1 ppm RMS
	Vertical	3.5 mm + 0.4 ppm RMS
STATIC AND FAST STATIC		
	Horizontal	3 mm + 0.5 ppm RMS
	Vertical	5 mm + 0.5 ppm RMS
REAL TIME KINEMATIC SURVEYING		
Single Baseline <30 km		
	Horizontal	8 mm + 1 ppm RMS
	Vertical	15 mm + 1 ppm RMS
Network RTK[5]		
	Horizontal	8 mm + 0.5 ppm RMS
	Vertical	15 mm + 0.5 ppm RMS
RTK start-up time for specified precisions[6]		2 to 8 seconds
TRIMBLE RTX (SATELLITE AND CELLULAR/INTERNET (IP))		
CenterPoint RTX		
	Horizontal	4 cm RMS
	Vertical	9 cm RMS
	RTX convergence time for specific precisions[7]	< 30 min (typical)
	RTX QuickStart convergence time for specific precisions[7]	< 5 min (typical)
	Operating range (inland)	Nearly worldwide
CenterPoint RTX Fast		
	Horizontal	2 cm RMS
	Vertical	5 cm RMS
	RTX convergence time for specific precisions[7]	1-5 min (typical)
	Operating range (inland)	In select regions
TRIMBLE XFILL[8]		
	Horizontal	RTK[9] + 10 mm/minute RMS
	Vertical	RTK[9] + 20 mm/minute RMS

HARDWARE		
PHYSICAL		
Dimensions (W×H)	11.9 cm x 13.6 cm (4.6 in x 5.4 in)	
Weight	1.12 kg (2.49 lb) with internal battery, internal radio with UHF antenna, 3.57 kg (7.86 lb) items above plus range pole, controller & bracket	
Temperature[10]		
	Operating	−40° C to +65° C (−40° F to +149° F)
	Storage	−40° C to +75° C (−40° F to +167° F)
Humidity		100%, condensing
Ingress Protection		IP67 dustproof, protected from temporary immersion to depth of 1 m (3.28 ft)
Shock and vibration (Tested and meets the following environmental standards)		
	Shock	Non-operating: Designed to survive a 2 m (6.6 ft) pole drop onto concrete. Operating: to 40 G, 10 msec, sawtooth
	Vibration	MIL-STD-810F, FIG.514.5C-1
ELECTRICAL		
	Power 11 to 24 V DC external power input with over-voltage protection on Port 1 and Port 2 (7-pin Lemo)	
	Rechargeable, removable 7.4 V, 3.7 Ah Lithium-ion smart battery with LED status indicators	
	Power consumption is 5.1 W in RTK rover mode with internal radio[11]	
Operating times on internal battery[12]		
	450 MHz receive only option	5.5 hours
	450 MHz receive/transmit option (0.5 W)	4.5 hours
	450 MHz receive/transmit option (2.0 W)	3.7 hours
	Cellular receive option	5.0 hours
COMMUNICATIONS AND DATA STORAGE		
	Serial	3-wire serial (7-pin Lemo)
	USB v2.0	Supports data download and high speed communications
	Radio Modem	Fully Integrated, sealed 450 MHz wide band receiver/transmitter with frequency range of 403 MHz to 473 MHz, support of Trimble, Pacific Crest, and SATEL radio protocols:
		Transmit power: 2 W
		Range: 3–5 km typical / 10 km optimal[13]
	Cellular	Integrated, 3.5 G modem, HSDPA 7.2 Mbps (download), GPRS multi-slot class 12, EDGE multi-slot class 12, UMTS/HSDPA (WCDMA/FDD) 850/1900/2100MHz, Quad-band EGSM 850/900/1800/1900 MHz, GSM CSD, 3GPP LTE
	Bluetooth	Fully integrated, fully sealed 2.4 GHz communications port (Bluetooth®)[14]
	Wi-Fi	802.11 b,g, access point and client mode, WPA/WPA2/WEP64/WEP128 encryption
	USB v2.0	Supports data download and high speed communications
	External communication devices for corrections supported on	Serial, USB, TCP/IP and Bluetooth ports
	Data storage	4 GB internal memory; over seven years of raw observables (approx. 1.4 MB /day), based on recording every 15 seconds from an average of 14 satellites
	CMR+, CMRx, RTCM 2.1, RTCM 2.3, RTCM 3.0, RTCM 3.1, RTCM 3.2 input and output	
	24 NMEA outputs, GSOF, RT17 and RT27 outputs	

Trimble R10 GNSS SYSTEM

COMMUNICATIONS AND DATA STORAGE	
WEBUI	
	Offers simple configuration, operation, status, and data transfer
	Accessible via Wi-Fi, Serial, USB, and Bluetooth
SUPPORTED TRIMBLE CONTROLLERS	
	Trimble TSC3, Trimble Slate, Trimble CU, Trimble Tablet Rugged PC
CERTIFICATIONS	
	IEC 60950-1 (Electrical Safety); FCC OET Bulletin 65 (RF Exposure Safety); FCC Part 15.105 (Class B), Part 15.247, Part 90; PTCRB (AT&T); Bluetooth SIG; WFA IC ES-003 (Class B); Radio Equipment Directive 2014/53/EU, RoHS, WEEE; Australia & New Zealand RCM; Japan Radio and Telecom MIC

1 There is no public GLONASS L3 CDMA ICD. The current capability in the receivers is based on publicly available information. As such, Trimble cannot guarantee that these receivers will be fully compatible with a future generation of GLONASS satellites or signals.
2 Current BeiDou capability is based on publicly available information. The hardware of this product is designed for BeiDou B3 compatibility (trial version) and its firmware will be enhanced, where possible, to fully support such new signals as soon as the officially published signal interface control documentation (ICD) becomes available. As such, Trimble cannot guarantee full compatibility with future generations of BeiDou satellites or signals.
3 Precision and reliability may be subject to anomalies due to multipath, obstructions, satellite geometry, and atmospheric conditions. The specifications stated recommend the use of stable mounts in an open sky view, EMI and multipath clean environment, optimal GNSS constellation configurations, along with the use of survey practices that are generally accepted for performing the highest-order surveys for the applicable application including occupation times appropriate for baseline length. Baselines longer than 30 km require precise ephemeris and occupations up to 24 hours may be required to achieve the high precision static specification.
4 Depends on WAAS/EGNOS system performance.
5 Network RTK PPM values are referenced to the closest physical base station.
6 May be affected by atmospheric conditions, signal multipath, obstructions and satellite geometry. Initialization reliability is continuously monitored to ensure highest quality.
7 Receiver convergence time varies based on GNSS constellation health, level of multipath, and proximity to obstructions such as large trees and buildings. Convergences times decrease significantly when using a "RTX Quickstart" on a previously surveyed point or a known survey control point.
8 Precisions are dependent on GNSS satellite availability. xFill positioning without a RTX subscription ends after 5 minutes of radio downtime. xFill positioning with a RTX subscription will continue beyond 5 minutes providing RTX has converged, with typical precisions not exceeding 6 cm horizontal, 14 cm vertical. xFill is not available in all regions, check with your local sales representative for more information.
9 RTK refers to the last reported precision before the correction source was lost and xFill started.
10 Receiver will operate normally to –40° C, internal batteries are rated to –20° C.
11 Tracking GPS, GLONASS and SBAS satellites.
12 Varies with temperature and wireless data rate. When using a receiver and internal radio in the transmit mode, it is recommended that an external 6 Ah or higher battery is used.
13 Varies with terrain and operating conditions.
14 Bluetooth type approvals are country specific.

Specifications subject to change without notice.

Contact your local Trimble Authorized Distribution Partner for more information

NORTH AMERICA
Trimble Inc.
10368 Westmoor Dr
Westminster CO 80021
USA

EUROPE
Trimble Germany GmbH
Am Prime Parc 11
65479 Raunheim
GERMANY

ASIA-PACIFIC
Trimble Navigation
Singapore Pty Limited
80 Marine Parade Road
#22-06, Parkway Parade
Singapore 449269
SINGAPORE

PN 022543-544I (08/17)

Trimble TSC3 Controller

Key Features

Large, bright, high-resolution screen makes instrument control easy

Optimized for Trimble Access field software

Fully-integrated camera, GPS navigation, and communications

Improved collaboration and control through **constant connectivity**

The Trimble® TSC3 controller with Trimble Access™ software is a groundbreaking handheld field computing solution that streamlines the flow of everyday surveying work and the number of devices you need in the field.

A POWERFUL ENGINE FOR DRIVING TRIMBLE ACCESS SOFTWARE

Part of a trusted line of field controllers, the Trimble TSC3 controller is rugged and designed for surveyor's workflows. It performs Trimble Access operations fast and delivers ample power to run third-party applications on the Windows® platform.

Make Pictures an Essential Part of Your Workflow

With a built-in 5 MP Autofocus camera and LED flash, you can take digital photographs of your job site right from the controller. No extra devices, batteries, or file transfers are required, and images are automatically geotagged for easy identification.

Easily record the qualitative information that survey data alone can miss, such as site conditions or work progress. The benefits of including images as part of your workflow are almost limitless: from easy data handover to in-field quality assurance.

Communications that Bridge Field and Office in Real-Time

The TSC3 controller enables wireless Internet connectivity through an integrated GSM/GPRS/CDMA2 modem. This allows Trimble Access software to facilitate a constant flow of information between field and office, including real-time synchronization of field and office data with Trimble AccessSync software. You can download and upload important files any time and from anywhere, as needed. Data collection, processing, analysis, and delivery are faster and more efficient.

A wealth of communication options let you transfer critical information no matter the environment: Connect with VRS™ connections using the internal modem. Access your office network through 802.11 LAN, or USB and serial RS232 communication options.

For All of Your Surveying Applications

The rugged TSC3 controller is purpose-built to make both Integrated Surveying and Spatial Imaging jobs easier, more efficient, and more flexible:

Easy-to-Use Interface

Control your survey and verify your work on the large, bright, high-resolution LCD touchscreen. With the option of a QWERTY or conventional alpha-numeric keyboard, data entry is quick and easy.

An Internal Compass

Receive direction cues even when you are stationary or moving backwards.

Integrated GPS

Employ GPS Search on a conventional survey without an external GPS receiver. You can also navigate and find control points and other assets quickly.

Cables Eliminated

Bluetooth® wireless technology eliminates cables in surveying systems. An internal 2.4 GHz radio option is also ideal for controlling Trimble robotic systems.

Designed to Support Your Daily Workflows

Trimble Access field software available on the TSC3 controller offers numerous features and capabilities to streamline the flow of everyday surveying work. Streamlined workflows – such as Roads, Monitoring, Mines, and Tunnels —guide crews through common project types and allows crews to get the job done faster with less distractions.

Survey companies can also implement their unique workflows by taking advantage of the customization capabilities available in the Trimble Access Software Development Kit (SDK). The Trimble Access SDK provides software developers with the tools to customize and extend Trimble Access.

With a bright, daylight readable display, integrated communications, and integrated survey workflows, the fully integrated TSC3 controller will make your field work more efficient.

Trimble

Trimble TSC3 Controller

TECHNICAL SPECIFICATIONS

Standard software

Windows Embedded Handheld 6.5 Professional operating system, including:

- SMS Text Messaging Support
- Microsoft Office Mobile:
  - Word Mobile
  - Excel Mobile
  - PowerPoint Mobile
  - Outlook Mobile
- Internet Explorer Mobile
- Notes / Tasks
- Task Manager
- Calculator
- Microsoft Pictures and Videos
- Customized Camera and Flash control including geo-tagging through Microsoft Pictures & Videos software
- Flashlight mode control application
- Calendar / Contacts
- Windows Media Player
- Messenger
- Adobe Acrobat Reader
- Trimble SatViewer (GPS interface software application)

Operating system languages options (customer provisionable):
Simplified Chinese, English, French, German, Japanese, Spanish

Trimble Field Software Solutions

The Trimble TSC3 controller runs the Trimble Access field software. In addition, a number of regional solutions are available. For more information on the field software that's best for you, contact your local Trimble authorized distribution partner.

Standard Accessories (included)

- 28.9 Wh Li-Ion battery
- International AC power supply
- Hand strap
- USB cable (mini)
- Stylus tether
- Stylus with spring tip (pkg of 2)
- Screen protectors
- Audio port dust cover
- I/O port dust covers
- Standard soft case
- Quick start guide sheet
- Radio antenna for integrated 2.4 GHz radio modem (optional)

Optional Accessories

- Deluxe carry case
- Individual battery charger
- Range pole bracket
- 12 V vehicle charging kit
- Desk docking cradle with USB host, USB client, and 10/100 Mbps Ethernet connections

All standard accessories are also available to order separately.

HARDWARE

Physical Specifications

Size . . . . . 141 mm x 278 mm x 64 mm (5.6 in x 10.9 in x 2.5 in)
80 mm (3.2 in) at handgrip

Weight . . . . . 1.04 kg (2.3 lb) including rechargeable battery
1.10 kg (2.4 lb) including rechargeable battery and optional internal 2.4 GHz radio-modem

Housing . . . . . Polycarbonate (case), Hytrel® (overmold)

ENVIRONMENTAL SPECIFICATIONS

Meets or exceeds:

Operating Temperature . . . . . –30 °C to 60 °C (–22 °F to 140 °F)

Storage Temperature . . . . . –40 °C to 70 °C (–40 °F to 158 °F)

Temperature shock . . . . . –35 °C/65 °C (–31 °F/149 °F)
MIL-STD-810G, Method 503.5, Procedure I

Humidity . . . . . 90%RH temp cycle –20 °C/60 °C (–4 °F/140 °F)
MIL-STD-810G, Method 507.5

Sand & dust . . . . . IP6x: 8 hours of operation with blowing talcum powder (IEC-529)

Water . . . . . IPx7: Immersed in 1 m of water for 30 minutes (IEC-529)

Drop . . . . . 26 drops at room temperature from 1.22 m (4 ft) onto plywood over concrete
MIL-STD-810G, Method 516.6, Procedure IV

Vibration . . . . . General Minimum Integrity and Loose Cargo test
MIL-STD 810G, Method 514.6, Procedures I, II

Altitude . . . . . 4,572 m (15,000 ft) at 23 °C (73 °F)
and 12,192m (40,000 ft.) at –30 °C (–22 °F)
MIL-STD-810G, Method 500.5, Procedures I, II, III

ELECTRICAL SPECIFICATIONS

- Processor: Texas Instrument Sitara™ 3715 series ARM® Cortex™–A8 Processor (800 MHz)
- Memory: 256 MB RAM
- Storage: 8 GB non-volatile NAND Flash onboard
- Expansion: SDHC memory slot, USB host internal embedded expansion slot (for future use)
- Batteries: 11.1 V, 2600 mAh, 28.9 Wh Li-Ion rechargeable pack
  - Battery life of 34 hours under normal operating conditions[1].
  - Full charge in 3.0 hours.
- Notification LEDs: 3 x tri-colored notification LEDs
- Display:
  - 4.2 in (107 mm) landscape VGA display, 640 x 480 pixels
  - Sunlight-readable color TFT with LED backlight, resistive touchscreen
- Keyboard:
  - Full QWERTY keypad with 10-key number pad, directional buttons, and 4 programmable buttons
  - "ABCD" style keypad option with 10-key number pad, directional buttons, and 4 programmable buttons available
- Audio: Integrated speaker and microphone with 3.5 mm stereo headset connection for audio system events, warnings, and notifications.
- I/O: USB Host (full speed), USB Client (high speed), DC power port, 9-pin serial RS-232
- Wireless:
  - Integrated Bluetooth 2.0+EDR, integrated Wi-Fi 802.11 b/g
  - Integrated quad-band GSM/GPRS/EDGE: 850/900/1800/1900 MHz
  - 2/6 Mbit/s 3G HSDPA GSM WWAN
  - Integrated 2.4 GHz frequency-hopping spread-spectrum radio modem (optional)
  - Dual band CDMA2000 in Bands BC0 and BC1 (800/900MHz)[2]
- Camera / GPS / Compass / Accelerometer:
  - 5 MP auto focus camera with dual white light LED flash, LED flashlight function
  - Integrated GPS (WAAS enabled)
  - Integrated compass
  - Integrated accelerometer

CERTIFICATIONS

Class B Part 15 FCC certification, CE Mark approval and C-tick approval. RoHS compliant. Bluetooth type approvals and regulations are country specific.
MIL-STD-810G, IP 67, MIL-STD-461, PTCRB, GCF compliant, Wi-Fi Alliance certified, AT&T Network Compatible.
Country type certifications: USA, Canada, EU, New Zealand, Australia, Brazil.
Pending certifications: Malaysia, China (PRC), India, Japan, Republic of Korea, Russia, Taiwan, Thailand, UAE

RECYCLING INFORMATION

For product recycling instructions and more information, please go to www.trimble.com/environment/summary.html.

1 Unit is idle with backlight turned on, no radios turned on, moderate temperatures.
2 CDMA modem only supports the Verizon network (USA).

Specifications subject to change without notice.

TRIMBLE AUTHORIZED DISTRIBUTION PARTNER

NORTH AMERICA
Trimble Navigation Limited
10368 Westmoor Dr
Westminster CO 80021
USA

EUROPE
Trimble Germany GmbH
Am Prime Parc 11
65479 Raunheim
GERMANY

ASIA-PACIFIC
Trimble Navigation
Singapore Pty Limited
80 Marine Parade Road
#22-06, Parkway Parade
Singapore 449269
SINGAPORE

ODOM

HYDROTRAC™

odom
HYDROGRAPHIC SYSTEMS

- IDEAL FOR SMALL BOATS AND HARSH CONDITIONS
- FREQUENCY AGILE
- HIGH RESOLUTION THERMAL PRINTER
- INTERNAL DGPS (OPTIONAL)
- WATERPROOF
- FLASH UPGRADEABLE
- SIDE SCAN OPTION

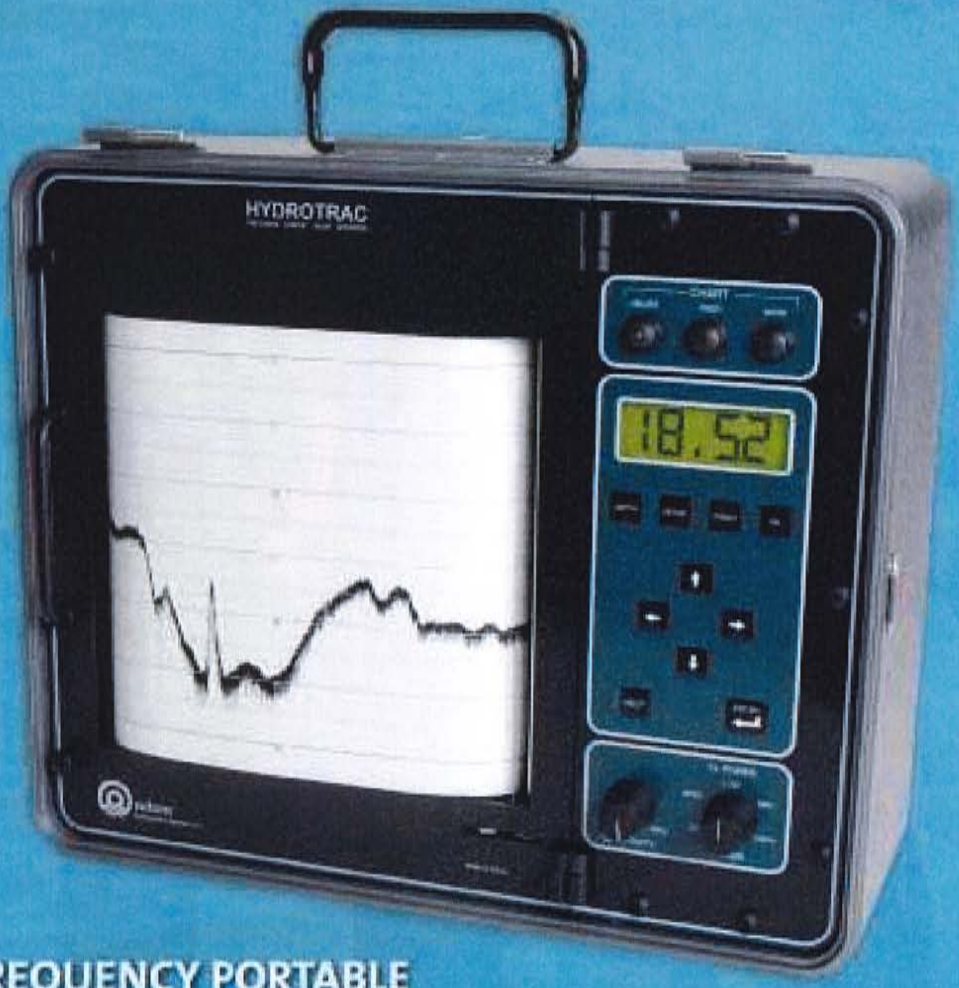

SINGLE FREQUENCY PORTABLE HYDROGRAHIC ECHO SOUNDER

ODOM HYDROTRAC™

Specifically designed for work in less-than-ideal circumstances on small survey boats and inflatable watercraft, the **Hydrotrac**™ offers compact portability and the confidence of knowing you're using a proven **Odom** product. It is completely waterproof and comes equipped with the same advanced features you've come to trust and depend on in **Odom** echo sounders.

Buy Odom – invest in your peace of mind.

SPECIFICATIONS

Frequency Agile
- Operator selectable – 24, 33, 40, 200, 210 and 340 kHz

Output Power
- 600 watts

Power Requirement
- 11-28 V DC (standard)

Resolution
- 0.1 ft / 0.01 m

Accuracy
- 200 kHz – 1 cm 0.1% of depth value (corrected for sound velocity)
- 33 kHz – 10 cm 0.1% of depth value (corrected for sound velocity)

Depth Range
- Max 600 m / 1968 ft

Environmental Operating Conditions:
- 0 – 50 C

Communication
- 2 RS232 or RS422 ports

Dimensions
- 368 mm (14.5 in) H x 419 mm (16.5 in) W x 203 mm (8 in) D

Weight
- Lightweight (24.8 lbs / 11.25 kg)

Features
- 8.5 in / 216 mm thermal printer (fax paper)
- Annotation printed on chart
- LCD display (1 inch high)
- Sealed keypad controls
- Manual/remote mark command
- Auto scale change (phasing)
- GPS input
- Heave input from motion sensor
- Auto pulse length TVG
- Output: NMEA, ECHOTRAC, DESO 25, etc.
- Waterproof (with cover in place)
- Fix mark annotation: date, time, fix no., depth (and GPS if input)
- Flash memory upgradeable
- Built-in simulator
- Software included: Comlog
- Operation and installation manuals provided on CD

Controls
- Sensitivity
- Chart ON/OFF and advance
- Event mark (internal selectable timer)
- Transmit power (high / med / low)

Touch Pad Settings
- Draft, velocity and tide inputs
- Time and date
- Scale width and center
- Blanking
- Calibration gate
- Alarm filter
- Fix interval
- Chart speed
- HELP function (prints on chart)
- Current parameters (prints on chart)

Options
- 200 kHz or 340 kHz side scan transducer
- Built-in DGPS
- Remote display

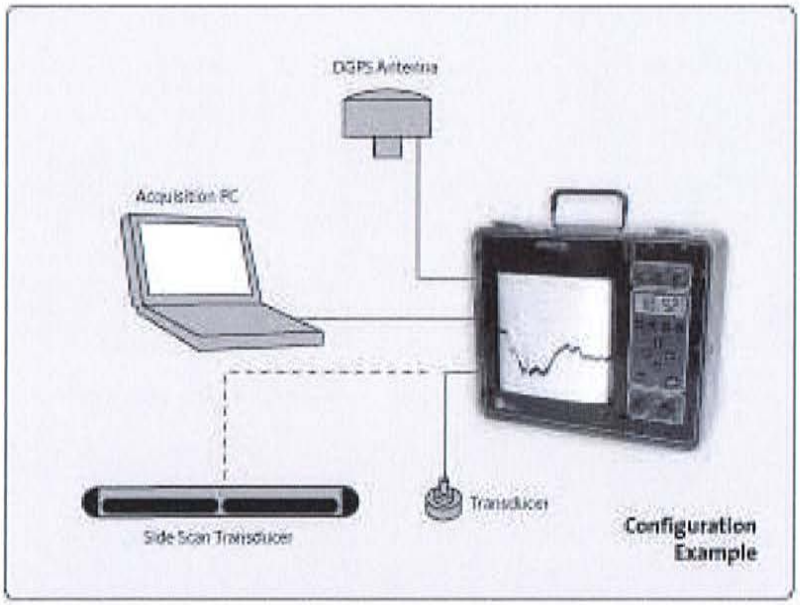

Configuration Example

odom
HYDROGRAPHIC SYSTEMS

1450 Seaboard Avenue
Baton Rouge, Louisiana 70810-6261 USA
E-mail: email@odomhydrographic.com
www.odomhydrographic.com

4/01/08

YSI 600LS Level Sonde

Precise level measurement

The YSI 600LS compact sonde measures level, flow, temperature, and conductivity. The 600LS will seamlessly integrate with the YSI 650MDS, laptop, or data collection platform.

With the 600LS, tide gauge measurements have never been so easy!

- **Sonde fits down 2-inch wells**
- **Easily connects to data collection platforms such as the YSI 6200 DAS**
- **Detachable cable lengths**
- **Compatible with the YSI 650 Multiparameter Display System**
- **Temperature/conductivity/vented level**
- **Optional battery compartment for unattended, internal logging**

Ideal for use with the YSI 6200 DAS, connecting via SDI-12 for remote and real-time data acquisition applications. Rugged waterproof, the YSI 600LS is perfect for tide gauge monitoring, wetlands level applications, groundwater, estuaries, rivers, and more.

Features

The YSI 600LS is an economical logging system for long-term, in situ monitoring. It logs at programmable intervals and stores 150,000 readings. The 600LS has extreme level accuracy of ±0.01 feet (0.003 m) from 0 to 30 foot depths.

Pure Data for a Healthy Planet.®

Precise Level Measurement in a Compact Sonde

To order, or for more information, contact YSI Environmental.

+1 937 767 7241

800 897 4151 (US)

www.ysi.com

YSI Environmental
+1 937 767 7241
Fax +1 937 767 9353
environmental@ysi.com

Endeco/YSI
+1 508 748 0366
Fax +1 508 748 2543
systems@ysi.com

SonTek/YSI
+1 858 546 8327
Fax +1 858 546 8150
inquiry@sontek.com

YSI Gulf Coast
+1 225 753 2650
Fax +1 225 753 8669
environmental@ysi.com

YSI Hydrodata (UK)
+44 1462 673 581
Fax +44 1462 673 582
europe@ysi.com

YSI Middle East (Bahrain)
+973 1753 6222
Fax +973 1753 6333
halsalem@ysi.com

YSI (Hong Kong) Limited
+852 2891 8154
Fax +852 2834 0034
hongkong@ysi.com

YSI (China) Limited
+86 10 5203 9675
Fax +86 10 5203 9679
beijing@ysi-china.com

YSI Nanotech (Japan)
+81 44 222 0009
Fax +81 44 221 1102
nanotech@ysi.com

ISO 9001
ISO 14001

Yellow Springs, Ohio Facility

Printed in USA 1206 E22-01

CE

YSI *incorporated*
Who's Minding the Planet?®

YSI 600LS Sensor Specifications

	Range	Resolution	Accuracy
Conductivity•	0 to 100 mS/cm	0.001 to 0.1 mS/cm (range dependent)	±0.5% of reading + 0.001 mS/cm
Salinity	0 to 70 ppt	0.01 ppt	±1% of reading or 0.1 ppt, whichever is greater
Temperature	-5 to +50°C	0.01°C	±0.15°C
Shallow Vented Level	0 to 30 ft, 9.1 m	0.001 ft, 0.001 m	±0.01 ft, 0.003 m

• Report outputs of specific conductance (conductivity corrected to 25° C), resistivity, and total dissolved solids are also provided. These values are automatically calculated from conductivity according to algorithms found in *Standard Methods for the Examination of Water and Wastewater* (ed 1989).

YSI 600LS Sonde Specifications

Medium	Fresh, sea or polluted water	Software	EcoWatch®
Temperature	-5 to +50°C	Dimensions Diameter Length (no batteries) Weight	1.65 in, 4.2 cm 15 in, 38 cm 1.10 lbs, 0.5 kg
Communications	RS-232, SDI-12	Power (optional)	4 AA-size alkaline batteries, or external 12 V DC

Ordering Information

600LS-10	Temperature, Shallow vented level
600LS-11	Temperature, Shallow vented level, Battery option
600LS-12	Temperature, Conductivity, Shallow vented level
600LS-13	Temperature, Conductivity, Shallow vented level, Battery option
Cables	
6195	10 ft vented detachable cable
6191	25 ft vented detachable cable
6192	50 ft vented detachable cable (Shallow vented level maximum depth is 30 feet.)

About Conductivity

The YSI 600LS is available with conductivity and without conductivity. In order to achieve the most accurate level measurements, it is highly recommended you use the **600LS-12** or **600LS-13** with conductivity if your application will require deployments in saline environments. Tidal, estuarine, salt water intrusion in groundwater, and freshwater/saltwater mixing zone studies are typical examples where a higher conductivity reading would require the conductivity sensor to achieve the most accurate, reliable level measurements.

As with all YSI products, there are several accessories available, from calibration solution to carrying cases, to keep your equipment protected and operating well. Please visit **www.ysi.com** or call **800-897-4151** for more information.

YSI 650 Multiparameter Display System

Rugged and Reliable Display and Data Logging System

The YSI 650 Multiparameter Display System

Easily log real-time data, calibrate YSI 6-Series sondes, set up sondes for deployment, and upload data to a PC with the feature-packed YSI 650MDS (Multiparameter Display System). Designed for reliable field use, this versatile display and data logger features a waterproof IP-67, impact-resistant case.

- **Compatible with EcoWatch® for Windows® data analysis software**
- **User-upgradable software from YSI's website**
- **Menu-driven, easy-to-use interface**
- **Multiple language capabilities**
- **Graphing feature**
- **Three-year warranty**

Feature-Packed Performance

Battery Life

With the standard alkaline battery configuration of 4 C-cells, the YSI 650 will power itself and a YSI 6600 sonde continuously for approximately 30 hours. Or, choose the rechargeable battery pack option with quick-charge feature.

Optional Barometer

Temperature-compensated barometer readings are displayed and can be used in dissolved oxygen calibration. Measurements can be logged to memory for tracking changes in barometric pressure.

Optional GPS Interface

Designed to NMEA protocol, the YSI 650 MDS will display and log real-time GPS readings with a user supplied GPS interfaced with YSI 6-Series sondes.

Memory Options

Standard memory with 150 data sets, or a high-memory option (1.5 MB) with more than 50,000 data sets; both options with time and date stamp.

Pure Data for a Healthy Planet.®

A powerful logging display for your data collection processes

The 650MDS can be used with YSI sondes for spot sampling as well as short-term data logging.

Supply a GPS with NMEA 0183 protocol, connect with the YSI 6115 kit, and collect GPS data along with water quality data.

Upload data from the 650 to EcoWatch® for instant data viewing.

YSI 650MDS Specifications

Temperature	Operating Storage	-10 to +60°C for visible display -20 to +70°C
Waterproof Rating		IP-67 for both the standard alkaline battery configuration and for the rechargeable battery pack option
Connector		MS-8; meets IP-67 specification
Dimensions	Width Length Weight with batteries	4.7 in, 11.9 cm 9 in, 22.9 cm 2.1 lbs, 0.91 kg
Display		VGA; LCD with 320 by 240 pixels with backlight
Power	Standard Optional	4 alkaline C-cells with detachable battery cover Ni metal hydride battery pack with attached battery cover and 110/220 volt charging system
Communications		RS-232 to all sondes, for data transfer to PC, and for software updates
Optional GPS		NMEA 0183; requires user-supplied GPS and YSI 6115 Y-cable
Backlight		4 LEDs illuminating LCD; user-selectable
Keypad		20 keys, including instrument on/off, backlight on/off, enter, esc, 10 number/letter entry keys, 2 vertical arrow keys, 2 horizontal arrow keys, period key, and minus key
Warranty		3 years

Ordering Information

650-01	Instrument, standard memory
650-02	Instrument, high memory
650-03	Instrument, standard memory, barometer
650-04	Instrument, high memory, barometer
6113	Rechargeable battery pack kit with 110 volt charger and adapter cable
616	Charger, cigarette lighter
4654	Tripod
614	Ultra clamp, C-clamp mount
5081	Carrying case, hard-sided
5085	Hands-free harness
5065	Form-fitted carrying case
6115	Y-cable for interface with user-supplied GPS system

The 650MDS can interface with any YSI sonde for
- *spot sampling*
- *short-term studies*
- *surface and ground water monitoring*
- *water level monitoring*

Packaged together, the 600QS system includes a 600R conductivity sonde, 650MDS, field cable, and additional sensor options such as pH, dissolved oxygen, ORP, and vented level.

To order, or for more information, contact YSI

+1 937 767 7241

800 897 4151 (US)

www.ysi.com

YSI Environmental
+1 937 767 7241
Fax +1 937 767 9353
environmental@ysi.com

YSI Integrated Systems & Services
+1 508 748 0366
Fax +1 508 748 2543
systems@ysi.com

SonTek/YSI
+1 858 546 8327
Fax +1 858 546 8150
inquiry@sontek.com

YSI Gulf Coast
+1 225 753 2650
Fax +1 225 753 8669
environmental@ysi.com

YSI Hydrodata (UK)
+44 1462 673 581
Fax +44 1462 673 582
europe@ysi.com

YSI Middle East (Bahrain)
+973 1753 6222
Fax +973 1753 6333
halsalem@ysi.com

YSI (Hong Kong) Limited
+852 2891 8154
Fax +852 2834 0034
hongkong@ysi.com

YSI (China) Limited
+86 10 5203 9675
Fax +86 10 5203 9679
beijing@ysi-china.com

YSI Nanotech (Japan)
+81 44 222 0009
Fax +81 44 221 1102
nanotech@ysi.com

ISO 9001
ISO 14001
Yellow Springs, Ohio Facility

Ocean Sensor Systems, Inc.

Wave Gauge, OSSI-010-003B/C

A Self Logging/Self Powered Pressure Sensor

General Description

The OSSI-010-003B/C Wave Gauge combines a highly stable Pressure Sensor, a Compact Flash Card Data Logger, a rugged waterproof package and 12 or 28 C size Alkaline Batteries. A Low Power Microprocessor records up to 2 Gigabytes of data on a Compact Flash Card in an ASCII or Binary format with time and date. Then the Card is easily removed and can be read on any PC with a standard Compact Flash Card Reader. The Logger will collect months of continuous data or years of burst data. A serial port is provided as a user interface to configure and monitor the Wave Gauge. Standard pressure ranges are 0 to 1 Bar, 0 to 3 Bars and 0 to 10 Bars.

Features

- **Standard Compact Flash Card Data Storage**
- **Data storage up to 2 Gigabytes**
- **Standard Card Reader Compatible**
- **Power with 12 or 28 C Size Alkaline Batteries**
- **Flush Hastelloy Diaphragm**
- **ABS Plastic Housing Rated to 100 Meters**
- **Months of Continuous Operation**
- **Years of Burst Operation**
- **Rugged Sealed Waterproof Design**
- **Fully Programmable via RS232**
- **PC Interface Software**
- **Binary or ASCII Data Format**
- **Sample Rate From 2 Hz to 30Hz**
- **Burst or Continuous Sampling**
- **Accuracy ± 0.05% FS, 10 to 40** °C
- **Resolution 0.0033%FS**
- **Long Term Stability ± 0.05%FS**
- **Optional Water Temperature Logging**

Dimensions and Ordering Information

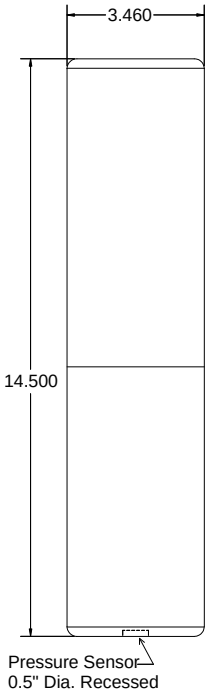

Pressure Range	Battery	Part Number
0 to 1 Bar (obsolete)	6 volt	OSSI-010-003B-01
0 to 3 Bars (obsolete)	6 volt	OSSI-010-003B-03
0 to 10 Bars (obsolete)	6 volt	OSSI-010-003B-10
0 to 1 Bar	18 volt	OSSI-010-003C-01
0 to 3 Bars	18 volt	OSSI-010-003C-03
0 to 10 Bars	18 volt	OSSI-010-003C-10
0 to 1 Bar Extended Case,	21 Volt	OSSI-010-003C-01E
0 to 3 Bars Extended Case	21 Volt	OSSI-010-003C-03E
0 to 10 Bars Extended Case	21 Volt	OSSI-010-003C-10E

Extended case for Dual 21V, 28 cell Battery Pack

Electrical Characteristics

Parameter	**Conditions**	Min.	Typ.	Max.	**Units**
Battery Voltage	6 V, 12 cell battery	3.6	6.0	7.0	VDC
	18V, 12 cell battery (4)	9	18	35	VDC
	21V, 28 cell battery (3)	9	21	35	VDC
Temperature Range		-10		65	°C
Battery Drain, Sleep Mode	6 V battery Pack		3		mW
	18V battery Pack (4)		3.4		mW
	21 V battery Pack (3)		3.5		mW
Battery Drain	Sleep mode with RS232 Monitoring (1)		15.0		mW
Battery Drain, Continuous Sampling	6 V battery Pack		74.0		mW
	18V battery Pack (4)		65.2		mW
	21 V battery Pack (3)		66.2		mW
Battery Drain	Continuous Sampling with RS232 Monitoring (1)		90.0		mW
Battery Type, See schematic below	Alkaline 6V		12		C Cells
	Alkaline 18V		12		C Cells
	Alkaline 21V		28		C Cells
Battery Life Continuous Sampling	6 V battery Pack		2.5		Month
	18V battery Pack (4)		3.0		Month
	21 V battery Pack (3)		6.5		Month
Battery Life 25% Sample (2)	6 V battery Pack		8.5		Month
	18V battery Pack (4)		9.7		Month
	21 V battery Pack (3)		21.7		Month
Battery Life 10% Sample (2)	6 V battery Pack		16.7		Month
	18V battery Pack (4)		17.8		Month
	21 V battery Pack (3)		40.3		Month

(1) Powered up External Monitoring PC connected to RS232 Serial port.
(2) Industrial Alkaline Batteries 12 C cells totaling 102 Watt hr. Typ. or 28 calls totaling 238 Watt hr. Typ.
(3) Only available with the extended Wave Gauge case (Identified with the letter E at the end of the Wave Gauge part number)
(4) Version C Wave Gauge only

The 6V 12 alkaline C cells are connected in a Series, parallel arrangement.

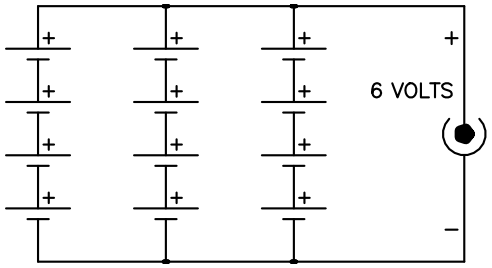

The 18V 12 alkaline C cells are connected in a Series.

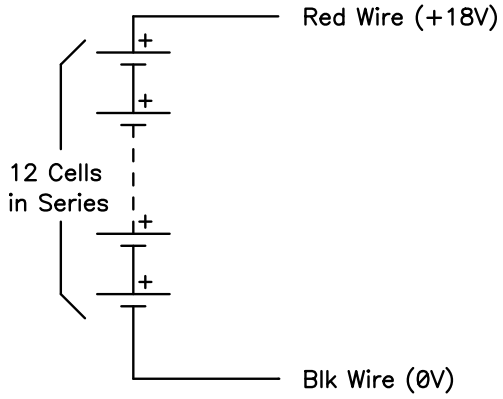

The 21V 28 alkaline C cells are connected in two groups of 14 cells connected in series.

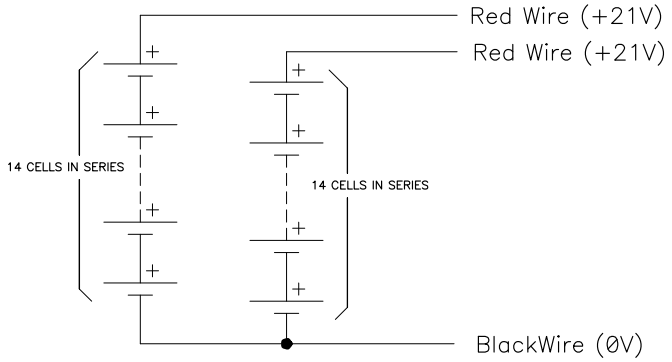

Data Characteristics, Pressure

Parameter	**Conditions**	Min.	Typ.	Max.	**Units**
Pressure Numeric (4) Format & Units	OSSI-010-003C-01			+.99999	Bars
Pressure Numeric Format & Units	OSSI-010-003C-03			+3.0000	Bars
Pressure Numeric Format & Units	OSSI-010-003C-10			+9.9999	Bars
Data Accuracy (1)(2)(3)	10 to 40 °C			0.05	±% FS
Data Accuracy (1)(2)(3)	-10 to 65 °C			0.1	±% FS
Data Resolution			0.0033		% FS
Long Term Stability	OSSI-010-003C-01		0.0005		Bar
Long Term Stability	OSSI-010-003C-03, -10		0.05		% FS

(1) Linearity + Hysteresis + Repeatability + Temperature Coefficients + Zero + Span Tolerance
(2) Accuracy and Resolution are valid for Basic Pressure Range
(3) Linearity: Best Straight Line
(4) The 1 bar unit data format when over full scale (greater than +.99999) reads 1.00000 to 1.25000

Data Characteristics, Temperature

Parameter	**Conditions**	Min.	Typ.	Max.	**Units**
Temperature Numeric Format & Units	0 to 62.4375 °C			+999	counts
Temperature Data Resolution	Per count from 0°C		0.0625		°C
Temperature Accuracy	-10°C to 65°C			1.25	± °C

Timing and Interfacing Characteristics

Parameter	**Conditions**	**Min.**	**Typ.**	**Max.**	**Units**
Sample Frequency	Programmable	2		30 (1)	Hz
Serial Baud Rate			9.6		Kbaud
Flash Card Size	FAT16 format	64		2000	Mbytes
Sample Capacity 2000 Mbyte Flash Card	Binary IEEE 754 ASCII data			468 232	Msamples
Sample Burst Time	Programmable	1		60	minutes
Sample Burst Interval	Programmable	1		60	minutes
New File Interval	Programmable	1		255	days
Real Time Clock Accuracy				20	ppm

(1) Either Serial Output or Air Temperature must be off for 30 Hz sample rate.

Battery Life Calculation:

Battery life is a function of Burst Time and the Burst Interval. It may be calculated with the following formula.

Calculate Drain power first: Dp = Sl + (Fs * (Bt / Bi))

Where Dp = Drain power in mW
Bt = Burst Time in minutes
Bi = Burst Interval in minutes

Power used with the 6V 12 Cell Battery Pack:
Fs = Power used during sampling = 74mW
Sl = Power used during sleep time = 3.0mW

Power used with the 18V 12 Cell Battery Pack:
Fs = Power used during sampling = 65.2mW
Sl = Power used during sleep time = 3.5mW

Power used with the 21V 28 Cell Battery Pack:
Fs = Power used during sampling = 66.2mW
Sl = Power used during sleep time = 3.5mW

Now Calculate Battery Life: Bl = Bc / Dp

Where Bl = Battery Life in Hours
Bc = Battery Capacity in mWhr = 140,000mWhrs typ. for 12 C size alkaline batteries
Bc = Battery Capacity in mWhr = 326,000mWhrs typ. for 28 C size alkaline batteries
Dp = Drain Power in mW

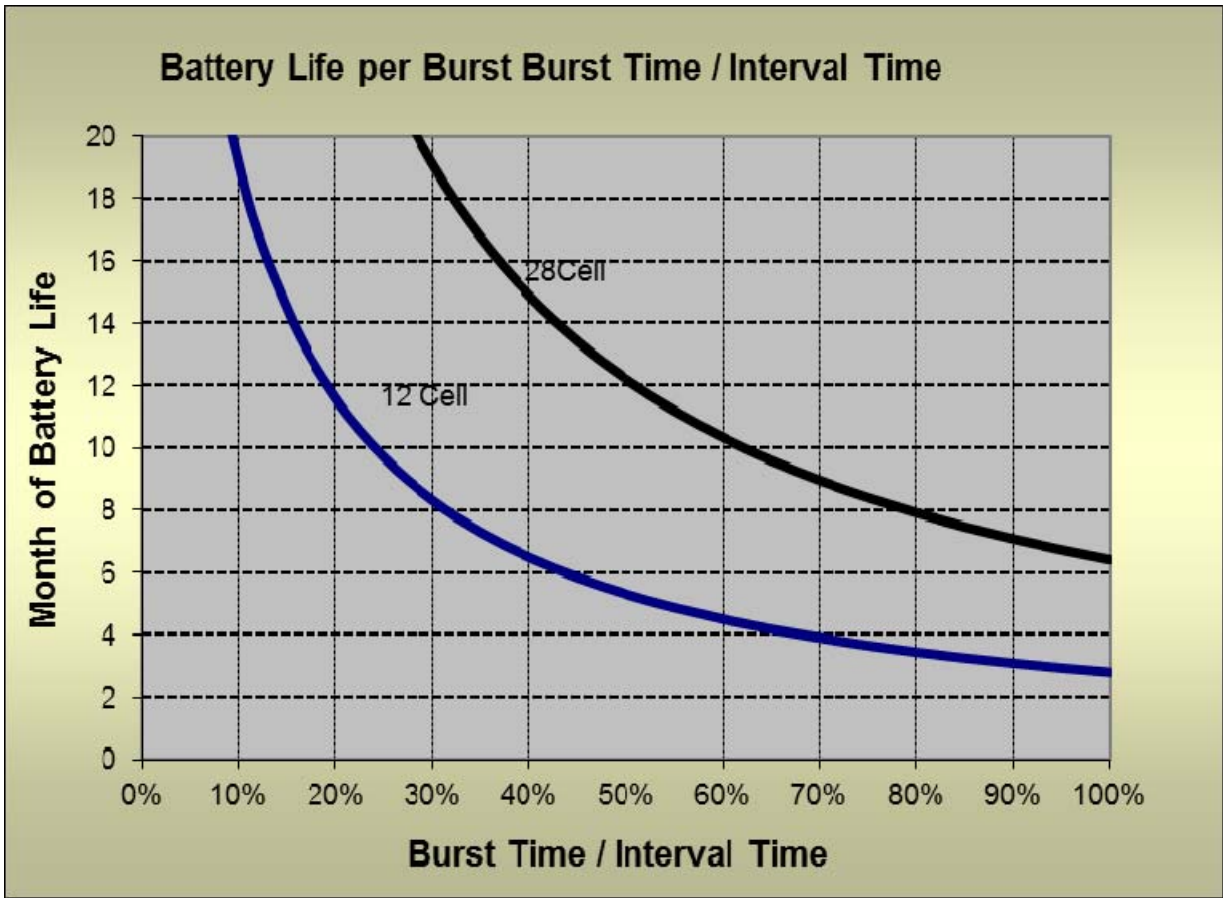

Data Storage Time:

Data Storage Time is a function of Sample Frequency, Burst Time, Interval and Data format.

The number of months of Data Storage for a Compact Flash Card may be calculated with the following formula.

St = (Sm * CF) / (F * (Bt / Bi) * 2,626,560)

Where St = Storage Time in months

Sm = Samples per Mbyte per storage format type

122,000 samples per Mbyte for ASCII

115,000 samples per Mbyte for ASCII format with Air Temperature sampling

230,000 samples per Mbyte for Binary

230,000 samples per Mbyte for Binary format with Air Temperature sampling

CF = Compact Flash card size in Mbytes

F = Programmed Sample Frequency 2Hz, 5Hz, 10Hz, 20Hz, or 30Hz

Bt = Burst Time in minutes

Bi = Burst Interval in minutes

2,626,560 = Seconds per month

512 M byte Compact Flash card:

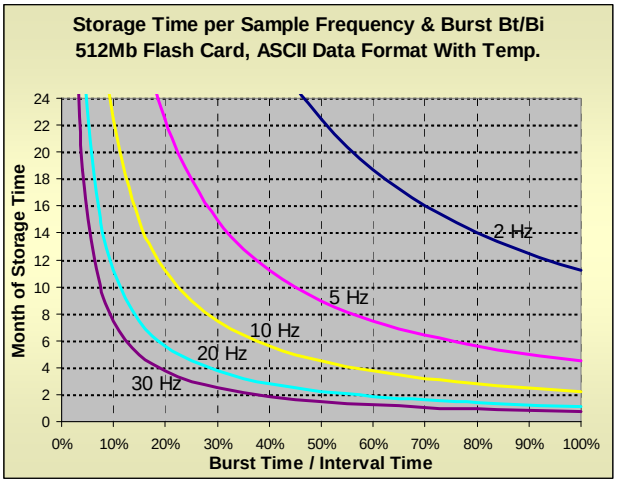

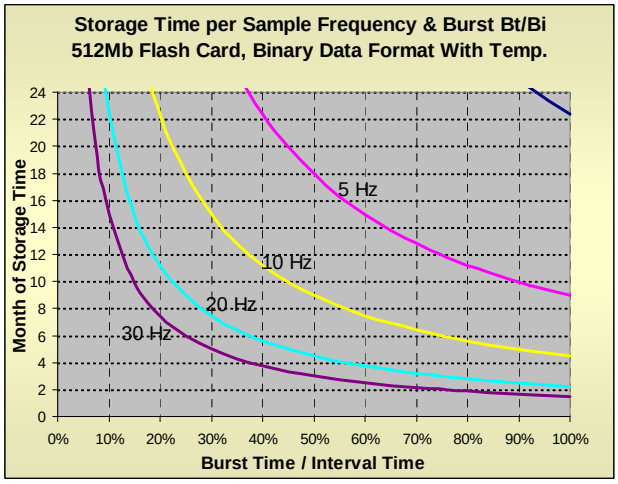

256 M byte Compact Flash card:

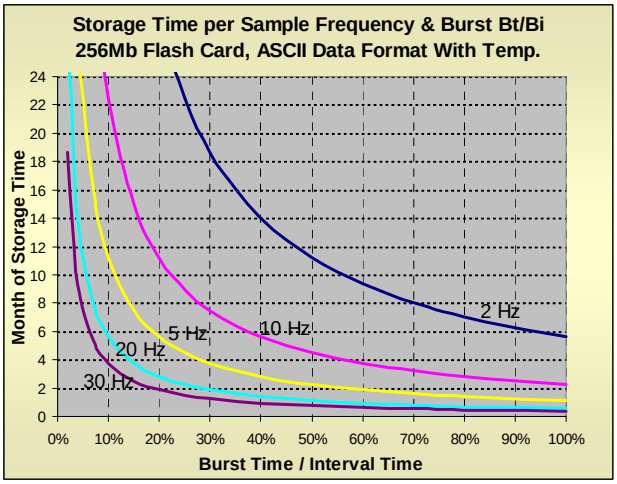

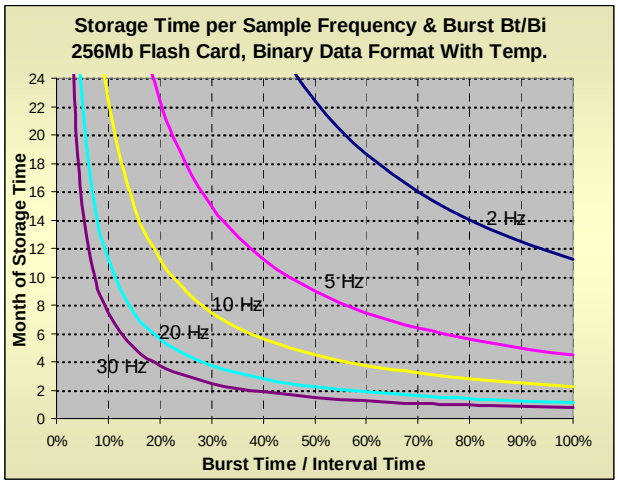

128 M byte Compact Flash card:

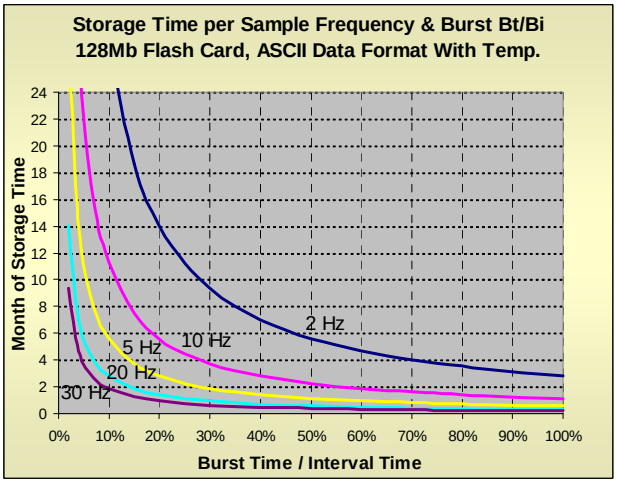

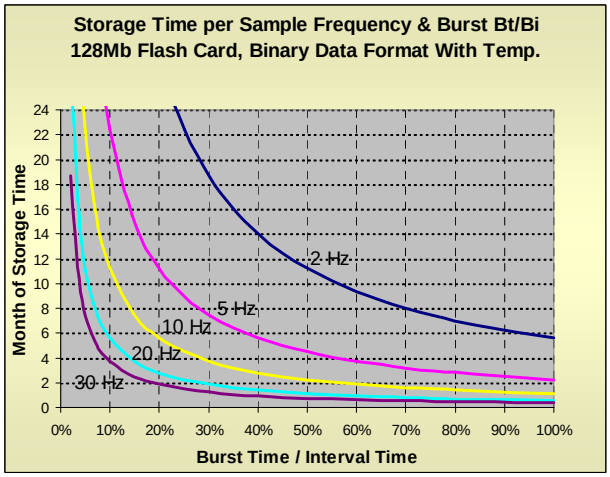

Number of Files and File Name:

The maximum number of files that the Wave Gauge can create is 512. The file names are automatically created starting at WLOG_000 and sequence up to WLOG_511. If previous files were left on the Compact Flash card those file names will be skipped. Note file name (location) WLOG_000 may be reserved and hidden by the Compact Flash Card manufacture.

File Format:

A File Header is placed at the start of each file when created. The Header contains the creation time, date and configuration information. The time and date are also placed at the start of each new burst.

New File Header Layout, Comma Delimited (separated)

Offset	Length & Type	File Status: Time, Date and Configuration Data
00h	4 ASCII bytes	Y00, to Y99, for Year 2000 to 2099
04h	4 ASCII bytes	M01, to M12, for Month Jan to Dec
08h	4 ASCII bytes	D01, to D31, for Day of month 1 to 31
0Ch	4 ASCII bytes	H00, to H23, for Hour of Day midnight to 23:00 hrs
10h	4 ASCII bytes	M00, to M59, for Minute of Hour 00 to 59
14h	4 ASCII bytes	S00, to S59, for Second of Minute 00 to 59
18h	4 ASCII bytes	F02, F05, F10, F20, F30, Sample Frequency in Hz
1Ch	4 ASCII bytes	L01, to L60, Burst Length 1 to 60 Minutes (note 1)
20h	4 ASCII bytes	I01, to I60, Burst Interval 1 to 60 Minutes
24h	5 ASCII bytes	N001, to N255, New File Interval 1 to 255 days (note 1)
28h	3 ASCII bytes	Z00 Min. Pressure Range in Bars
2Dh	5 ASCII bytes	X01, X03, X10, X30 Max. Pressure Range in Bars
30h	4 ASCII bytes	T10, Wave Gauge Type 10 = OSSI-010-003C
35h	6 ASCII bytes	R0000, Reserved
3Bh	4 Binary bytes	0Dh 0Ah 0Dh 0Ah Two carriage return line feeds

Note 1: 0 = continuous

New Burst Header Layout, Comma Delimited (separated)

Offset	Length & Type	Burst Status: Start Time and Date
3Fh	4 ASCII bytes	Y00, to Y99, for Year 2000 to 2099
43h	4 ASCII bytes	M01, to M12, for Month Jan to Dec
47h	4 ASCII bytes	D01, to D31, for Day of month 1 to 31
4Bh	4 ASCII bytes	H00, to H23, for Hour of Day midnight to 23:00 hrs
4Fh	4 ASCII bytes	M00, to M59, for Minute of Hour 00 to 59
53h	4 ASCII bytes	S00, to S59, for Second of Minute 00 to 59
57h	2 Binary bytes	0Dh 0Ah One carriage return line feed

File Data Format:

The file data may be stored in ASCII or Binary format and with or without Air Temperature. After each set of 12 Pressure Data samples stored, an Air Temperature sample is inserted if the temperature option is selected. Then a carriage return line feed is added if in ASCII format. In binary format two hex FE bytes will be added. At the end of each burst two carriage return line feeds are added in ASCII format or two hex FF bytes in binary format. The Binary Pressure Data is in IEEE 754 single precision floating point.

Sampled Data in ASCII Format, Comma Delimited with Air Temperature

Offset	**Length & Type**	**Data Description** (for a 0 to 3 Bar Sensor)
59h	8 ASCII bytes	-0.3000, to +3.0000, Pressure Sample #1
61h	8 ASCII bytes	-0.3000, to +3.0000, Pressure Sample #2
69h	8 ASCII bytes	-0.3000, to +3.0000, Pressure Sample #3
71h	8 ASCII bytes	-0.3000, to +3.0000, Pressure Sample #4
79h	8 ASCII bytes	-0.3000, to +3.0000, Pressure Sample #5
81h	8 ASCII bytes	-0.3000, to +3.0000, Pressure Sample #6
89h	8 ASCII bytes	-0.3000, to +3.0000, Pressure Sample #7
91h	8 ASCII bytes	-0.3000, to +3.0000, Pressure Sample #8
99h	8 ASCII bytes	-0.3000, to +3.0000, Pressure Sample #9
A1h	8 ASCII bytes	-0.3000, to +3.0000, Pressure Sample #10
A9h	8 ASCII bytes	-0.3000, to +3.0000, Pressure Sample #11
B1h	8 ASCII bytes	-0.3000, to +3.0000, Pressure Sample #12
B9h	6 ASCII bytes	-0640, To +1024, Air Temp. -40 to +65 C, 0.0625 C per count
BEh	2 Binary bytes	0Dh 0Ah One carriage return line feed
C91h	8 ASCII bytes	-0.3000, to +3.0000, Pressure Sample #13
??h	8 ASCII bytes	-0.3000, to +3.0000, Pressure Sample #??
??h	4 Binary bytes	0Dh 0Ah 0Dh 0Ah Two carriage return line feeds

Sampled Data in ASCII Format, Comma Delimited without Air Temperature

Offset	Length &/ Type	Data Description (for a 0 to 3 Bar Sensor)
59h	8 ASCII bytes	-0.3000, to +3.0000, Pressure Sample #1
61h	8 ASCII bytes	-0.3000, to +3.0000, Pressure Sample #2
69h	8 ASCII bytes	-0.3000, to +3.0000, Pressure Sample #3
71h	8 ASCII bytes	-0.3000, to +3.0000, Pressure Sample #4
79h	8 ASCII bytes	-0.3000, to +3.0000, Pressure Sample #5
81h	8 ASCII bytes	-0.3000, to +3.0000, Pressure Sample #6
89h	8 ASCII bytes	-0.3000, to +3.0000, Pressure Sample #7
91h	8 ASCII bytes	-0.3000, to +3.0000, Pressure Sample #8
99h	8 ASCII bytes	-0.3000, to +3.0000, Pressure Sample #9
A1h	8 ASCII bytes	-0.3000, to +3.0000, Pressure Sample #10
A9h	8 ASCII bytes	-0.3000, to +3.0000, Pressure Sample #11
B1h	8 ASCII bytes	-0.3000, to +3.0000, Pressure Sample #12
B9h	2 Binary bytes	0Dh 0Ah One carriage return line feed
BBh	8 ASCII bytes	-0.3000, to +3.0000, Pressure Sample #13
??h	8 ASCII bytes	-0.3000, to +3.0000, Pressure Sample #??
??h	4 Binary bytes	0Dh 0Ah 0Dh 0Ah Two carriage return line feeds

File Data Format cont:

Sampled Data in Binary Format with Air Temperature:

Offset	Length & Type	Data Description
59h	4 Binary bytes	32 bit floating point Pressure Sample #1
5Dh	4 Binary bytes	32 bit floating point Pressure Sample #2
61h	4 Binary bytes	32 bit floating point Pressure Sample #3
65h	4 Binary bytes	32 bit floating point Pressure Sample #4
69h	4 Binary bytes	32 bit floating point Pressure Sample #5
6Dh	4 Binary bytes	32 bit floating point Pressure Sample #6
71h	4 Binary bytes	32 bit floating point Pressure Sample #7
75h	4 Binary bytes	32 bit floating point Pressure Sample #8
79h	4 Binary bytes	32 bit floating point Pressure Sample #9
7Dh	4 Binary bytes	32 bit floating point Pressure Sample #10
81h	4 Binary bytes	32 bit floating point Pressure Sample #11
85h	4 Binary bytes	32 bit floating point Pressure Sample #12
89h	2 Binary bytes	82 80h to 04 00h, Air Temp. -40 to +65 C, 0.0625 C per count
8Bh	2 Binary bytes	FE FEh every 12 samples
??h	4 Binary bytes	32 bit floating point Pressure Sample #??
??h	2 Binary bytes	FF FFh at end of each Burst
??h	26 bytes	New Burst Header ending with FE FE

Sampled Data in Binary Format without Air Temperature:

Offset	Length / Type	Data Description
59h	4 Binary bytes	32 bit floating point Pressure Sample #1
5Dh	4 Binary bytes	32 bit floating point Pressure Sample #2
61h	4 Binary bytes	32 bit floating point Pressure Sample #3
65h	4 Binary bytes	32 bit floating point Pressure Sample #4
69h	4 Binary bytes	32 bit floating point Pressure Sample #5
6Dh	4 Binary bytes	32 bit floating point Pressure Sample #6
71h	4 Binary bytes	32 bit floating point Pressure Sample #7
75h	4 Binary bytes	32 bit floating point Pressure Sample #8
79h	4 Binary bytes	32 bit floating point Pressure Sample #9
7Dh	4 Binary bytes	32 bit floating point Pressure Sample #10
81h	4 Binary bytes	32 bit floating point Pressure Sample #11
85h	4 Binary bytes	32 bit floating point Pressure Sample #12
8Eh	2 Binary bytes	FE FEh every 12 samples
??h	4 Binary bytes	32 bit floating point Pressure Sample #??
??h	2 Binary bytes	FF FFh at end of each Burst
??h	26 bytes	New Burst Header ending with FE FE

Example - Sampled Data in ASCII Format Comma Delimited with Air Temperature Viewed in WordPad:

Y02,M11,D09,H21,M48,S10,F30,L02,I01,N001,Z00,X03,T10,R0000,

Y03,M03,D30,H00,M53,S00,
+0.0068,+0.0069,+0.0069,+0.0068,+0.0068,+0.0068,+0.0070,+0.0069,+0.0069,+0.0069,+0.0069,+0.0070,+0374,
+0.0069,+0.0068,+0.0069,+0.0069,+0.0070,+0.0070,+0.0069,+0.0069,+0.0069,+0.0070,+0.0069,+0.0068,+0374,
+0.0068,+0.0069,+0.0069,+0.0069,+0.0069,+0.0069,+0.0069,+0.0070,+0.0069,+0.0069,+0.0068,+0.0068,+0374,
+0.0068,+0.0069,+0.0070,+0.0069,+0.0068,+0.0067,+0.0066,+0.0068,+0.0068,+0.0068,+0.0068,+0.0068,+0375,
+0.0069,+0.0068,+0.0069,+0.0069,+0.0068,+0.0068,+0.0069,+0.0068,+0.0068,+0.0068,+0.0068,+0.0068,+0373,
+0.0068,+0.0068,+0.0069,+0.0068,+0.0069,+0.0068,+0.0069,+0.0069,+0.0068,+0.0069,+0.0068,+0.0068,+0373,
+0.0070,+0.0069,+0.0068,+0.0067,+0.0066,+0.0069,+0.0069,+0.0069,+0.0069,+0.0068,+0.0070,+0.0070,+0375,
+0.0069,+0.0069,+0.0069,+0.0070,+0.0070,+0.0069,+0.0068,+0.0068,+0.0069,+0.0069,+0.0068,+0.0068,+0374,
+0.0067,+0.0069,+0.0068,+0.0067,+0.0067,+0.0067,+0.0069,+0.0069,+0.0068,+0.0069,+0.0069,+0.0071,+0374,
+0.0069,+0.0069,+0.0069,+0.0069,+0.0071,+0.0070,+0.0069,+0.0069,+0.0067,+0.0069,+0.0068,+0.0068,+0374,
+0.0069,+0.0068,+0.0070,+0.0069,+0.0069,+0.0069,+0.0070,+0.0071,+0.0069,+0.0069,+0.0068,+0.0068,+0374,

Y03,M03,D30,H00,M55,S00,
+0.0000,+0.5526,+0.3264,+0.1937,+0.1160,+0.0704,+0.0436,+0.0281,+0.0188,+0.0135,+0.0103,+0.0083,+0374,
+0.0075,+0.0068,+0.0064,+0.0061,+0.0061,+0.0062,+0.0061,+0.0060,+0.0059,+0.0058,+0.0060,+0.0059,+0373,
+0.0060,+0.0060,+0.0061,+0.0063,+0.0061,+0.0061,+0.0059,+0.0058,+0.0060,+0.0059,+0.0060,+0.0059,+0373,
+0.0060,+0.0062,+0.0061,+0.0061,+0.0062,+0.0060,+0.0062,+0.0062,+0.0062,+0.0061,+0.0061,+0.0063,+0374,

Example - Sampled Data in ASCII Format Comma Delimited without Air Temperature Viewed in WordPad:

Y02,M11,D09,H21,M48,S10,F30,L02,I01,N001,Z00,X03,T10,R0000,

Y03,M03,D30,H00,M53,S00,
+0.0068,+0.0069,+0.0069,+0.0068,+0.0068,+0.0068,+0.0070,+0.0069,+0.0069,+0.0069,+0.0069,+0.0070,
+0.0069,+0.0068,+0.0069,+0.0069,+0.0070,+0.0070,+0.0069,+0.0069,+0.0069,+0.0070,+0.0069,+0.0068,
+0.0068,+0.0069,+0.0069,+0.0069,+0.0069,+0.0069,+0.0069,+0.0070,+0.0069,+0.0069,+0.0068,+0.0068,
+0.0068,+0.0069,+0.0070,+0.0069,+0.0068,+0.0067,+0.0066,+0.0068,+0.0068,+0.0068,+0.0068,+0.0068,
+0.0069,+0.0068,+0.0069,+0.0069,+0.0068,+0.0068,+0.0069,+0.0068,+0.0068,+0.0068,+0.0068,+0.0068,
+0.0068,+0.0068,+0.0069,+0.0068,+0.0069,+0.0068,+0.0069,+0.0069,+0.0068,+0.0069,+0.0068,+0.0068,
+0.0070,+0.0069,+0.0068,+0.0067,+0.0066,+0.0069,+0.0069,+0.0069,+0.0069,+0.0068,+0.0070,+0.0070,
+0.0069,+0.0069,+0.0069,+0.0070,+0.0070,+0.0069,+0.0068,+0.0068,+0.0069,+0.0069,+0.0068,+0.0068,
+0.0067,+0.0069,+0.0068,+0.0067,+0.0067,+0.0067,+0.0069,+0.0069,+0.0068,+0.0069,+0.0069,+0.0071,
+0.0069,+0.0069,+0.0069,+0.0069,+0.0071,+0.0070,+0.0069,+0.0069,+0.0067,+0.0069,+0.0068,+0.0068,
+0.0069,+0.0068,+0.0070,+0.0069,+0.0069,+0.0069,+0.0070,+0.0071,+0.0069,+0.0069,+0.0068,+0.0068,

Y03,M03,D30,H00,M55,S00,
+0.0000,+0.5526,+0.3264,+0.1937,+0.1160,+0.0704,+0.0436,+0.0281,+0.0188,+0.0135,+0.0103,+0.0083,
+0.0075,+0.0068,+0.0064,+0.0061,+0.0061,+0.0062,+0.0061,+0.0060,+0.0059,+0.0058,+0.0060,+0.0059,
+0.0060,+0.0060,+0.0061,+0.0063,+0.0061,+0.0061,+0.0059,+0.0058,+0.0060,+0.0059,+0.0060,+0.0059,
+0.0060,+0.0062,+0.0061,+0.0061,+0.0062,+0.0060,+0.0062,+0.0062,+0.0062,+0.0061,+0.0061,+0.0063,

Checking the Battery Pack:

Measuring the open circuit voltage of the Alkaline battery pack to determine the amount of service life will only yield a rough estimate.

An open circuit reading of 6 volts or greater for the 4 cell Alkaline Battery Pack indicates essentially that the battery pack has at least 90% capacity.

Communications and Configuration:

The Wave Gauge may be configured with a PC's RS232 serial port. Use our convenient programming software or a Hyper Terminal with the following commands.

Commands are one byte and Acknowledgements are 3 bytes

Commands:
s = Stop running sample routine and wait for command instructions.
w = Write configuration data to Wave Gauge from PC.
r = Read back configuration data to PC.
i = Read back ID number to PC.
g = Go run main sample and store data to Compact Flash card routine.

Acknowledgements:
SOK = Acknowledge Stop running command and wait for command instruction.
WOK = Acknowledge Write configuration and wait to receive data from PC. (Time out in 15 sec)
ROK = Acknowledge Transmit configuration and transmit configuration data to PC.
IOK = Acknowledge ID Command and transmit ID (serial) number to PC.
GOK = Acknowledge go command and go run main sample and store data routine.
BAD = Receive failure or check sum on configuration data error
DOW = Do, write to configure Wave Gauge. Wave Gauge has not been configured.

Monitoring the sampled data:
The sampled data may be monitored via the RS232 serial port if the configuration control byte is set to enable the RS232 port:
Example with Air Temperature enabled:
+1.2345, +0384
+1.2345, +0384
: :
+1.2345, +0384
Example without Air Temperature enabled:
+1.2345
+1.2345
:
+1.2345

To Configure the Wave Gauge a 44 comma separated 2 ASCII character string must be sent to it.

Configuration String, Comma Delimited, Transmitted via RS232 serial port to Wave Gauge

Offset	Length & Type	Name	Range and Description
00h	3 ASCII bytes	Sensor Type	0A, = Wave Gauge
03h	3 ASCII bytes	Max Pressure	01, 03, 10, or 30, The max. pressure range in Bars
06h	3 ASCII bytes	Min Pressure	00, Bars
09h	12 ASCII bytes	(reserved)	00,00,00,00,
15h	3 ASCII bytes	Sample Frequency	02, or 05, or 0A, or 14, or 1E, Hex. Selects Sample Frequency 02, or 05, or 10, or 20, or 30 Hz
18h	3 ASCII bytes	Burst Time	01, to 3C Hex value, Burst Time value, 1 to 60 Minutes (note 4)
1Bh	3 ASCII bytes	Burst Interval	01, to 3C Hex value, Burst Interval value, 1 to 60 Minutes
1Eh	3 ASCII bytes	New File Interval	01, to FF, Hex value, New File Interval 1 to 255 days (note 1)
21h	3 ASCII bytes	Set RTC seconds	00, to 59 Dec. Value, Real Time Clock, set only when control byte bit 3 is set
24h	3 ASCII bytes	Set RTC Minutes	00, to 59 Dec. Value, Real Time Clock, set only when control byte bit 3 is set
27h	3 ASCII bytes	Set RTC Hours	00, to 23 Dec. Value, Real Time Clock, set only when control byte bit 3 is set
2Ah	3 ASCII bytes	Set RTC Day of week	01, to 07 Dec. Value, Real Time Clock, set only when control byte bit 3 is set
2Dh	3 ASCII bytes	Set RTC Date	01, to 31 Dec. Value, Real Time Clock, set only when control byte bit 3 is set
30h	3 ASCII bytes	Set RTC Month	01, to 12 Dec. Value, Real Time Clock, set only when control byte bit 3 is set
33h	3 ASCII bytes	Set RTC Year	00, to 99 Dec. Value, = 2000 to 2099, set only when control byte bit 3 is set
36h	3 ASCII bytes	Start Minutes	00, to 59 Dec. Value, Start logging data on compact Flash Card
39h	3 ASCII bytes	Start Hours	00, to 59 Dec. Value, Start logging data on compact Flash Card
3Ch	3 ASCII bytes	Start Date	00, to 31 Dec. Value, Start logging data on compact Flash Card
3Fh	3 ASCII bytes	Start Month	00, to 12 Dec. Value, Start logging data on compact Flash Card
42h	3 ASCII bytes	Start Year	00, to 99 Dec. Value, Start logging data on compact Flash Card
45h	54 ASCII Bytes	(reserved)	00,00,00,00,00,00,00,00,00,00,00,00,00,00,00,00,00,00, = Reserved space, 18 comma delimited 2 ASCII char.
7Bh	3 ASCII bytes	CF Status	00, read only, Compact Flash status
7Eh	3 ASCII bytes	Control Byte	See Control Byte Table below
81h	3 ASCII bytes	Check Sum	00, to FF Hex value, is the sum of the Hex values in offset 00h to 81h (Note: Treat all Dec. values as Hex Values)

Note 4: 00, = continuous

Control Byte	
Bit 7	0
Bit 6	0
Bit 5	1 = Enable Start Sampling Time control
	0 = Start Sampling Immediately
Bit 4	1 = Water Temp. enabled
	0 = Water Temp disabled
Bit 3	1 = Set Real Time Clock Time and Date per this file
	0 = No change to Real Time Clock
Bit 2	0 = 9600 baud, default
Bit 1	1 = RS232 output enabled battery power drain 70 mW in cont. sample mode
	0 = RS232 output disabled, battery power drain 54 mW in cont. sample mode
	Note Transmit data always sent in ASCII format
Bit 0	1 = BINARY Data file format
	0 = ASCII Data File comma delimited and carriage return every 12 samples.

Installing and Removing the Compact Flash card:

Install the Compact Flash card with the top label facing down as viewed below. If the power plug is connected the File Status LED will turn on for 3 seconds. If the power plug is not connected the File Status LED will turn on for 3 seconds when it is connected. If the card size or format is incorrect the File Status LED will blink fast for 4 seconds. If the battery voltage is low the LED will not turn on at all.

To remove the card, first press the Close File Button. The File Status LED will indicate that it's ok to unplug the card by a continuous 1 second on and 1 second off blinking. The File Status LED will stop blinking when the card is removed. If the card is removed before pressing the Close File Button **the last file will be corrupted.** The File Status LED will blink fast for 4 seconds to indicate this error.

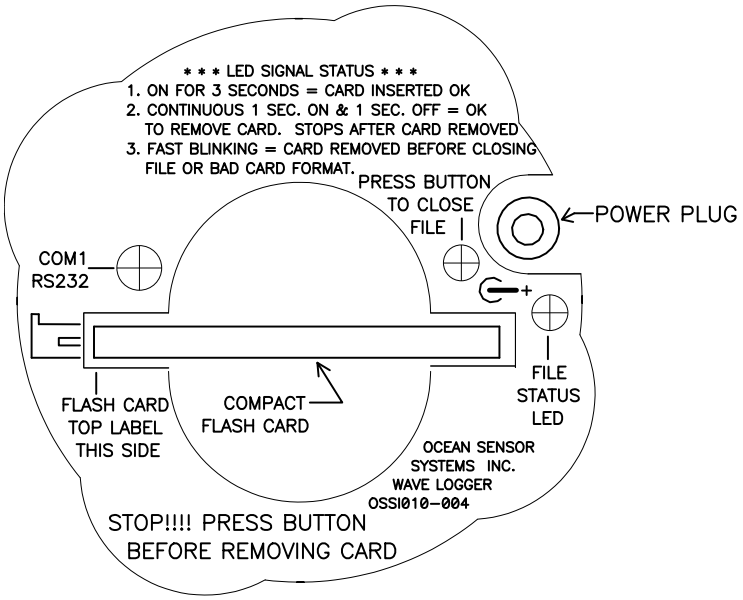

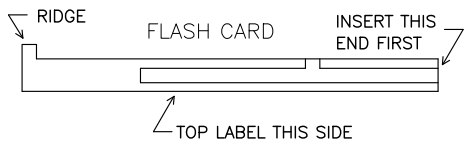

APPENDIX B

SURVEY BENCHMARK DATASHEETS

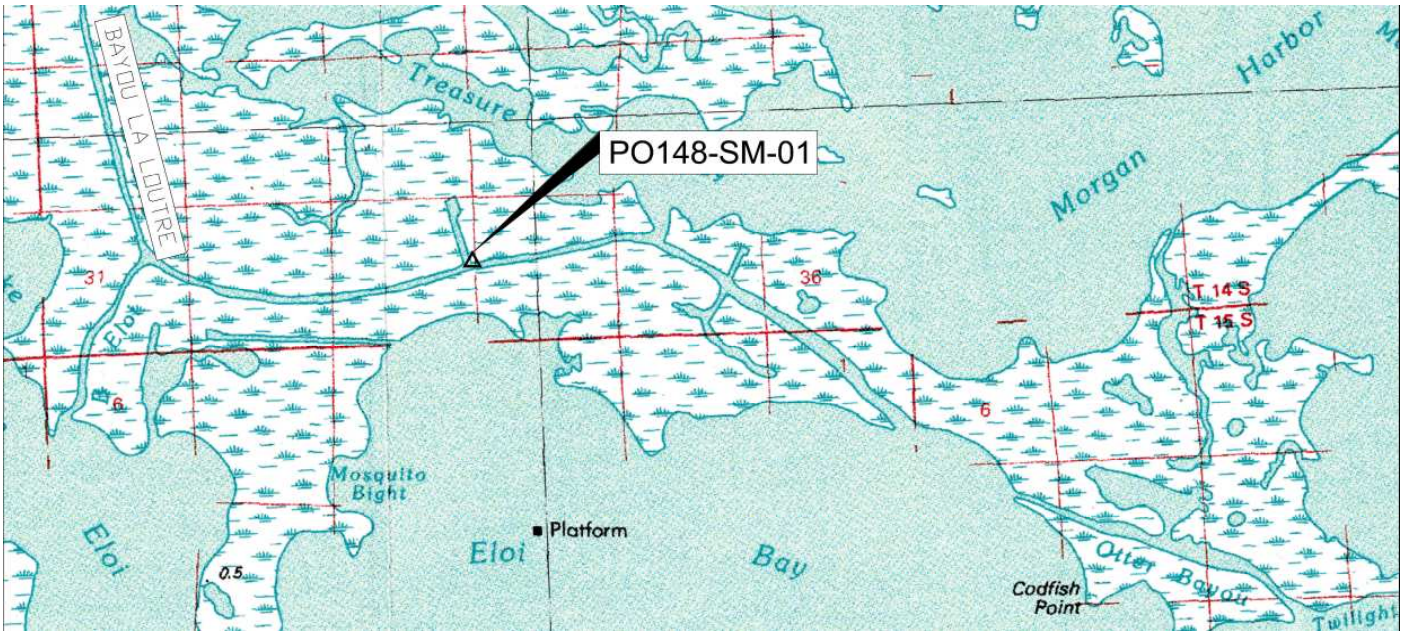

VICINITY MAP

Reproduced from U.S. Geological Survey, Aerial dated 1983

Station Name: PO148-SM-01

Monument Location: This station is located on the corner of Bayou La Loutre and a north-south canal that intersects with Bayou La Loutre. The Monument is situated on the east bank of the north-south canal and is approximately 30 feet east of the water's edge and is approximately 35 feet northerly from Bayou La Loutre's water's edge.

Monument Description: NGS Style Floating Sleeve Monument: 9/16" Stainless steel sectional rods driven 64 feet to refusal within a greased sleeve and sand filled 6" PVC pipe with protective cover and is set above the ground.

Monument Established By: T. Baker Smith, LLC

For: Coastal Protection and Restoration Authority, CPRA

Stamping: "PO148-SM-01"

Installation/Survey Date: April 2013

Adjusted NAD83 (2011) Geodetic Position
Lat. 29° 47' 43.67278"N
Long. 89° 23' 20.72523"W

Adjusted NAD83 (2011) Datum LSZ (1702) Ft
N= 476,343.280
E= 3,897,480.698

Adjusted NAVD88 Height (Epoch 2010.0)
Elevation = 4.83 feet (1.472 mtrs)

Ellipsoid Height = -24.079 mtrs.
Geoid12A Height = -25.551 mtrs.

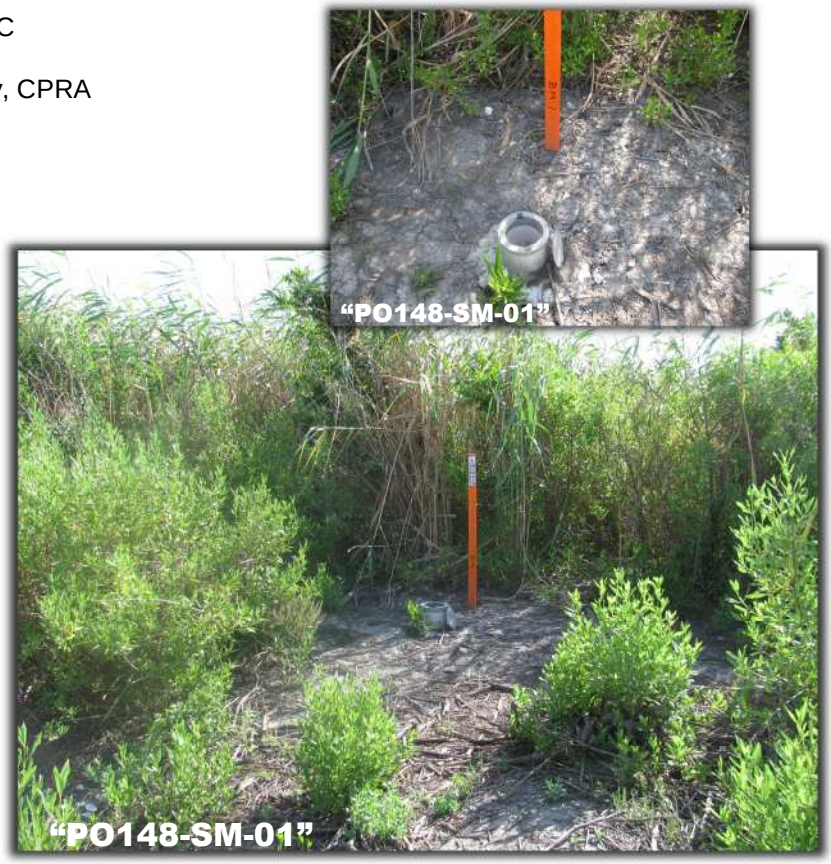

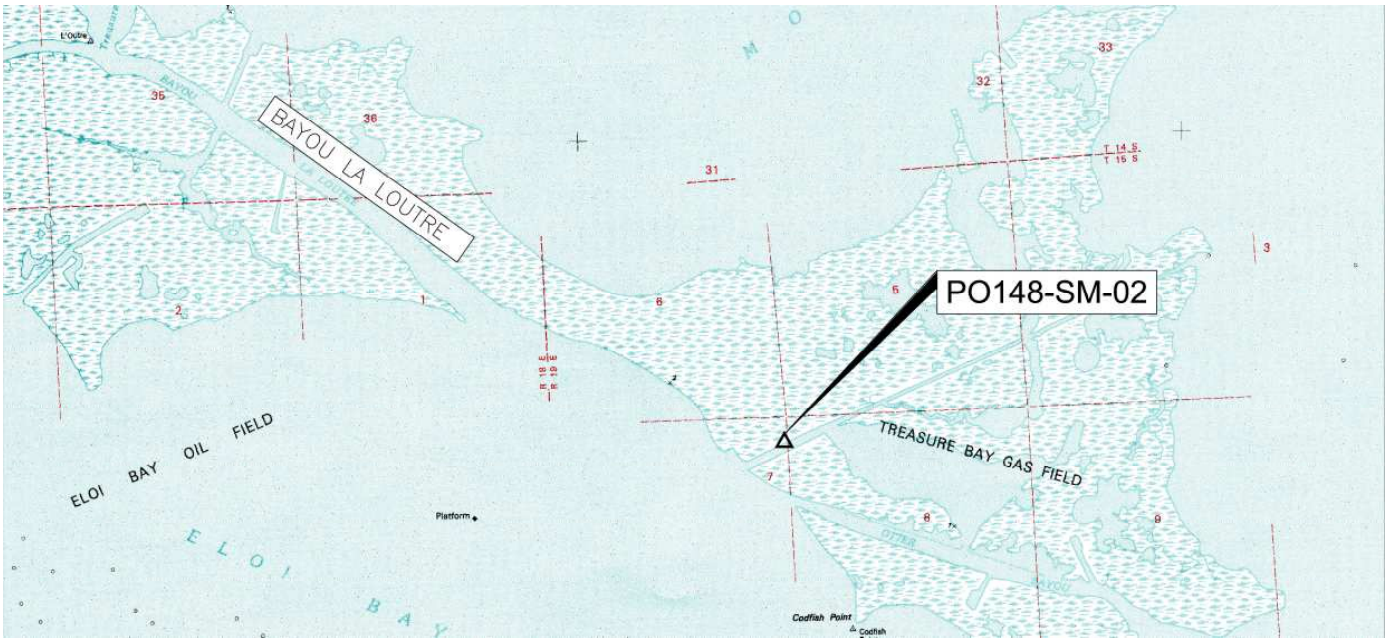

VICINITY MAP Reproduced from U.S. Geological Survey, Aerial dated 1994

Station Name: PO148-SM-02

Monument Location: This station is located in a southwest-northeast canal near the northeastern side of Eloi Bay in between Bayou La Loutre and Otter Bayou. The Monument is situated on the north bank of the canal and is approximately 630 feet from Eloi Bay and approximately 25 feet north of the water's edge from the canal.

Monument Description: NGS Style Floating Sleeve Monument: 9/16" Stainless steel sectional rods driven 100 feet to refusal within a greased sleeve and sand filled 6" PVC pipe with protective cover and is set above the ground.

Monument Established By: T. Baker Smith, LLC

For: Coastal Protection and Restoration Authority, CPRA

Stamping: "PO148-SM-02"

Installation/Survey Date: April 2013

Adjusted NAD83 (2011) Geodetic Position
Lat. 29° 46' 24.80905"N
Long. 89° 19' 09.89810"W

Adjusted NAD83 (2011) Datum LSZ (1702) Ft
N= 468,759.796
E= 3,919,716.739

Adjusted NAVD88 Height (Epoch 2010.0)
Elevation = 3.53 feet (1.076 mtrs)

Ellipsoid Height = -24.413 mtrs.
Geoid12A Height = -25.489 mtrs.

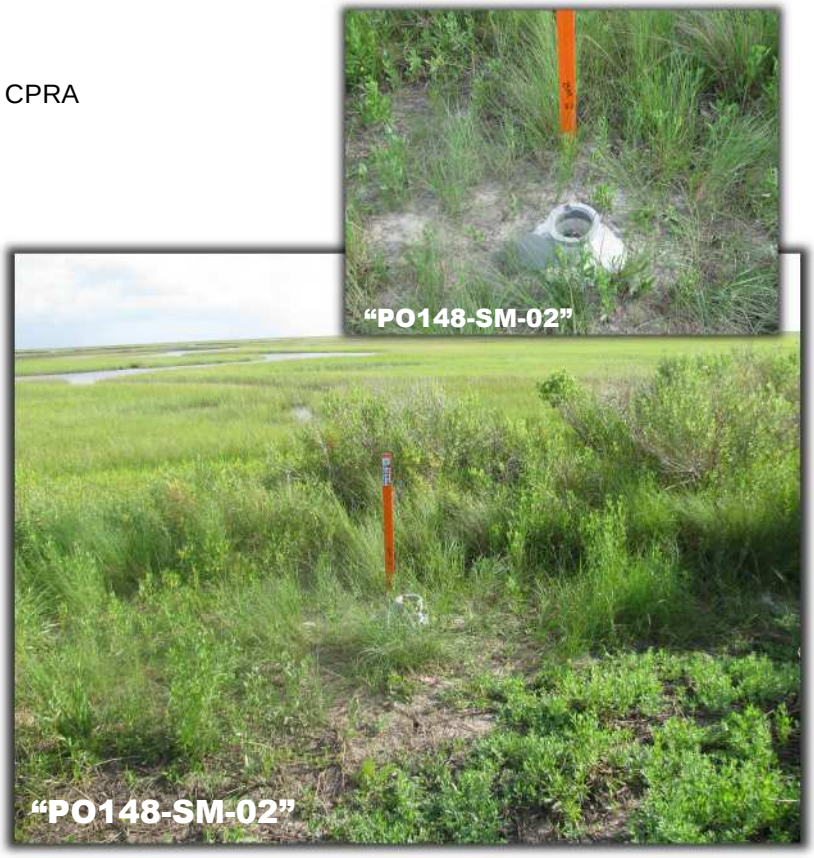

Adjusted Position Established by T. Baker Smith, LLC for the Coastal Protection and Restoration Authority, CPRA

APPENDIX C

FIELD NOTES

2017.0470 MOTT MACDONALD
CPRA PO-174

π PO148-SM-02 SP83/LA SOUTH 1702/ GEOID 12A
@ 2M

PT	X	Y	ELEV	DESC	DURATION
1002	3907369.31	476290.90	2.497	TBM CHK (¾" IRON ROD)	3 MIN
2000			0.85	TOW	
2001			0.82	TOW	
2002	3919756.36	468737.04	4.84	TOP OF BOX	
2003			0.96	TOW	
2004			0.89	TOW	
2005			0.91	TOW	
2006	3893714.87	473080.50	4.74	TOP OF BOX	
2007			0.86	TOW	
2008			0.90	TOW	
2009			0.94	TOW	
2010			0.91	TOW	

GAGE 001 INSTALLATION @ 13:00 SND = 4.5'
GAGE 002 INSTALLATION @ 14:15 SND = 4.1'

J. CHAUVIN
D. DAGENHARDT
A. SZUSH

9/21/2017

NE WIND 5 KNOTS

VESSEL: SURVEYOR 9

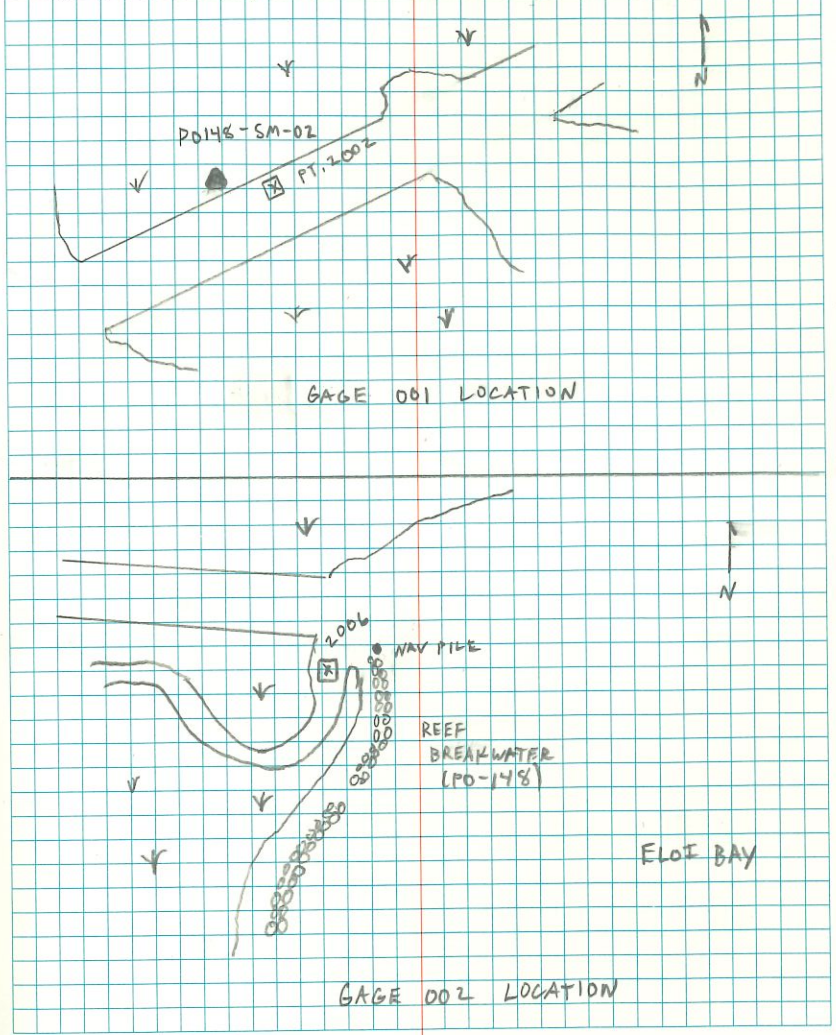

B-2991

2017.0470 MOTT MACDONALD
CPRA PO-0174

π PO148-SM-01 SP83/LASOUTH 1702/GEOID12A

PT	X	Y	ELEV	DESC	SND
1				CHKPT-3	
2				CHKPT-3A	
3			-0.134	TOW 10:24AM	
4			-0.14	TOW 10:24AM	
8	3891812.77	466015.34	-5.9	505	5.9'
9	3891146.30	466454.20	-1.2	501	1.3'
10	3891651.98	466794.42	-1.5	502	1.5'
12	3893228.13	469163.17	-6.1	506	5.9'
14	3892709.69	469737.20	-2.0	503	2.0'
17	3894206.85	471586.82	-6.1	507	6.0'
18	3893383.84	472087.53	-2.3	504	2.7'

* POINTS + SOUNDINGS TAKEN AT TOP OF GAGE BASEPLATE

LOCATION	GAGE ID	BASEPLATE #	TIME OF DEPLOYMENT
505	P05	1	10:55
501	PB	17	11:22
502	P0042 RENTAL	13	11:39
506	P02	10	11:56
503	P06	12	12:13
507	P01	18	12:32
504	P04	4	12:47

J. CHAUVIN
B. PELLEGRIN
T. EVERETT

11/21/2017
ENE WIND 5 KNOTS

VESSEL: SURVEYOR 6

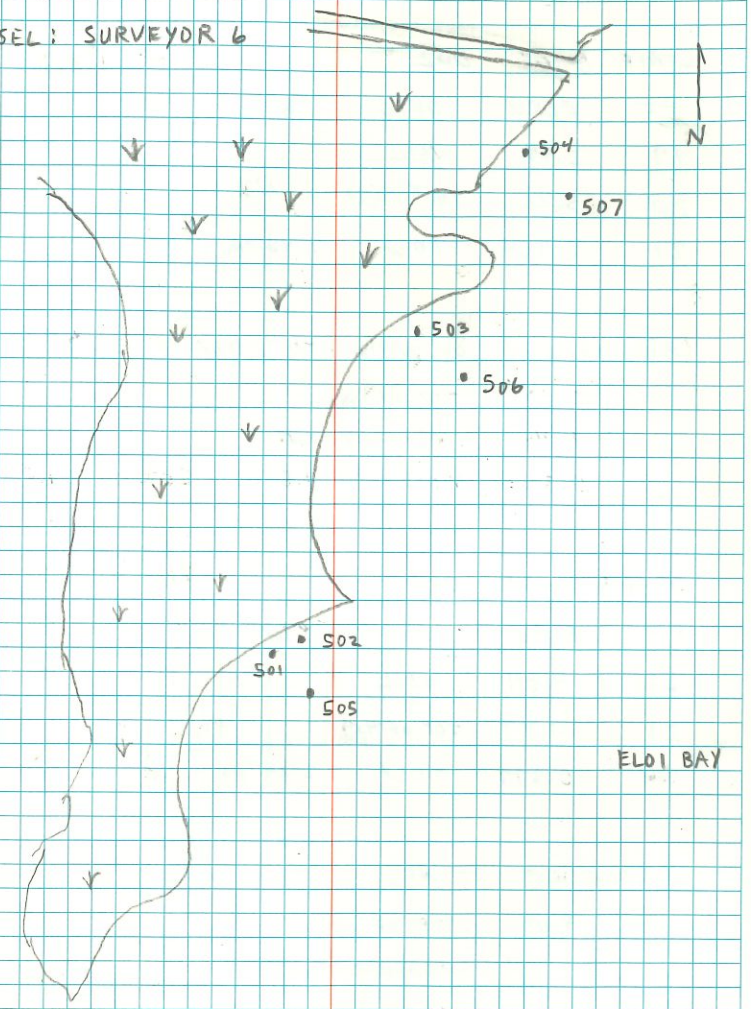

B-2994

2017.0470 MOTT MACDONALD
CPRA PO-0174

STAFF GAGE 002

PT	ELEV	DESC	TIME
19	2.84	NAIL	
20	5.72	TOP OF 4x4	
21	0.364	TOW	1:46 PM

MEASUREMENT OF NAIL TO TOW = 2.48'

2.84' TOP OF NAIL
- 2.48' MEASUREMENT
0.36' TOW

STAFF GAGE 001

PT	ELEV	DESC	TIME
22	4.04	NAIL	
23	7.47	TOP OF 4x4	
26	0.377	TOW	2:34 PM

MEASUREMENT OF NAIL TO TOW = 3.70'

4.04' TOP OF NAIL
- 3.70' MEASUREMENT
0.34 TOW

J. CHAUVIN
B. PELLEGRIN
T. EVERETT

11/21/2017

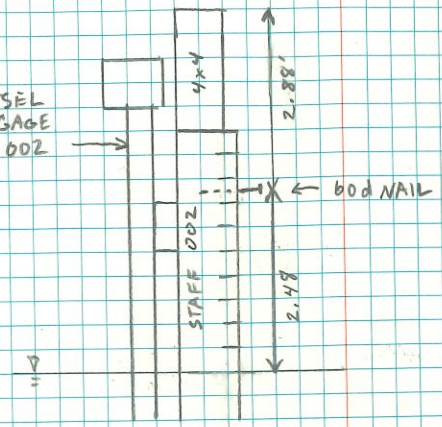

WSEL GAGE 002

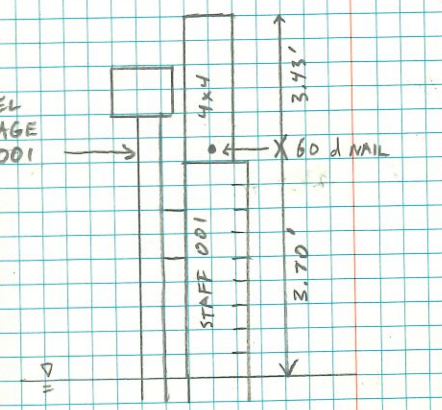

WSEL GAGE 001

B-2994

2017.0945 JOB FILE: 17.0945.12.13.JR

(PO-148) LIVING SHORELINE DEMONSTRATION PROJECT

CPRA

ELOI BAY, LA

USED RTK

BASE SET UP ON PO148-SM-01

N: 476343.280

E: 3897480.698

ELEV: 4.830 (OPUS START @ 7:47)

CHECK SHOT ON PO148-SM-02

PT#1 - 3MIN SHOT FOR X,Y,Z

PT#2 CHK IN H: 0.043 V: -0.005

PT#475 CHK OUT H: 0.074 V: 0.042

OPUS END @ ± 3:58

BASE HEIGHT 2.25m ROVER HEIGHT 2m

PT#	REMARKS		PT#	REMARKS	
3-31	OYSTER BREAK X-SEC		245-271	DOUBLE CIRCLE	X-SEC 3
32-56	TRIPLE CIRCLE X-SEC 1		272-299	"	X-SEC 4
57-83	"	X-SEC 2	300-325	"	X-SEC 5
84-111	"	X-SEC 3	326-354	"	X-SEC 6
112-137	"	X-SEC 4	365-383	OYSTER BREAK	X-SEC 2
138-163	"	X-SEC 5	384-411	DOUBLE TRIANGLE	X-SEC 1
164-191	"	X-SEC 6	412-439	"	X-SEC 2
192-217	DOUBLE CIRCLE	X-SEC 1	440-466	OYSTER BREAK	X-SEC 3
218-244	"	X-SEC 2	467-474	"	X-SEC 3

CHECK PTS 35-59 FOR BASE INTERRUPTION

J. RODRIGUE
J. DUPRE
L. ROBINSON

12-13-17

BREEZY

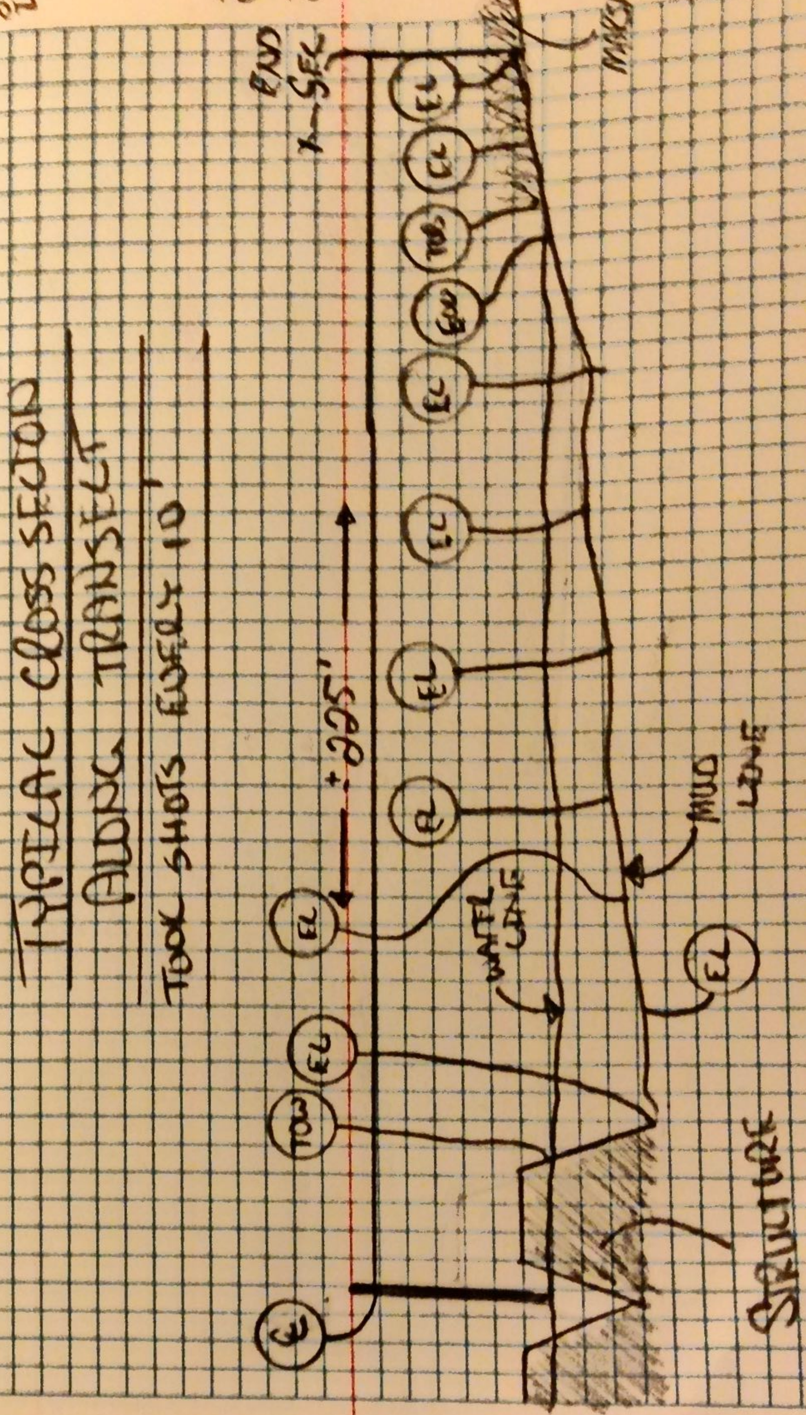

4260

2017.0945 JOB FILE: 17.0945.12-14.JR

LIVING SHORELINE DEMONSTRATION PROJECT (PO-148)

CPRA

ELOI BAY, LA

USED RTK

BASE SET UP ON PT PO148-SM-01

N- 476343.280 OPUS START

E- 3897480.698 OPUS END

ELEV. 4.830 BASE HT 2.25m ROVER HT 2m

CHECK SHOT ON TBM03A PT 476 3 MIN SHOT

PT# 477 CHECK IN H_L: 0.005 Vt: 0.015

PT# 962 CHECK OUT H_L: 0.043 Vt: 0.021

Pt #	Remarks		Pt #	Remarks	
478-497	CONT. DOUBLE TRIANGLE	X-SEC 3	BAY SIDE DATA		
498-525	DOUBLE TRIANGLE	X-SEC 4	847-849	BAY SIDE	X-SEC 1
526-555	OYSTER BREAK	X-SEC 4	850-852	"	2
556-584	DOUBLE TRIANGLE	X-SEC 5	853-855	"	3
585-612	"	X-SEC 6	856-858	"	4
613-643	5 CIRCUITS	X-SEC 1	859-861	"	5
644-673	"	X-SEC 2	862-864	"	6
674-702	OYSTER BREAK	X-SEC 5	865-868	"	7
703-761	5 CIRCLE	X-SEC 3	869-872	"	8
762-789	"	X-SEC 4	873-876	"	9
790-817	OYSTER BREAK	X-SEC 6	877-880	"	10
818-846	5 CIRCLE	X-SEC 5	881-884	"	11

J. ROBICHEAUX
T. ACKER
L. ROBINSON

12-14-17

62

Pt #	Remarks		Pt #	Remarks	
885-888	BAY SIDE	X-SEC 12	922-925	BAY SIDE	X-SEC 21
889-893	"	13	926-929	"	22
893-896	"	14	930-933	"	23
897-900	"	15	934-937	"	24
901-905	"	16	938-943	STACKS	X-SEC 1
906-909	"	17	944-949	"	2
910-913	"	18	950-955	"	3
914-917	"	19	956-961	"	4
918-921	"	20			

TYPICAL BAY SIDE CROSS SECTION

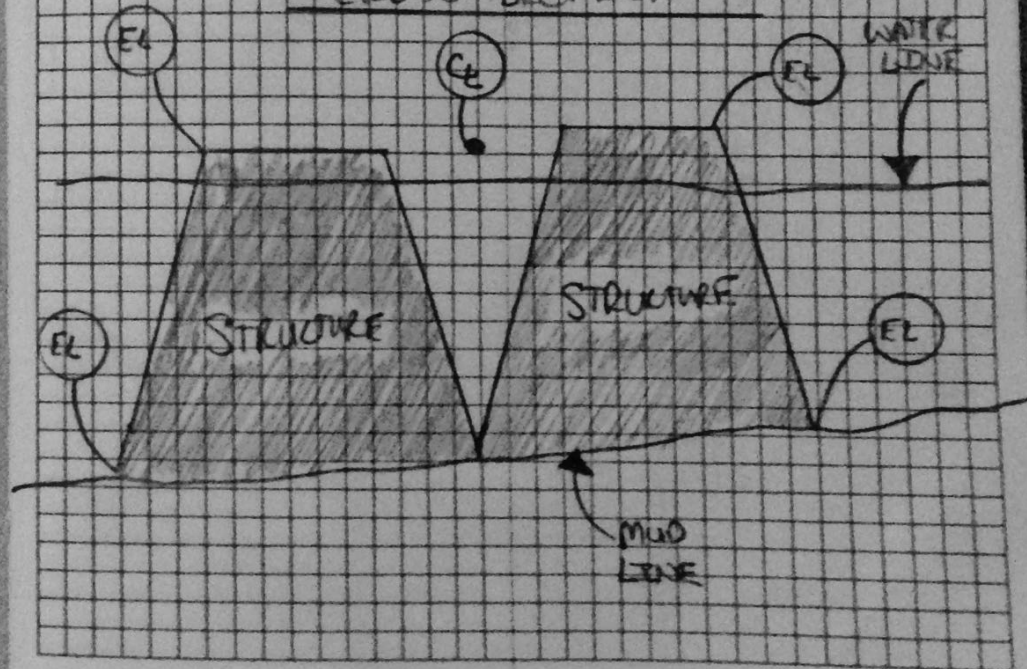

4260

2017.0945 CPRA

Living Shores

Break waters

Base on TBM 03A

TBM 03A	476300.503	Inside ¾" GIP
	3907362.455	El. 1.782 7.054' Hight

Line Log

STA	Time Start	Time Stop
1	10:22	10:28
2	11:10	11:18
3	11:26	11:33
4	11:40	11:47
5	11:56	12:02

Check Pts

446	TBM 03
503	P0148-sm-02

1-15-18

D. Richard
A. Nagwin
J. Chauvin

23

Bar Check 10:00
5.1' + 10' Vel 4766

Water shots

447-449	9:28
455	12:26
466	12:46
496	13:17
497	13:44
499	14:28
501	15:15
502	15:15

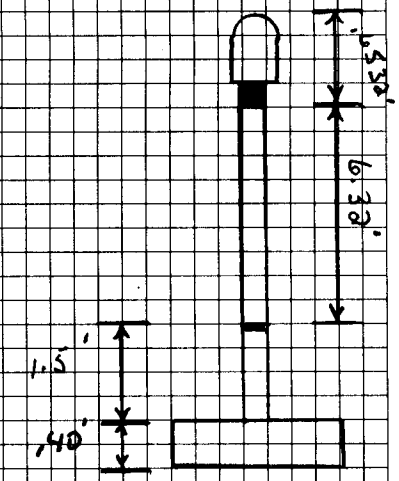

4702

2017.0945 CPRA

Living Shores Breakwater

Base on TBM 03A

(see pg 23)

Check Gauge

29° 47' 12.003

89° 24' 04.096

@ 13:45

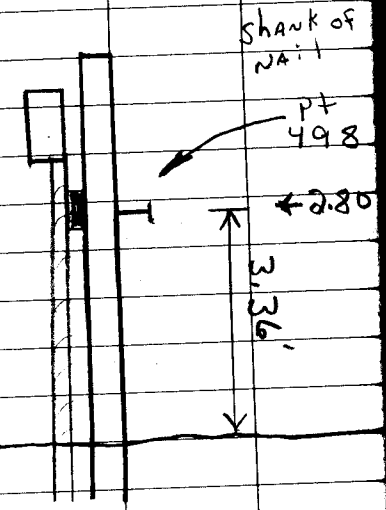

Pt 497

-.666'

1-15-18

Check Gauge

29° 46' 27.583

89° 19' 09.450

@ 17:30

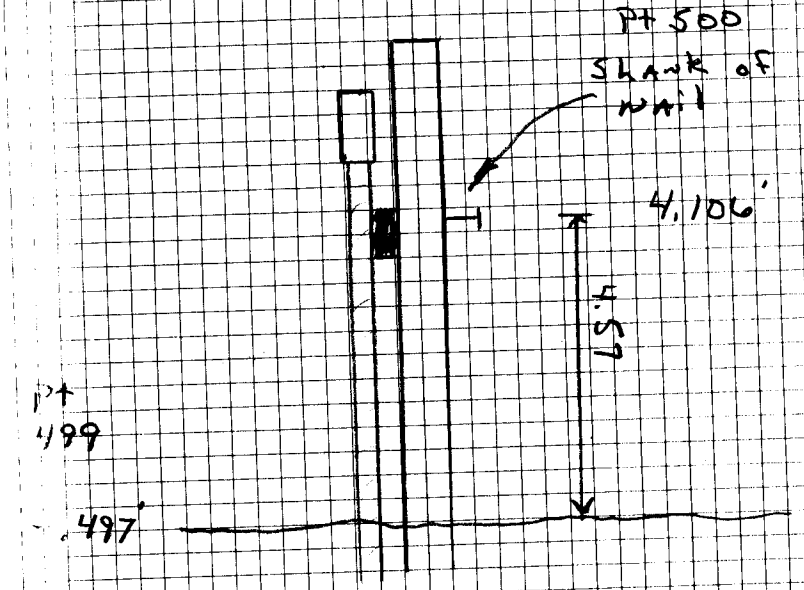

4702

2017, 0470 MOTT MACDONALD
CPRA PO-174

T PO-148-SM-01 SP83/LA SOUTH 1702/GEOID12A

CHKPT TBM-03A

WAVE GAGE RETRIEVAL

LOCATION	TIME OF RETRIEVAL
SOS	11:01
SO6	11:11
SO7	11:22
SO1	11:40
SO2	12:13
SO3	12:34
SO4	12:57

WSEL GAGE 002/003 (WELL CANAL LOCATION)

PT	ELEV	DESC	TIME
17	-0.18	TOW	13:16
18	-0.16	TOW	13:16
19	-0.16	TOW	13:16
20	-0.18	TOW	13:17
21	2.81	NAIL	13:17
22	5.71	TOP OF 4x4	
23	4.86	TOP OF BOX	

J. CHAUVIN
B. PELLEGRIN
T. EVERETT

02/14/2018
SE WINDS 8MPH

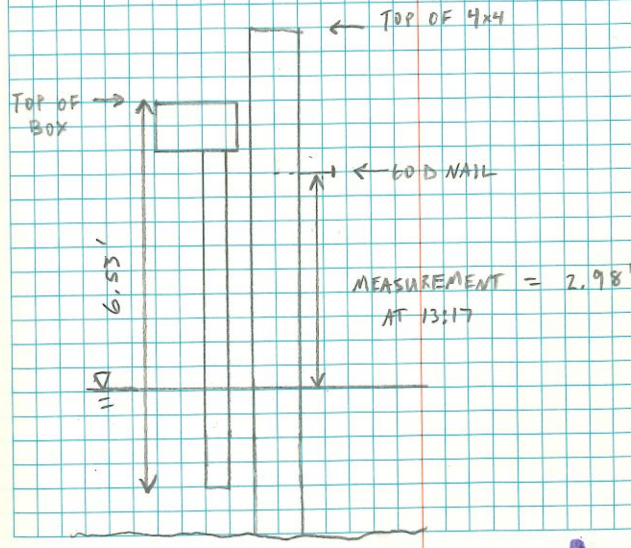

B-2994

2017.0470 MOTT MacDONALD
LPRA PO-174

WSEL GAGE 001 (PO148-SM-02 LOCATION)

PT	ELEV	DESC	TIME
25	-0.18	TOW	14:14
26	-0.19	TOW	14:15
27	-0.16	TOW	14:15
28	4.09	NAIL	14:16
29	7.45	TOP OF 4x4	
30	4.72	TOP OF BOX	

CHKPT PO148-SM-02
CHKPT TBM-03A

J. CHAUVIN
B. PELLEGRIN
T. EVERETT

02/14/2018

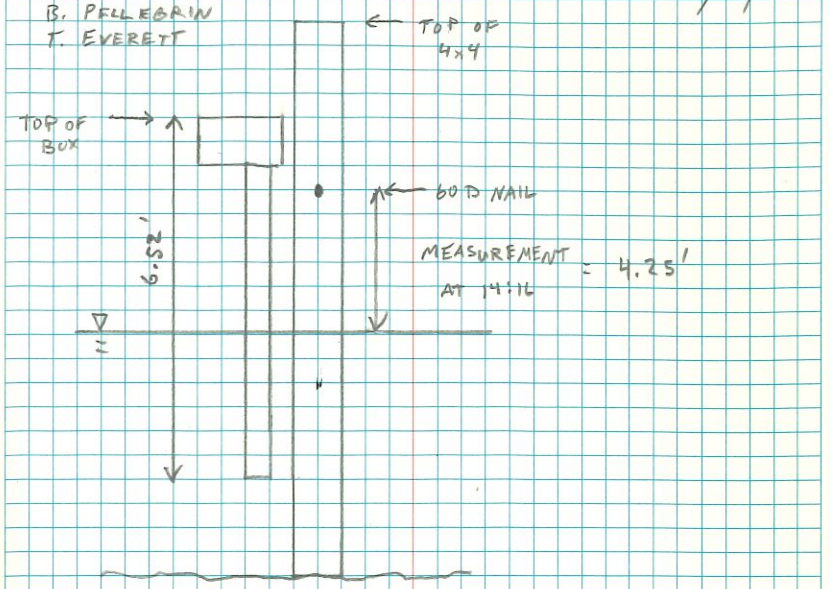

R-2994

VITA

Jason Chauvin was born and raised in Houma, Louisiana. Growing up in Houma and working for his family's century old hardware store along Bayou Petit Caillou in Chauvin, Louisiana instilled in him a passion for south Louisiana culture and an understanding of the bounties and challenges of the landscape. Jason graduated from Vandebilt Catholic High School in May 2006. He graduated from Louisiana State University in May 2011 with a Bachelor of Science degree in Civil Engineering. He anticipates graduating from Louisiana State University with a Master of Science degree in Coastal and Ecological Engineering in August 2018.

Jason is a registered Professional Engineer in the state of Louisiana and currently works as a Project Manager for T. Baker Smith. He has experience in topographic, hydrographic, and hazard surveying, construction administration, civil site design, drainage, flood protection, and coastal restoration.